Structure of Optimal Schedules for Charging Non-ideal Energy Storage

by
Rozanna Nadeera Jesudasan
Student id: 6626742

A thesis submitted in fulfillment of the
requirements for the degree of
Master of Engineering (Research)
at

Swinburne University of Technology
Australia

Supervised by
A/Prof. Lachlan Andrew
and
Prof. Le Hai Vu

2013

Abstract

Energy storage is becoming increasingly important to maintain the stability of the grid, to mitigate the intermittency of renewable generation and to reduce the peak demand in the grid. However, if energy storage is not managed optimally, the utility and the users might not be able to reap the benefits due to energy storage being an expensive technology. Therefore this thesis provides and finds the long term optimal operation schedule for non-ideal storage systems under real-time and arbitrary price increases and discusses the impact of the optimal policy when used for peak shaving in the power grid.

Since the long term storage problem can be infinite when electricity prices increase arbitrarily, an alternate formulation of studying the long term storage schedule by finding the limit of the finite horizon solution is presented using convex optimisation and simulated using the dynamic programming algorithm. Based on this formulation, we show that under certain conditions, convergence and renewal points exists for ideal and non-ideal storage systems with charging inefficiency and self-discharge. Because of the existence of renewal points, the results in this thesis show that future demand and price do not affect the scheduling decisions before the renewal point for a given convergence time, allowing to investigate the behaviour of the long term schedule by investigating the properties of the finite horizon solution with convergence.

The major findings on the structure of the optimal storage management schedule show that for ideal storage systems, the marginal generation cost is constant while storage does not fully saturate or empty. However for energy storage with charging inefficiency, fluctuations in generation are seen that depends on the efficiency of the storage. For peak shaving with inefficient storage systems, the simulations show that a trade-off exists in purchasing a smaller more efficient storage device or a larger less efficient storage device to achieve the same amount of peak shaving. Additionally, the same amount of peak shaving can also be achieved for a range of efficiency values for smaller energy storage systems allowing utilities and users to benefit if the utility provides a cheaper storage system for peak shaving and cost savings. Finally the structure of the generation schedule for storage devices with self-discharge shows that the generation would increase exponentially due to the self-discharge and that having rapid price increases greater than the rate of self-discharge caused the generation schedule to decrease exponentially, suggesting that moderate price increase could balance the generation and provide better peak shaving in the grid.

Acknowledgment

I would like to express my sincere gratitude to my supervisors Associate professor Lachlan Andrew and Professor Hai Vu without whom this thesis would not have been possible. I thank Lachlan for his guidance, support, encouragement and patience during these two years. His immense knowledge and enthusiasm enabled me to better understand and appreciate the need for energy efficiency. I would also like to thank Hai Vu for his encouragement, support and advice which enabled me to achieve my research goals.

I also extend my gratitude to Professor Grenville Armitage and everyone at CAIA (Centre for Advanced Internet Architectures) Swinburne for supporting me and providing me with the necessary feedback.

Finally, I wish to thank my family and friends for their encouragement during my studies.

Declaration

Thesis contains no material which has been accepted for the award to the candidate of any other degree or diploma. To the best of my knowledge this thesis contains no material previously published or written by another person except where due reference is given in the text.

Signed:

Date:

Contents

List of Figures

List of Tables

Chapter 1

Introduction

As increasing demands are placed on an aging electricity grid, there is an increased need to incorporate energy storage to smooth the peak demand placed on the generation, transmission and distribution system. To minimise demands in the network, the storage systems are usually placed near the loads, so that the energy storage systems are able to store power during low demand periods from the grid, and supply power to the loads during peak demand. Because of this, utilities are trying to encourage customers to install energy storage systems in households to reduce the peak demand in the grid, by providing price incentives for the customers to shift their energy consumption using energy storage. With recent developments in more advanced storage technologies and the reduced cost of storage systems, the use and operation of energy storage to manage demand and reduce the variability of renewable generation has become an popular and much needed area of research [1, 2, 42, 48, 54, 55].

The use of energy storage in the power grid affects two groups of stakeholder: the end users who consume energy and pay for it, and the utilities who operate the generation, transmission and distribution systems and need to maintain the stability and reliability of the grid, while reducing the operational cost in providing electricity. These circumstances forces both the utility and the user to consider the behaviour of energy storage under optimal operation conditions. In particular, both stakeholders need to be able to implement the best possible operation strategy considering electricity prices, user demand, generation cost and the most suitable storage system based on the storage device characteristics, such as capacity and energy loss. Therefore in this thesis we investigate and study the structure of the long term optimal solution in managing demand and reducing energy cost for the stakeholders by using energy storage systems under real-time and arbitrary price increases.

For users to be able to profit from using energy storage, the utility needs to set electricity prices to reflect the demand in the grid, so that users charge their storage devices during low prices and discharge when the prices are high. That is, high demand would see high electricity prices and low demand would cause the real-time electricity prices to reduce, encouraging users to charge their energy storage. However,with peak oil and reducing energy resources, it is also necessary to factor in the rapid increase in energy prices which ultimately affect the overall cost of generation for the utility. This requires the study of the long term optimisation of energy storage under rapid price increases, that will ultimately help the utilities and users understand the implication and trade-offs associated with using energy storage for cost minimisation and peak shaving in the grid.

The operational optimisation of energy storage can be quite complex, when considering that it has to be able to anticipate future saturation and starvation of the storage system [15], by factoring in future demand and electricity price trends. This is especially true when looking at the long term optimisation of energy storage. In the context of long term energy storage, the utility or user might choose to buy and store energy early and save it for a long period to use when prices are much higher than the daily price peaks, possibly reducing the desired peak shaving in the grid, especially when future price trends increase rapidly. As a result we see that it is necessary to study the effects of the storage on the long term optimal solution under such price trends.

The long term storage scheduling problem with arbitrary price increase, typically results in an infinite horizon energy storage cost minimisation problem that results in a total infinite cost if the average cost per stage is increasing. Because of this, we first models and provide an alternate method of analysing the finite horizon(short term) energy storage problem, and use its structural properties to study numerically the behaviour and optimal solution for the long term energy storage problem with charging inefficiency and self-discharge. Here, the inefficiency of a storage device is the loss of energy during the charging and discharging phase of the storage, and self-discharge for a storage device is a form of energy loss due to internal chemical reactions in chemical storage or friction in flywheels that occurs over time. Therefore since the inefficiency and self-discharge of a storage system are characteristics that result in the loss of energy from a storage device, it is possible that the utility might have to generate more in order to compensate for the energy loss when using an energy storage system between the utility and the user. Because of this we see it important to study the impact on the structure of the optimal schedule cause by such non-ideal characteristics of energy storage. As a result, we individually study the impact on the cost and peak shaving for the above mentioned inefficiency and self-discharge, and show the structure of the optimal charging and generation schedule due to these storage characteristics. Moreover, we also discuss the trade-offs for the utility and the user and the change to the total generation by considering the storage capacity and storage loss under real-time and arbitrary price increases.

This thesis thus investigates and discusses the structural properties of the infinite horizon optimal storage scheduling problem, for cost minimisation and peak shaving under different electricity pricing mechanisms and demand trends, when using energy storage systems. Based on these structural properties, the implications and trade-off for the utility and users are presented, considering separately the inefficiency and self-discharge losses for different capacity energy storage systems.

1.1 Outline and Contribution of the Thesis

The outline of each chapter and the contribution of this thesis is presented as follows,

1.1.1 Chapter 2

This chapter contains the background and overview of the research carried out in optimising the use of energy storage systems in the grid. Here we show the algorithms, pricing mechanisms, optimisation methods and storage characteristics considered when optimally managing the schedule of energy storage for demand management and other grid based optimisations. Based on this, the focus of our research is introduced.

1.1.2 Chapter 3

In Chapter 3 we proposes a model for minimising the operational cost of generation using energy storage. The optimal solution of the model is then presented and used to analyse the structural properties of ideal energy storage systems. The structure of the optimal solution when using an ideal energy storage shows that the marginal generation cost is constant between storage saturation and empty points, which also results in the generation being constant between such points under constant price increase. Furthermore, by using the optimal expression for energy storage, we show that the finite horizon solution of the storage and generation schedule converges in finite time T under certain conditions, and that renewal point exist for some time $t \in (0, T)$ for which the storage schedule of any optimal problem with terminal storage level $b(T) \in [0, B]$ is the same for any time $t' < t$. Further even when the time horizon is extended, we show that the renewal point stays the same, which allows us to decouple the long term solution into multiple finite horizon solutions and study the behaviour of the long term scheduling problem.

Therefore, the main contribution of this chapter is to demonstrate the above mentioned structural properties and to provide an alternate method to study the infinite horizon infinite cost storage problem. Furthermore the the optimal charging and generation schedule are also numerically simulated using dynamic programing and the behaviour of the scheduling decisions are demonstrated in this chapter

1.1.3 Chapter 4

This chapter extends the ideal energy storage system to incorporate storage with charging inefficiency and shows the structural properties of the optimal solution with losses due to inefficiency. This chapter shows that for a storage device with charging efficiency, the marginal generation cost is not constant when the storage level $b \in (0, B)$ as an ideal storage device, but instead fluctuates between some upper and lower value.

This chapter also investigates the peak shaving behaviour when using inefficient energy storage under real-time prices and arbitrary price increases. We show that for smaller storage systems, the peak shaving remains the same for a range of efficiency values, which allows a utility to purchase a less expensive more inefficient storage device to provide to the user, based on the assumption that the utility is willing to provide the storage device for the user for peak shaving in the grid. Further we also show that a trade-off exists to provide the user with a larger less efficient storage system or a smaller more efficient storage system to provide the same amount of peak shaving. Additionally, chapter also discusses the effect of rapidly increasing prices on peak shaving in the grid, and discusses the impact of inefficiency on the total generation of the grid with real-time prices.

1.1.4 Chapter 5

Chapter 5 discusses and presents the structural properties for energy storage systems with self-discharge. Here we demonstrate that the optimal generation schedule exponentially increases due to the increase self-discharge, and that this increase in generation is greater at higher rates of self-discharge which increases the peak generation of the system. We also demonstrate that the structure of the generation schedule is such that whenever the generation decreases for a low rate of leakage, the generation also decreases for a higher rate of leakage. Conversely, whenever the generation jumps up for a high rate of leakage, it also jumps up for a lower rate.

Additionally, we carry out a study on the behaviour of peak shaving when using energy storage devices with self-discharge under rapid price increases. We show that the structure of the generation schedule due to self-discharge causes the optimal generation to be piecewise increasing and that the increase in prices cause the the optimal generation to be piecewise decreasing, which results in the possibility of a cancellation in which steadily increasing prices can improve the effectiveness of peak shaving.

1.1.5 Chapter 6

This is the last chapter of the thesis containing the conclusion and possible future work in the area of optimal operation of energy storage in the grid.

1.2 List of Publications and Technical Reports

- Rozanna N. Jesudasan, Lachlan L. H. Andrew, and Hai L. Vu. Scheduling inefficient storage. In *Proceedings of the 2013 IEEE Power & Energy Society General Meeting*, Vancouver, British Columbia, Canada, July 2013

- Rozanna N. Jesudasan and Lachlan L. H. Andrew. Scheduling long term energy storage. In *The fourth International Conference on Future Energy Systems (ACM e-Energy)*, Berkeley, CA, May 2013. In preperation

- Rozanna N. Jesudasan, Lachlan L. H. Andrew, and Hai L. Vu. User-optimal Storage with Rising Energy Prices. Technical Report 120906A, Centre for Advanced Internet Architectures, Swinburne University of Technology, Melbourne, Australia, 06 September 2012

Chapter 2

Background and Literature Review

This chapter gives the background and overview of other research that has been carried out in modeling and optimising the usage of energy storage systems. The algorithms, pricing mechanisms, storage characteristics and peak shaving are discussed providing a short description of the research in each area. Finally, the focus of our research and the research issues that we will address in our thesis are presented.

2.1 Overview

The electricity grid is responsible for supplying power on demand to many households and businesses, making it one of the most complex and critical infrastructures to maintain. The grid needs to be reliable and stable through balancing energy supply and demand [53]. One of the key issues with this static behaviour in generation and demand is that the grid also must supply energy during sudden peak demand. This sudden demand requires utilities to use more expensive fast ramping generators [23] that provide the required extra power than the planned base load generation in the grid. Moreover, this peak generation on the grid can cause a strain in the grid which can result in blackouts [14]. Because of this, utilities are interested in employing methods that will allow them to reduce the peak demand by providing users with incentives to manage and shift their demand from high peak periods to low peak periods [5].

One proposed method to shift user demand is by autonomously scheduling user appliances, which require certain appliances such as air conditioners and washing machines that can be scheduled to operate at off peak periods based on price signals sent by the utility reflecting the demand in the grid. That is, if the demand in the grid is low, the electricity price will be low allowing users to use their devices during such periods. Similarly, high price signals indicate high demand in the grid, so the devices will shift their operation schedules to a different period [48, 54]. A second proposed method to manage demand in the grid is by using energy storage to store energy during low demand and to supply energy to user loads during peak demand periods [15, 23, 42]. In this thesis, we will investigating the latter scenario, where energy storage is used to manage and optimise the user demand, and reduce the operational cost for the utility by reducing the required peak generation, also known as peak shaving. As per our problem setting in section 3.2, we are interested in optimising the charging and generation schedule when using an energy storage device installed between the user(s) and the utility to satisfy a single user or aggregate user demand using the power drawn from the electricity grid. Therefore, this chapter will present the literature that shows the optimisation and management methods for ideal and non-ideal storage systems for cost minimisation and peak shaving. Furthermore, we will also show how our research will contribute to finding the structural properties of non-ideal storage systems with real-time and arbitrary price increases.

2.2 Modeling and Optimal Scheduling of Energy Storage Systems

The energy storage management and scheduling problem has been studied from the perspective of the end user [15, 23, 29, 30, 62] as well as the utility [9, 11, 37, 38, 59]. In general, the literature optimises the storage schedule, finds the structure of the operational schedule or investigates the optimal sizing of the storage for different objectives and storage characteristics. These studies are usually carried out considering the short term(finite horizon- minutes, hours, days) or the long term(infinite horizon- months, years) management of energy storage when having either deterministic or stochastic demand and prices.

Chandy et al. [15] study the finite horizon optimal policy for a single generator and single load using dynamic programming and discuss the structural properties of the generation and storage policy. In particular, they look at minimising a total convex generation and a holding cost, which applies a penalty for not having a certain storage level for an ideal energy storage device. Similar to Chandy et al. in [15], Van de ven et al. [62] also looks at the optimal policy when minimising the cost of generation subject to deterministic user demand and prices. However, instead of looking at the short term cost, [62] studies the long term optimal policy using Markov Decision process and shows, that the optimal policy has a two threshold structure that requires the storage to charge when the storage level drops below the lower threshold and discharge when the storage level is above the upper threshold. Koustsopoulos et al. [38] also look at the long term optimal energy storage problem, but instead of considering the profit for the user, they consider the cost minimisation for the utility when using energy storage. Similar to Chandy et al. in [15], the electricity cost in [38] is a convex function of the power drawn from the grid, modeling the fact that each extra unit of generation needed to serve the user is more expensive as the required generation increases. In [38], Koustsopoulos et al. derive a threshold based optimal policy similar to [62] for the infinite horizon case, but using an on-line algorithm. Finally they show that the performance of their algorithm approaches the optimal policy as the storage capacity increases comparing their results with the dynamic programming algorithm.

2.2.1 Algorithms Used for Optimisation

Since our main aim is to investigate and understand the structure of the long term storage solution, we use the fact that the solution solves a dynamic program (DP) similar to [45, 15, 24, 37, 38, 62] to numerically simulate the optimal schedule for the energy storage problem. Since dynamic programming (in section 3.5) allows a complex optimisation to be solved by solving smaller sub problems which lead to the optimal solution of the original problem, it provides a per stage and overall minimum cost for the given complex cost minimisation problem with energy storage. Dynamic programming has also been used in optimal management for electric vehicles [56]. In the case of Romaus et al. [56], dynamic programming is used to optimise the size and the usage of a car battery.

Though dynamic programming has been used by many to optimise the short and long term energy storage problem, others [30, 58, 61, 65], have proposed or used different algorithms to solve the storage problem. Here Urganokar et al. [61], develop an algorithm that provides near optimal performance as storage size increases, for optimal management of energy storage in data centers. They use a technique which requires no prior knowledge of the workload known as Lyapunov optimisation,which is used to reduce the average operational cost of electricity by using UPS(uninterruptible power supply) systems in data centers. As mentioned above, they show that for their algorithm, the deviation from optimality reduces as the storage capacity increases.

On the other hand, Sortomme et al. [58] use a method called particle swarm optimization (PSO), to manage the optimal dispatch and consumption of energy for micro grids which contain localised renewable generation, energy storage and loads. Further, in [30], Huang et al. consider the problem of energy storage management to maximise the user profit, for a user that is able to buy and sell energy to and from the power grid. For this they develop an algorithm called Demand Response with Energy Storage Management (DM-ESM), that does not require statistical knowledge of the system dynamics unlike the Dynamic programing algorithm.

Other on-line algorithms such as Receding horizon control(RHC) and Model predictive control (MPC) have also been used by [39, 64] to optimise the scheduling of energy storage under real-time pricing. These on-line algorithms carry out the optimisation dynamically by finding the optimum for a finite window including the current and future states of the horizon and progress forward in time while updating each of its states in real-time to provide a more accurate optimisation based on the updated state. The advantage of these algorithms compared to dynamic programing is that the optimal decision can be updated progressively through the horizon as the demand and price signals change. Finally, Linear programming is used by Youn et al. in [65] to minimise the operational cost of a small power producing facility that can buy and sell energy to the grid. Here they make assumptions about the distribution of the load and the on-site generation facility to determine the optimal operation of the energy storage device.

2.2.2 Overview of Objectives for Scheduling Energy Storage

As stated by [15, 26, 38, 39, 62], the energy storage problem with variable demand and pricing is non linear and non convex, and hence requires non linear and more complex methods to optimise the use of energy storage. Most of the literature in the area of optimal use of energy storage apply convex optimisation to model the energy storage problem with pricing to find a global optimal solution quickly and efficiently. Lin et al. [44] solve their power dispatch problem by solving a piecewise quadratic cost function. Lavaei et al. [40] provides sufficient conditions under which a non convex optimal power flow problem can be solved as a convex problem. In both [40] and [44], the optimal power flow problem of the grid that aims to find an optimal operation to minimise some cost function based on generation or transmission losses is non-linear and hard to solve. As a result, both [40, 44] show that by using convex optimisation it is possible to solve this complex non-linear optimal power flow problem. Based on this [15, 26] solve the problem of optimising the usage schedule for single and distributed energy storage systems respectively. Similar to the literature in the area of optimal energy storage management our objective is to minimise the cost of generation. In our model we assume that our generation cost is convex, allowing us to efficiently optimise the energy storage problem. Further, since the convexity of generation relates to an increase in the overall cost for every extra unit of power generated; minimising a convex cost also models the fact that we want to reduce our generation to shave the peak in the grid, thereby reducing the cost and the strain on the grid.

2.2.3 Pricing Schemes for Optimising Energy Storage

Another important aspect of modeling and scheduling storage is the pricing signals that are set by the utility, to reflect the strain and other factors affecting the grid. Some of these common pricing schemes are [5, 47],

- Time of Use (TOU) pricing, where electricity prices are charged according to peak, mid-peak and off peak periods of the day.
- Critical peak pricing (CPP), where an additional charge on top of the TOU is applied for power drawn beyond a certain threshold.
- Real time pricing (RTP), where users are charged according to price fluctuations in real-time, usually applied every 30 or 60 minutes.

For our research we are particularly interested in real-time prices, where the utility applies some time varying price to reduce peak demand in the grid. A study that looks at optimising the operation strategy for energy storage systems based on real-time electricity prices to benefit the user is carried out by Weihao et al. in [29]. Weihao et al. compare two types of energy storage systems with inefficiency and compare the benefit for the user based on the performance of the schedules storage system based on Denmark's real-time pricing. They show that even though a battery with higher efficiency has a better performance in shifting user demand and reducing cost for the user, the cost of the storage affects the payback period making the battery with lower efficiency more profitable to install, since it is cheaper than the battery with a higher efficiency. These studies show that the scheduling decisions are affected by the battery characteristics as well as the user demand and pricing signals applied by the utility. Xu et al. [64] optimise the storage schedule under demand and price uncertainties. They observe the scheduling decision due to the variations in the day-ahead pricing and real-time pricing using MPC. Their case studies show that by using MPC, the electricity cost can be minimised under price and load uncertainties.

The problem of scheduling residential energy consumption with real-time prices is carried out by Mohsenian-Rad et al. in [47]. Though their studies are for scheduling residential devices and not using storage, the results are applicable to storage, since their scheduling algorithm provides a method to shift demand by storing energy during low electricity prices and uses the stored energy during peak electricity prices. Their results show that a user can decrease their payment up to 25% and at the same time the utility can reduce their peak to average generation ratio to 38%, which results in both a reduction in cost for the user and peak shaving for the utility. Korpaas et al. [37], optimise the operation schedule of energy storage for wind power plants in electricity markets and show that by choosing the proper sizing of storage it is possible to take advantage of hourly variation in pricing. Harsha et al. [27] look at the long term average cost minimisation of renewable generation with energy storage when using real-time pricing. Harsha et al. also use dynamic programming to optimise the scheduling behaviour of energy storage and generation. Their work mainly focuses on the profitability of storage, showing that for storage to be profitable under their policy, the ratio of the amortized cost of storage to the peak energy price should be less than 1/4.

The literature shows that the utility set pricing plays an important role in scheduling and optimising the storage schedule. However, the literature does not consider situations where electricity prices rise arbitrarily due to fuel shortages or other grid related expenses. Though such as [38, 62] literature consider the effect of inflation on the optimal schedule, they do not discuss or model scenarios for which prices can rise faster than the rate of inflation. That is, the cost per stage as well as the long term cost is unbounded due to rapid increases in pricing, which results in an infinite horizon infinite cost problem. One method to handle this increase in cost is by applying a weighted limit as suggested by [20], but since we are interested in arbitrary rates of increase, such a technique does not apply. Therefore subsequent chapters of this thesis will contribute by providing an alternate method to solve and observe the structure of the infinite horizon infinite cost problem.

The foregoing work assumes the load is fixed. The alternative to this is to schedule demand optimally. These studies on optimising energy usage range from scheduling household devices with and without energy storage and scheduling storage for Electric Vehicles (EV) [63, 42, 57, 49]. Particularly, Wu et al. [63] looks at minimising the energy purchase cost by optimising the charging and discharging of energy storage for EV power demand. Their research focuses on the algorithm that minimises the purchase cost while being able to meet the power demand of the EV. A study that looks at optimising the scheduling for household devices and energy storage on the other hand is carried out by Li et al. [42]. According to Li et al., these storage devices can be batteries that are bought specifically for saving cost or PHEVs (Plug-in hybrid electric vehicles). Here Li et al. maximise a utility function that benefits both the customer as well as the utility in the way that the customer purchases electricity and the way that the utility sets the real-time prices. Their results show that by maximising these functions, the utility can reduce the peak in the grid and the customer can benefit by reducing their electricity bill when using energy storage.

2.3 Non-ideal Energy Storage

The characteristics of energy storage devices are also factors that affect the charging and generation scheduling behaviour. That is, characteristics such as storage capacity, inefficiency, self-discharge, discharge time, depth of discharge etc. [31] determine the energy lost from the device, the time it takes to charge the device and how fast the device can be charged and discharged, which affect the optimal operation of a storage system. Faghih et al. [23] research into the optimal use of storage with ramp constraints and price elasticity for a finite horizon. The ramp constraint of the storage limits how fast power can be drawn in and out of a storage system. Their studies provide the optimal policy using non-ideal storage and also demonstrates that a user can profit by selling energy to the grid when prices are above some mean value and charge the storage device only when the prices are below a certain threshold, similar to [62]. Similarly, Bejan et al. [9] model a storage system with ramp constraints that limit the rate of charging and discharging, to study the behaviour of large scale fast response storage with wind power. Here they use the storage to find a trade-off between the wind spill, which is the energy lost due to excess generation from wind power, and the use of expensive fast response generators. Han et al. [59] also looks at balancing the loss of energy and the use of fast ramping generators with the use of energy storage. In their studies, the storage device is considered to be inefficient, with both charging and discharging efficiency, where the charging efficiency is the ratio of charged power to the power input and the discharge efficiency is given by the the ratio between the output power to the power discharged. Their result is for balancing both loss and fast response generation based on a threshold policy which decides when to use the fast response generation based on how much loss is profitable for certain charging/discharging efficiencies of the storage system.

Gast et al. [25] extend the model by Bejan et al. in [9] to study the performance of energy storage with energy efficiency and wind prediction. They provide trade-off bounds on the energy loss due to both wind spill, storage efficiency and fast response generation. Unsurprisingly, they show that when the storage is non-ideal and the charging/discharging efficiency $\eta < 1$, the total energy loss and fast response generation will be positive regardless of the storage size. This suggests that the efficiency of a storage device impacts the storage and generation scheduling decisions in the grid, possibly increasing the amount of generation required due to the loss in energy as expected. The problem of managing wind energy commitments with co-located inefficient energy storage is discussed by Bitar et al. in [11]. Bitar et al. demonstrate that the problem can be solved using convex programming and that the solution results in trade-offs between storage capacity and expected profit. Their main results show that a storage policy that always stores the maximum allowable energy is optimal when there is surplus generation, but the overall profit depends also on the price of the storage device. As indicated in [11], the capacity of the storage plays an important role in storing and providing power. Additionally, the efficiency of the storage can also affect the price of the storage device. Because of this, we have observed the behaviour of the optimal scheduling solution to understand the cost and peak shaving trend with increasing storage capacity and charging/discharge efficiency.

Though many [28, 39, 50, 62] model the the charging/discharging efficiency and self-discharge of energy storage, they do not discuss the qualitative effects of these non-ideal characteristics with decreasing efficiency, increasing self-discharge or storage capacity. Kraning et al. in [39] look at modeling and optimising multiple storage devices to operate as a single storage device by using receding horizon control (RHC). The objective of their problem is to minimise the average cost of operating the storage devices. Here, they consider the trade-off between battery sizing and storage cost. Though larger storage devices provide better performance, they are more expensive; therefore Kraning et al. [39] minimises this trade-off between the average cost per stage and the initial cost of the storage device. Similar to Chandy et al in [15], Kraning et al. [39] applies a penalty cost for not being able to meet the required energy demand. As a result their research provides a method to minimise the total operation cost taking into consideration the penalty cost, by using convex optimisation for storage devices with charging/discharging efficiency.

The self-discharge of energy storage also affects the optimal scheduling decisions when using energy storage, since it affects the amount of energy retained in the storage device over time [31]. This loss in energy can vary from low self-discharge in lithium ion batteries to high self-discharge in flywheels [21]. Similar to the charging/discharging efficiency, some papers [19, 39, 60] include self-discharge in their models, but do not consider the qualitative effect of increasing self-discharge with time varying prices when scheduling short term or long term energy storage. As mentioned above, though Kraning et al. [39] include self-discharge in their modeling they do not investigate the impact of such self-discharge of storage devices on the optimal behaviour of the schedule. Taylor et al. [60] focus on storing and scheduling renewable variable generation using energy storage in energy markets to profit multiple independent utilities. Their studies on storage consider charging/discharging efficiency and self-discharge in energy storage systems with capacity constraints on energy storage similar to our storage model. Devillers et al. [19], consider storage self-discharge for energy harvesting communication systems with storage constraints. Their objective is to maximise the amount of data transmitted by using energy storage to store the harvested energy. Their model assumes a constant rate self-discharge similar to our model. This demonstrates that research needs to be carried out by not only modeling the efficiency for an individual scenario, but also by understanding the impact of increasing self-discharge by observing the structural properties of the optimal solution, especially for long term storage, where the loss of energy can be significant over time.

Though the literature above models the energy storage problem with non-ideal characteristic of energy storage, little exists on the the structural behaviour of the optimal schedule due to non-ideal storage properties, especially energy loss. Because of this, we study the structural properties of the optimal charging and generation schedule subject to the influence of two effects that model the loss of energy when using energy storage. To be more precise, the charging/discharging efficiency and the self-discharge of storage that cause significant influence for long term energy storage. Moreover, we also discuss the performance of peak shaving in the grid when using our optimal solution to store energy in non-ideal energy storage systems.

2.4 Peak Shaving

Peak shaving is the reduction in peak power generation to satisfy some peak demand. Peak shaving can be achieved by either reducing the demand by shifting or shedding load in the grid; or by using energy storage to store power during low demand and supply power during peak demand periods. This allows the utility to generate less during such times. Since peak generation is expensive for the utility, and causes a strain on the grid, some [35, 41, 44, 46, 51] have studied the methods of reducing the peak generation in the grid by using energy storage. The reduction in cost of the electricity bill by peak shaving is studied by Maly et al. [46]. Maly et al. use dynamic programing to solve the optimisation problem by scheduling energy storage so that the generation in the grid is minimised. Their result show that trough leveling is not optimal since the battery charges faster when at minimum charge and that during off peak hours it is better to charge more evenly since a higher charge rate is undesirable since it can cause the demand to peak when charging the storage system. The authors state that by evenly charging the battery, it will not only reduce the electricity bill but will also reduce the battery wear and tear. Since their problem uses a TOU pricing model with peak and off peak pricing, the battery can charge evenly during off peak periods. But for our studies, since we use real-time prices the influence of such pricing may affect the scheduling decisions differently.

Oudalove et al. [51] minimise the customer electricity bill by using energy storage when the utility applies CPP. Their optimal policy shows that it is optimal to charge between two peaks and that it is not optimal to charge for longer periods. Instead they suggest that it might be more profitable to have shorter peaks to get a higher revenue which is highly dependent on the fixed as well as the peak pricing. These results agree with [22] Evan et al. that shows peak pricing rate and duration of peak demand affect the cost saving obtained by peak shaving.

Apart from pricing, Bar-Noy et al. [7] show that the storage size also can affect the peak shaving in the grid. They show that increasing the capacity of energy storage increases the peak shaving capabilities of a grid, even with inefficiencies. However, we show that this is not always the case since the inefficiency causes the generation to fluctuate between storage saturation and empty points which results in a maximum allowable energy level for a given demand profile. Therefore, our research focuses on understanding peak shaving capabilities for energy storage devices with charging/discharging efficiency and self-discharge with and without arbitrary increase in prices and increasing storage capacity. Since the loss affects the amount of power deliverable by the storage device, we see it necessary to understand the possible implication of such non-ideal storage devices.

2.5 Focus of our Research

The research in the area of optimising and scheduling generation and cost using energy storage, shows that the cost model, the pricing and the storage characteristics affect the optimal scheduling behaviour. Though many have provided methods to solve the optimal storage schedule, little has been done to understand the structure of the long term optimal solution, especially under real-time and arbitrary price increases. As a result, our research focuses on optimising the energy storage problem and also studying the behavioural patterns associated with the optimal solution for energy storage devices with charging/discharging efficiency and self-discharge. Furthermore, we have applied these structural results and investigated the peak shaving capabilities and cost saving for the utility/user. Additionally, since the peak shaving only benefits the utility, we have also investigated trade-offs that can be applied, so that the customer and the utility can both save cost by reducing the peak generation, under the assumption that the utility is willing to pass on some of the cost savings to the customer.

Chapter 3

Energy Storage Model

In this chapter, a model is developed for an ideal energy storage device installed between the generator and the customer to find the optimal scheduling behaviour that minimises the total electricity cost. The model is solved using convex optimisation techniques and the results of the optimal solution are used to prove structural properties that allow an infinite cost infinite horizon problem to be studied in finite time. The resulting structural results are then numerically simulated using dynamic programming to show the optimal charging and generation behaviour for an ideal energy storage device.

3.1 Overview

Managing the demand in the electricity grid is essential for stability and reducing the cost of generation in the grid. Sudden peaks in demand not only increases the cost of generation, but can also cause power outages, especially when supply is not able to meet demand. Therefore matching this supply with the consumption, shifting or reducing the peak demand and maintaining the stability at minimum cost are some of the major concerns for utilities [18]. Recent research has focused on methods of solving these problems by deploying and managing storage devices near loads [7, 9, 15, 16, 17, 23]. These loads can be daily user loads such as household devices, or more variable elements such as wind turbines and photovoltaic systems. Then by installing storage devices between loads and the utility, it is expected that the storage system would act as a buffer between the required generation and the user demand, so that the storage device can charge during low price and demand periods to later satisfy the peak demand by discharging the storage system. So, to get the maximum benefit from energy storage systems, it is necessary to properly optimise and schedule these devices to understand the implications of using such devices, in lowering the utilities generation cost, and reducing the peak generation in the grid. Though the cost minimisation in generation usually applies to the utility, here we consider the scenario where users are also able to benefit from using storage devices, provided utilities provide some price incentive for users reducing or shifting demand using storage devices [5, 22, 29]. Such arrangements are possible if the utility employs prices that reflect the demand in the grid known as dynamic pricing [8, 12], and also if the utility is willing to provide users with storage devices. The latter suggestion is considered due to the reluctance of users to purchase expensive storage devices which in the long term might not provide a return on investment for the user. But if the utility provides the user with such a device, then the user might be willing to install such a system, as long as they can reduce their electricity bill. This price incentive will then not only benefit the user, but will also ultimately allow the utility to reduce the peak demand in the grid.

Therefore, in this thesis we focus on optimising the storage schedule and finding the structural properties of the optimal solution that will allow utilities and users to make informed decisions when choosing storage device with different capacities and inefficiencies. We discuss the the trade-offs between cost and storage characteristics such as charging efficiency, self-discharge and storage sizing, that will allow the user and the utility to decide on the 'type of storage device' they wish to install. Particularly in this chapter we investigate the potential of using energy storage to minimise the long term user cost by optimising the charging and generation schedules and show structural properties that are present when using an ideal energy storage system. At present though a short term scheduling problem can be studied to minimise the user cost, the need for renewable energy in the long term encourages us to investigate a long timescale for scheduling storage systems [3]. This is because the availability and the demand for energy varies on longer timescales [4].

Though this thesis mainly focuses on user type storage systems, our model and results also apply to large scale energy storage systems that need to be scheduled in the long-term. This is especially important when considering a future grid that is fully or partially powered by renewable energy. Additionally, in subsequent chapters we will also study the structural properties of the charging and generation schedules for non-ideal storage devices and explore the peak shaving benefit that results from using storage devices in the grid with and without arbitrary price increases, allowing us to weigh the advantages and disadvantages when installing storage systems between the utility and the users.

3.2 Problem Setting

The electricity grid relies on the balance between supply and demand. This means that without energy storage, the power drawn from the grid $g(t)$, should be able to satisfy the user load $d(t)$ at all time t with $g(t) = d(t)$. Now consider an isolated energy storage system installed between the generator and the user load as shown in figure 3.1. This system would enable the user to either consume energy directly from the grid, or to store some energy $b(t)$ in the storage device, by drawing power from the grid during low price and demand periods, and using the stored energy at a later time when the demand and electricity prices are high. In this setting, it would seem natural to optimise the usage of the storage device by scheduling it, so that the total cost of generation is minimised. That is,

$$Minimise \sum_{t=1}^{\infty} \gamma(t) N(g(t)),$$

which is the total cost of generation. That is to say, we are interested in minimising the long term(infinite horizon) cost with arbitrarily varying prices $\gamma(.)$ and a convex cost function representing a penalty for drawing high power $N(.)$. However, this is not well defined in the full generality of the setting we consider. Note that with the use of renewable energy and a possible shortage of fossil fuels [43], the future prices of energy can increase impacting the long term scheduling behaviour of large and small scale storage systems. However, the impact on the cost due to varying energy prices are usually greater for large scale storage systems which require seasonal planning in months and years [4]. Therefore this motivates us to study the structure of problem (3.1) by taking the limit of of the solution of (3.2)

Therefore, though our studies mainly focuses on user type storage systems, our model and the structural behaviour in general can also be applied to large scale storage systems, since our constraint on the storage allows us to choose the capacity of the storage system.

Usually without increasing prices, the long term cost minimisation can be carried out by discounting the future costs, which models inflation and the fact that people are more interested in costs in the near future than those in the distant future. This discounting of the long term cost, reduces the tail end of the total cost to zero, resulting in a finite total cost as in [59, 62] for which an optimal solution can be found. In contrast, with arbitrary increase in prices that rise faster than the rate of inflation and unbounded cost per stage, the total cost of generation tends to be infinite for the above long term optimisation. Therefore to analyse this infinite horizon total infinite cost problem an alternative formulations in needed. This alternative approach uses the structure of the finite horizon solution to understand the infinite horizon solution. That is, instead of looking at the infinite sequence that solves a limiting problem, we look at the limit of the finite solution sequences of the finite horizon problem, subject to additional constraint on the terminal storage level of the finite horizon. Using these parameters, we will observe the structure of the finite horizon solution for a simple ideal storage device and show that the charging schedules with different terminal energy levels converge as the horizon $T \to \infty$ under certain conditions. This convergence as shown later, will allow us to study the behaviour of the finite horizon optimal solution and understand the behaviour of the infinite horizon optimal solution.

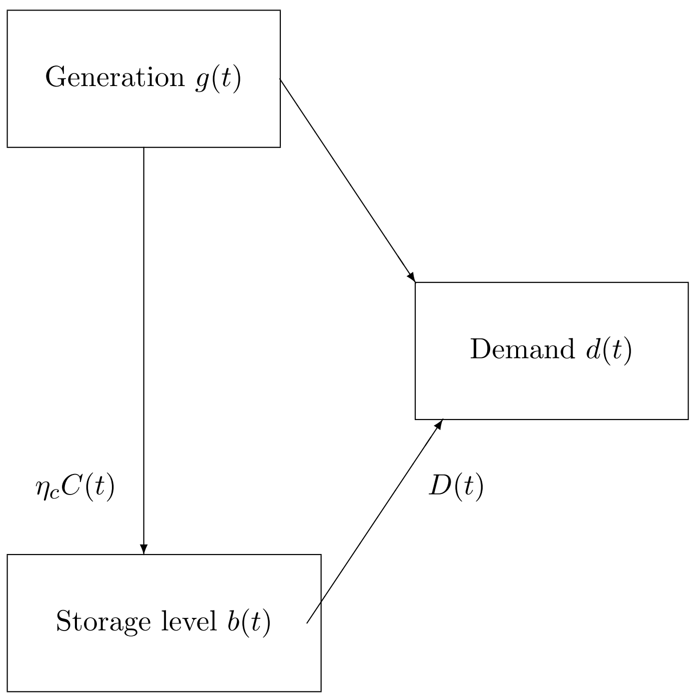

Figure 3.1: System model where the storage device with charging efficiency η_c and self-discharge β, draws an amount of power $C(t)$ or discharges $D(t)$ to satisfy the user demand $d(t)$, resulting in an energy level $b(t)$ in the battery. Here $g(t)$ is the amount of generation needed to satisfy both demand from the storage device and the user demand

Therefore in section 3.3, we present a finite horizon model for the above system shown in figure 3.1 for generation cost minimisation. Using this model, in subsequent sections, we will study the optimal solution and show structural properties of the optimal solution that will allow us to study the behaviour of the the long term charging and generation schedules when using ideal energy storage systems. Further, we will use the dynamic programming algorithm [10] to simulate this system and show numerically, the structural properties resulting from the optimal solution.

3.3 Model

In this section we present a model that can be used to solve the optimal storage scheduling problem discussed section 3.2. By optimally scheduling the charging($C(.)$) and discharging ($D(.)$) of a storage system with capacity B and storage level $b(.) \in [0, B]$, to satisfy user demand $d(.)$ as shown in equations (3.3)-(3.4); the model presented in this section aims to minimise the total generation cost given in equation (3.2), subject to the additional constraints on the generation, storage, charge and discharge levels in equations(3.5) - (3.12).

To elaborate further, consider user(s) with demand $d(t) \geq 0$, at each time slot t, and an energy storage device of capacity B, with charging efficiency $\eta_c \leq 1$ and self discharge loss factor β, as displayed in figure 3.1. If no charging or discharging occurs the energy loss in the storage is given by $b(t) = \beta b(t-1)$. Then, for each time slot t, this energy storage system draws power from the grid at a rate of $C(t) \geq 0$. This storage system is also able to satisfy the demand by discharging at a rate of $D(t) \geq 0$, from the available energy $b(t)$ stored in the battery, and the storage has a maximum charge and discharge rate of C_{max} and D_{max} respectively. Then, the total amount of power that is needed to satisfy the user demand and the demand from the energy storage is known as the generation $g(t)$ of the system. In the above system, the cost of drawing power from the grid is assumed to have the form $\gamma(t)N(g(t))$, for some time varying price $\gamma(.)$ and a nonlinear function $N(.)$, which is strictly convex in $g(.)$, modeling the fact that peak generation increases the power for the utility as well as the strain on the grid [15, 44].

The above setting then gives rise to an objective that requires the utility to minimise the operational cost of the system, provided the savings from the minimisation is passed from the utility to the user, as an incentive for the user to shift the demand by using a storage device.. Therefore a natural objective in minimising the generation cost would be,

$$\arg\min_{g} \sum_{t=1}^{\infty} \gamma(t) N(g(t)) \tag{3.1}$$

However, as mentioned in section 3.2, since we wish to study the long term scheduling behavior for a system with arbitrary price increase, the above objective leads to an infinite horizon infinite cost problem. As a result, instead of finding the solution to the limit of the above problem, we will instead find the limit of the solution as $T \to \infty$, for the finite horizon objective given below,

$$\arg\min_{g,b,C,D} \sum_{t=1}^{T} \gamma(t) N(g(t)) \tag{3.2}$$

Note that this is an offline problem with deterministic quantities, for which the storage dynamics are explained by the decision variables g, b, C, D, and it is not equivalent to solving the problem in equation (3.1). This is because a solution to the equation (3.1) does not exists for arbitrary varying prices. Then for the above mentioned system in figure 3.1, with non-ideal storage, the amount of energy $b(t)$ in the battery at each time slot is given by,

$$b(t) = \beta b(t-1) + \eta_c C(t) - D(t) \tag{3.3}$$

where $\eta_c C(t)$ of the power drawn is stored in the battery due to its charging inefficiency, and only $\beta b(t-1)$ of energy stored remains in the energy storage from the previous time slot due to the battery's self-discharge loss.

Then the system equation satisfying the user demand $d(t)$ and the storage demand is given as,

$$d(t) = g(t) - C(t) + D(t) \tag{3.4}$$

In the optimisation to follow, it will not be optimal to charge and discharge the storage device during a single time slot, and so $\min(C(t), D(t)) = 0$ for all t; this will be made precise in lemma 1 below. Then during each time slot, the power drawn from the grid is used either to satisfy the demand and charge the battery, or to discharge energy from the battery to satisfy the user demand according to equation (3.4).

Further, added to the above constraints on the power drawn and the storage level, the system is also subject to additional constraints on the maximum and minimum storage level, power input, power output and the minimum generation, which is given by,

$$b(t) \geq 0, \quad t < T \tag{3.5}$$

$$B - b(t)) \geq 0, \quad t < T \tag{3.6}$$

$$g(t) \geq 0 \tag{3.7}$$

$$C(t) \geq 0 \tag{3.8}$$

$$(C_{max} - C(t)) \geq 0 \tag{3.9}$$

$$D(t) \geq 0 \tag{3.10}$$

$$(D_{max} - D(t)) \geq 0. \tag{3.11}$$

Finally, since we wish to find the limits to the finite horizon solution, we also impose an additional constraint on the terminal energy level in the battery, which given by,

$$b(T) - bf = 0 \tag{3.12}$$

where $bf \in [0, B]$.

As a result, our aim is to minimise the total generation cost given by the objective equation (3.2) subject to constraints (3.3)-(3.12) for some time $t \in \{0, ..., T\}$.

Lemma 1. *For a storage device with charging inefficiency $\eta_c < 1$, $min(C(t), D(t)) = 0$, for any time $t \in (0, T)$.*

Proof. Let S be a storage device with capacity B, self-discharge $\beta = 1$ and charging inefficiency $\eta_c < 1$.

Now let the optimal storage schedule at some time $t \in (0, T)$ require the storage to change its energy level by some $x \in (0, B)$. i.e $b(t) - b(t-1) = x$, where $b(t)$ and $b(t-1)$ give the storage level at times t and $t-1$ respectively.

First consider a scenario in which the storage device charges $C(t)$ and discharges $D(t)$ at the same time $t \in (0, t)$, i.e $C(t) > 0$ and $D(t) > 0$ and its energy level $x \geq 0$. The other case when $x < 0$ is symmetric.

Then from equation (3.3) we get,

$$\eta_c C(t) - D(t) = b(t) - b(t-1) = x \tag{3.13}$$

whence

$$C(t) = (x + D(t))/\eta_c. \tag{3.14}$$

The above equation gives the amount of power that needs to be drawn from the grid by the storage device. Then, the generation $g_1^*(t)$, required at time t, with demand $d(t)$ is given by equation (3.4) as,

$$g_1^*(t) = d(t) + C(t) - D(t) \tag{3.15}$$

whence,

$$g_1^*(t) = d(t) + (x + D(t))/\eta_c - D(t) = d(t) + x/\eta_c + (1-\eta_c)D(t)/\eta_c. \tag{3.16}$$

Next consider a storage device which cannot charge and discharge at the same time, i.e $min(C(t), D(t)) = 0$. Then for a storage device that needs to increase its energy by x, at time t, $C(t) > 0, D(t) = 0$. Then equation (3.14) gives,

$$C(t) = x/\eta_c \tag{3.17}$$

and the generation $g_2^*(t)$ required from the grid is given as

$$g_2^*(t) = d(t) + C(t) - D(t) = d(t) + C(t) = d(t) + x/\eta_c \tag{3.18}$$

Comparing equations (3.16) and (3.18), we observe that $g_1^*(t) > g_2^*(t)$. Since our objective is to minimise the generation and the generation cost, as given by (3.2), we see that $g_2^*(t)$ would be the optimum generation at time t. Therefore, for a storage device with charging inefficiency $\eta_c < 1$, $min(C(t), D(t)) = 0$. $\square$

3.4 Optimal Solution Method

The optimisation problem, also known as the primal problem in section 3.3 with objective equation (3.2) subject to constraints (3.3)-(3.12), can be solved by applying the Karush-Kuhn-Tucker(KKT) conditions [13, 15] to the Lagrangian of the primal problem to find the optimal value of the objective (3.2),denoted by p^*. Here the KKT conditions give necessary conditions of stationarity, primal and dual feasibility and complementary slackness for the solution of primal problem to be optimal [13]. The complementary slackness conditions of the KKT are feasibility conditions that eliminate points which violate the boundary conditions given by the inequality constraints of the model 3.3. The dual feasibility of KKT conditions are feasible points for the dual of the primal problem. The dual problem of the primal problem is given by finding the best possible lower bound d^* on the Lagrange dual function (max{Lagrange dual function}) with $d^* \leq p^*$, taking into consideration the equality and inequality constraint of the original problem. Here the Lagrange dual function is given by taking the infimum of the Lagrangian which gives lower bounds on the optimal value of the primal problem [13].

Further, since our original problem in section 3.3 is strictly convex, strong duality holds for the primal and the dual, for any feasible point satisfying the KKT conditions [13]. This means that the solution to the dual is also the solution to the primal problem and $p^* = d^*$. As a result, we know that by applying the KKT conditions we are able to find the optimal expression for our energy storage problem. Therefore we first structure our original problem by augmenting the weighted sum of the constraints with its objective to give its Lagrangian, followed by using the KKT conditions to find the optimal solution for our problem. This allows us to analyse the solution obtained by using the KKT conditions to study the structure of the optimal behaviour of the original problem.

The Lagrangian of the objective and the constraints in section 3.3 is then given by,

$$
\begin{aligned}
L =& \sum_{t=1}^{T} \gamma(t) N(g(t)) + \sum_{t=1}^{T} \tilde{p}(t) \big[b(t) - \beta b(t-1) - \eta_c C(t) + D(t)\big] - \sum_{t=1}^{T} \tilde{\lambda}(t) g(t) \\
&+ \sum_{t=1}^{T} \tilde{q}(t) \big[d(t) + C(t) - D(t) - g(t)\big] - \sum_{t=1}^{T} \underline{b}(t) b(t) - \sum_{t=1}^{T} \underline{C}(t) C(t) \\
&- \sum_{t=1}^{T} \underline{D}(t) D(t) - \sum_{t=1}^{T} \bar{b}(t)(B - b(t)) - \sum_{t=1}^{T} \bar{C}(t)(C_{max} - C(t)) \\
&- \sum_{t=1}^{T} \bar{D}(t)(D_{max} - D(t)) + \tilde{e}(b(T) - F)
\end{aligned}
\tag{3.19}
$$

where the Lagrange multipliers assigned to the constraints are given by $\tilde{p}(t)$ for equation (3.3), $\tilde{q}(t)$ for equation (3.4), $\bar{b}(t)$ for equation (3.6), $\bar{C}(t)$ for equation (3.9), $\bar{D}(t)$ for equation (3.11), $\tilde{\lambda}(t)$ for equation (3.7), $\underline{b}(t)$ for equation (3.5), $\underline{C}(t)$ for equation (3.8), $\underline{D}(t)$ for equation (3.10) and $\tilde{e}$ for equation (3.12).

Next by differentiating the Lagrangian L with respect to $g(t), b(t), C(t)$ and $D(t)$ and applying stationarity conditions $dL/dg(t) = 0, dL/db(t) = 0, dL/dC(t) = 0, dL/dD(t) = 0$ the set of resulting equations can be written as,

$$\gamma(t) N^{'}(g^*(t)) - \tilde{q}^*(t) - \tilde{\lambda}^*(t) = 0 \tag{3.20}$$

$$\tilde{p}^*(t) - \beta \tilde{p}^*(t+1) \mathbf{1}(t < T) - \underline{b}^*(t) + \bar{b}^*(t) + \tilde{e}^* = 0 \tag{3.21}$$

$$\tilde{q}^*(t) - \eta_c \tilde{p}^*(t) - \underline{C}^*(t) + \bar{C}^*(t) = 0 \tag{3.22}$$

$$\tilde{p}^*(t) - \tilde{q}^*(t) - \underline{D}^*(t) + \bar{D}^*(t) = 0 \tag{3.23}$$

Next, by making the Lagrange dual variable $\tilde{q}^*(t)$ the subject, and subtracting equation (3.22) from equation(3.23), the expression representing the system equation can be written as,

$$\tilde{q}^*(t) = \frac{1}{2}[(1 + \eta_c)\tilde{p}^*(t) + \underline{C}^*(t) - \bar{C}^*(t) - \underline{D}^*(t) + \bar{D}^*(t)] \tag{3.24}$$

Similarly making $\tilde{p}^*(t)$ the subject of equation from solving(3.21) gives,

$$\tilde{p}^*(t) = \sum_{\tau=t}^{T-1} \beta^{\tau - t} \big[\underline{b}^*(\tau) - \bar{b}^*(\tau)\big]^+ + \tilde{e^*} \tag{3.25}$$

For the above problem the complementary slackness conditions from the KKT that apply for the inequality constraints are given by,

$$b^*(t)\underline{b}^*(t) = 0 \tag{3.26}$$

$$(B - b^*(t))\bar{b}^*(t) = 0 \tag{3.27}$$

$$C^*(t)\underline{C}^*(t) = 0 \tag{3.28}$$

$$(C_{max} - C^*(t))\bar{C}^*(t) = 0 \tag{3.29}$$

$$D^*(t)\underline{D}^*(t) = 0 \tag{3.30}$$

$$(D_{max} - D^*(t))\bar{D}^*(t) = 0 \tag{3.31}$$

$$g^*(t)\hat{\lambda}^*(t) = 0 \tag{3.32}$$

Here equations (3.26) and (3.27) provide values that are within the storage's maximum and minimum capacity, followed by the complementary slackness conditions in (3.28),(3.29),(3.30) and (3.31) which gives the lower bound and upper bound values for the charging and discharging power respectively. Finally equation (3.32) gives the generation feasible points that do not violate the lower bound of the generation.

Then, the optimal solution for our problem can be derived by substituting (3.24) and (3.25) in (3.20) and applying the primal feasibility condition $g^*(t) \geq 0$ and the complementary slackness condition (3.32) to give,

$$\gamma(t)N^{'}(g^*(t)) = \frac{1}{2}\big[(1+\eta_c)(\tilde{e^*} + \sum_{\tau=t}^{T-1} \beta^{\tau-t}(\underline{b}^*(\tau) - \bar{b}^*(\tau))) + \underline{C}^*(t) - \bar{C}^*(t) - \underline{D}^*(t) + \bar{D}^*(t)\big]^+ \tag{3.33}$$

as the dual formulation.

Here the left hand side of the equation represent the marginal generation cost and the right hand side of equation (3.33) shows the factors affecting the marginal generation cost. The right hand side of the equation shows, that future saturation and starvation of the storage device, its charging efficiency, self-discharge,charging and discharging constraints affect the scheduling decisions for the system when using energy storage.

Using this dual formulation, in sections 3.6, 4.4 and 5.4 we have analysed the structure of the optimal schedule for ideal and non-ideal storage systems. The dual formulation above has been used to prove monotonicity (2) of the charging and generation schedules. Further, the behaviour of the generation and charging schedules, such as fluctuation in generation due to inefficiency, exponential increase in generation caused by self-discharge has also been explained by using the dual formulation in equation (3.33).

3.4.1 Optimal Solution for an Ideal Energy Storage System

Let us first consider a system with an ideal energy storage device for the finite horizon. Then, for this device $\eta_c = 1$, $\beta = 1$ and $C_{max} = D_{max} = \infty$. That is, there are no charging or self-discharge losses or constraints on the maximum power drawn or discharged from the storage device. Then, the optimal solution for the dual in equation (3.33) becomes,

$$\gamma(t)N^{'}(g^{*}(t)) = \big[\sum_{\tau=t}^{T-1}(\underline{b}^{*}(\tau) - \bar{b}^{*}(\tau)) + \tilde{e^{*}}\big]^{+} \tag{3.34}$$

where $\gamma(t)N^{'}(g^{*}(t))$, gives the marginal cost of generation. Which is the change in total cost when the generation cost increases by one unit. Equation (3.34) shows that this marginal generation cost is affected by the Lagrange multipliers associated with the storage energy level. The lower bound on the storage with complementary slackness condition (3.26), is only active, when the storage fully discharges. Similarly, the upper bound of the storage constraint is active only when the storage is fully saturated, according to the slackness conditions in equation (3.27). Then, the right hand expression in equation (3.34) shows, that the storage has to anticipate future saturation and starvation of the storage system when deciding the optimal generation, similar to the optimal solution by Chandy et al. [15]. But, since our optimal solution does not have a holding cost for the storage level as in [15], the optimal marginal cost will be constant while the energy level in the storage $b^{*}(t) \in (0, B)$, but will change when the storage saturates or empties. To be exact, the storage decides to discharge when the marginal generation is high after saturation, and similarly charges after fully discharging which indicates a decrease in the marginal generation cost.

Therefore when $\gamma(.)$ is constant, due to the convexity of the generation cost $N'(.)$ in $g^{*}(.)$, the generation will also have the same scheduling behaviour as the marginal generation cost. That is, the generation is constant when $b^{*}(t) \in (0, B)$, and the generation increases when the battery fully saturates and decreases when the energy storage is fully discharged.

For the ideal energy storage system solution given by equation (3.34), the value of the

Lagrange multipliers $\underline{b}^*, \bar{b}^*, \tilde{e^*}$ are not known for each time $t \in [0, T]$. However, based on the complementary slackness conditions (3.26) and (3.27), we are able to determine the behaviour of the charging schedule. As a result, to numerically simulate the behaviour of the optimal charging schedule for storage systems, we use the Dynamic programming algorithm, which is able to give us the scheduling behaviour that minimises the total generation cost by charging and discharging the storage system as explained in section 3.5 below.

3.5 Dynamic Programming

To simulate the energy storage problem, we have formulated a Dynamic Programming(DP) algorithm that solves the storage model by considering the storage characteristics, generation and the demand of users in the power grid. Dynamic programming constructs its optimal solution for the initial problem by finding the optimal solution for each sub-problem. That is by solving smaller parts of a larger problem and then combining it to provide the solution for the overall problem. Usually, with finite horizon problems, the DP algorithm is applied to the tail sub-problem, or the final stage of the problem at the end of the horizon since the final state to the system is usually known or specified [10]. Then DP iterates backwards solving each sub-problem until it reaches the initial state. Therefore with DP, it is only necessary to know the the cost at the current state and the optimal cost of moving from the current state to the next state, which is given by applying Bellman's equation [10].

$$J_k(x_k) = \min\{cost_N(x_N) + \sum_{i=k}^{N-1} cost_i(x_i)\} \tag{3.35}$$

where the minimum cost is taken across all control policies and the average over all random disturbance, which in our case is the demand. The above equation gives the cost-to-go $J(.)$ from a particular state which is defined as the optimal cost for a $(N - k)$ stage problem starting at some state x and time $k \in (0, N)$ with a horizon time of N. In equation (3.35), the cost-to-go $J(x)$ at a particular state x and time k is given by, minimising the overall sum of the terminal cost at time N and the sum of the costs at being in some state x at each time moving backwards from $N - 1$ to k.

In our case, this would mean that the DP algorithm finds the minimum generation cost during each time step t of the horizon so that it can minimises the total generation cost. However, instead of applying the DP algorithm backwards, from the end of the horizon to the start of the horizon as in equation (3.35), we have chosen to implement the forward DP algorithm as described in [10]. According to Bertsekas [10], the optimal path from some point $p1$ to $p2$ in reverse is also optimal. Therefore with forward DP we will begin from the start of the horizon and find the optimal cost recursively for moving from the current state to the next state until the end of the horizon.

The DP algorithm evolves according to the state of the equation depending on the given input and the control (decisions) applied to the system, which results in an optimal solution to give the best path, or in our case the minimum cost. For our problem of optimal scheduling of energy storage, we define the system parameters as follows,

- **State:** The energy level in the battery $b(t)$ and $b(t+1)$ which is the output of the system once the control and disturbance is applied.

- **System Equation**: $b(t+1) = f(b(t), g(t), d(t))$, where t is the time or the stage of the system with time horizon T.

- **Decision Variable**: The generation of the system $g(t)$, which controls the amount of generation

- **Input to the system**: The demand of the system $d(t)$

- **Optimal Solution**: The Generation schedule for the applied parameters. Using this solution and the system equation we can get the charging schedule for the energy storage.

The workings of the forward DP algorithm that finds the optimal generation and charging schedules for some time horizon T, with terminal storage level $b(T)$ is given below.

Algorithm 1 Forward DP algorithm for finite horizon generation cost minimisation, equations (3.2)-(3.12)

▷ %Comment: input into algorithm-: initial storage level, final storage level, time horizon, storage capacity, price γ, demand, storage level discritisation%
input($b(0)$, $b(T)$, T , B , $price(.)$, $d(.)$,Num_Levels)
▷ %Optimal cost array per time slot%
$optimal\_cost[T] = 0$
$initial\_index = 1$
▷ % Find minimum optimal cost of generation at start of horizon for each storage level in array $b(.)$ and initial storage level $b(0)$. Here j and i are iterative indexes for the current and next storage level in $b(.)$
for j **do** = 1:Num_Levels
  $g(j) = d(1) + b(j) - b(0)$
  $optimal\_cost = price(1) * g(j)^2$
end for
▷ % Moving forward in time, find minimum generation cost per stage for each time step until time $T - 1$%
for t=2:T-1 **do**
▷ % The minimum generation is found iteratively for each storage level from zero to maximum capacity B%
  for j = 1:Num_Levels **do**
    for i = 1:Num_Levels **do**
▷ % The generation is calculated for each storage level from zero to maximum capacity B%
      $g(i) = d(t) + b(j) - b(i)$
      $cost\_per\_stage(i) = price(t) * g(i)^2$
    end for
▷ % Find the total minimum cost until time t %
    $minimum\_cost(j) = \min(costper\_stage + optimal\_cost)$
▷ % The $index\_of\_minimum$ matrix stores the index of storage value with minimum cost %
    $index\_of\_minimum(j, t-1) = index(costper\_stage + optimal\_cost)$
  end for
▷ % Store the new array of total minim cost per stage as the current optimal cost %
  $optimal\_cost = minimum\_cost$
end for
▷ % Find the minimum cost per stage and total minimum cost of generation at end of horizon%
for i **do** = 1:Num_Levels
  $g(i) = d(T) + b(T) - b(i)$
  $cost\_per\_stage(i) = price(N) * g(i)^2$
  $minimum\_cost(1) = \min(cost\_per\_stage + optimal\_cost)$
  $index\_of\_minimum(j, T-1) = index(cost\_per\_stage + optimal\_cost)$
  $total\_optimal\_cost = minimum\_cost(1)$
end for
▷ %Find optimal storage and generation schedule by iterating backwards from $b(T)$%
for r **do** = 1:T-1
  $initial\_index = index\_of\_minimum(initial\_index, T - r))$
  $b * (T - r) = b(initial\_index)$
  $g^*(T - r) = d(T - r) + b * (T - r) - b^*(T - r - 1)$
end for

3.6 Structure of Optimal Solution

Since the infinite horizon total cost can be infinite with arbitrarily increasing prices, the alternative method suggested in section 3.2, is to analyse the solutions of the finite horizon problem as $T \to \infty$. Accordingly, in this section we investigate the structural properties of the finite horizon scheduling solutions for different terminal battery levels, and show that under certain conditions, the charging schedule converges in finite time. That is, under certain conditions, any optimal storage schedule $(b_1^*, b_2^*, b_3^*..)$ having different terminal storage levels $(b_1^T, b_2^T, b_3^T...)$ at some time T, will converge to a storage schedule b_n^* at some time t, where $t \in (0, T)$ and $b^*(t) = 0$ or $b^*(t) = B$. This result allows us to decouple the infinite horizon optimisation into multiple finite horizon problems and observe the behaviour of the optimal schedule by using the finite horizon solution under certain conditions.

In this section, we first show that the storage schedule is monotonic with respect to the terminal storage level for an ideal storage device with $\eta_c = 1$ and $\beta = 1$. Secondly we use the monotonicity results of the schedules to show that convergence occurs under certain conditions. This allows us to use the finite horizon solutions to study numerically using dynamic programming the behaviour of the charging and generation schedule. Further, in Chapters 4 and 5 we will also show numerically, that convergence occurs and renewal points exists under the same conditions in this section, even when the storage device has changing inefficiency and self-discharge.

The theorems and lemmas presented below are for an ideal storage device with $\eta_c = 1$, $\beta = 1$, $C_{max} = \infty$ and $D_{max} = \infty$.

3.6.1 Monotonicity

Let $b_x^T(t)$ be a solution to (3.2) - (3.12), where T is the horizon of the solution and x is the terminal storage level of the storage device. So if $\lim_{T\to\infty} b_x^T(t)$ exists and is independent of x, then we can define the optimal battery occupancy to be

$$b^*(t) = \lim_{T\to\infty} b_x^T(t). \tag{3.36}$$

Then since $b(.)$ uniquely defined $g(.)$, this also characterizes the generation schedule. Based on these parameters, the following subsection gives the monotonicity lemmas and theorems.

Let b_1^* be the optimal charging schedule given $b_1(T) = bf_1$ and b_2^* be the optimal charging schedule given $b_2(T) = bf_2$, where bf_1, bf_2 are two terminal storage levels for a time horizon T. Then Theorem 2, shows that both the optimal schedules b_1^*, b_2^* are monotonic in the terminal storage level bf.

Theorem 2. *For any $bf_1, bf_2 \in [0, B]$ with $bf_1 < bf_2$, we have that $b_1^*(t) \leq b_2^*(t)$ for all $t \in [0, T]$.*

Proof. Since $bf_1 < bf_2$, the optimal solution of b_1^* b_2^* gives, $b_1^*(T) < b_2^*(T)$. Let us consider a time $t \in [0, T]$ which is the last time that $b_1^*(t) = b_2^*(t)$. Such a time exists since we know that $b_1(0) = b_2(0)$. Then, from Lemma 3 below we know that $b_1^*(t^{'}) = b_2^*(t^{'})$ for all $t^{'} \in [0, t]$. Also since we know that there is no such $\tau \in [t+1, T]$, that $b_1^*(\tau) = b_2^*(\tau)$, Lemma 4 states that $b_1^*(\tau) < b_2^*(\tau)$. Then from Lemmas 3 and 4 below we see that b_1^* and b_2^* is monotonic in bf (i.e $b_1^*(t) \leq b_2^*(t)$).

□

Lemma 3. *For any $bf_1, bf_2 \in [0, B]$, if $b_1^*(t) = b_2^*(t)$ for some $t \in [0, T]$, then $b_1^*(t^{'}) = b_2^*(t^{'})$ for all $t^{'} \in [0, t]$.*

Proof. We prove by that $b_1^*(t) = b_2^*(t)$ induction downward from t. Inductive steps: $b_1^*(t) = b_2^*(t)$ implies $b_1^*(t-1) = b_2^*(t-1)$.

Let $B_1(t+1)$ and $B_2(t+1)$ be the total generation cost from time $t+1$ to T, where $t \in [0, T-1]$, and $b_1^*(t) = b_2^*(t) = A$, with $A \in [0, B]$. The cost of generation at time t is in the form $\gamma(t)N(g^*(t))$ from the objective equation (3.2). Then the cost for b_1^* and b_2^* can be expressed as,

$$\gamma(t)N(g_1^*(t)) = \gamma(t)N(b_1^*(t) - b_1^*(t-1) + d(t)) = \gamma(t)N(A - b_1^*(t-1) + d(t)) \quad (3.37)$$

and

$$\gamma(t)N(g_2^*(t)) = \gamma(t)N(b_2^*(t) - b_2^*(t-1) + d(t)) = \gamma(t)N(A - b_2^*(t-1) + d(t)) \quad (3.38)$$

respectively. Furthermore, we know that the prefix up to time t of an optimal solution, is also optimal as in Dynamic Programming. Then, if $b_1^*(t-1), b_1^*(t), ..., bf_1$ is an optimal path to bf_1, $b_1^*(t-1), b_2^*(t), ..., bf_2$ is an optimal path to bf_2, since $b_1^*(t) = b_2^*(t)$. Therefore the cost equations for the optimal solutions can be written as,

$$\gamma(t)N(b_1^*(t) - b_2^*(t-1) + d(t)) = \gamma(t)N(A - b_2^*(t-1) + d(t)) \tag{3.39}$$

and

$$\gamma(t)N(b_2^*(t) - b_1^*(t-1) + d(t)) = \gamma(t)N(A - b_1^*(t-1) + d(t)) \tag{3.40}$$

respectively.

Next let us assume to obtain a contradiction that $b_i^*(t-1) < b_j^*(t-1)$, where $i, j \in \{1, 2\}$, and $i \neq j$, then the total cost from time t to T for b_i^* by using equations (3.37) and (3.39) is given by,

$$B_i(t+1) + \gamma(t)N(A - b_i^*(t-1) + d(t)) \tag{3.41}$$

and

$$B_i(t+1) + \gamma(t)N(A - b_j^*(t-1) + d(t)) \tag{3.42}$$

Then by comparing equation (3.41) and (3.42) and using the fact that N is strictly increasing we get,

$$B_i(t+1) + \gamma(t)N(A - b_i^*(t-1) + d(t)) > B_i(t+1) + \gamma(t)N(A - b_j^*(t-1) + d(t)) \tag{3.43}$$

The above equation shows that it is optimal for b_i^* to be at $b_j^*(t-1)$ at $t-1$ instead of $b_i^*(t-1)$. This contradiction implies that for optimality, at time $t-1$, $b_1^*(t-1) = b_2^*(t-1)$ as required. $\square$

Lemma 4. *For any $bf_1, bf_2 \in [0, B]$ with $bf_1 < bf_2$ and any $\tau \in [0, T]$, if there is no $t \in [\tau, T]$, such that $b_1^*(t) = b_2^*(t)$, then $b_1^*(t) < b_2^*(t)$ for all $t \in [\tau, T]$.*

Proof. (Proof by Contradiction) Since there is no t such that $b_1^*(t) = b_2^*(t)$, then the only way for Lemma 4 to be false is if there is a t for which $b_1^*(t) < b_2^*(t)$ and $b_1^*(t-1) > b_2^*(t-1)$.

Let $J_1(t)$, and $J_2(t)$ be the optimal costs for b_1^* and b_2^* respectively from time $[0, t-2]$, and $B_1(t)$,$B_2(t)$ be the optimal costs for b_1^* and b_2^* respectively from time $[t, T]$ and $b_1^*(0) = b_2^*(0)$. We will now define costs $N\{i, j\}$ for $i, j \in \{1, 2\}$, as the cost of going from $b_j(t-1)$ to $b_i(t)$. Equation (3.2) gives the optimal cost from time $[t-1, t]$ for b_1^* and b_2^* as $\gamma(t)N(g_1^*(t))$ and $\gamma(t)N(g_2^*(t))$ respectively. Then, by substituting the constraint equation (3.3) for g^*, we can express the cost functions as,

$$\gamma(t)N(g_1^*(t)) = \gamma(t)N(b_1^*(t) - b_1^*(t-1) + d(t)) \equiv \gamma(t)N\{1,1\} \tag{3.44}$$

and

$$\gamma(t)N(g_2^*(t)) = \gamma(t)N(b_2^*(t) - b_2^*(t-1) + d(t)) \equiv \gamma(t)N\{2,2\} \tag{3.45}$$

Additionally, the cost from $b_1^*(t-1)$ to $b_2^*(t)$ at time t and the cost from $b_2^*(t-1)$ to $b_1^*(t)$ at time t can be expressed as,

$$\gamma(t)(b_2^*(t) - b_1^*(t-1) + d(t)) = \gamma(t)N\{2,1\} \tag{3.46}$$

and

$$\gamma(t)N(b_1^*(t) - b_2^*(t-1) + d(t)) = \gamma(t)N\{1,2\} \tag{3.47}$$

respectively.

Now the total cost for b_1^*, and b_2^* to follow is original paths are given by,

$$J_1(t) + \gamma(t)N\{1,1\} + B_1(t) \tag{3.48}$$

and

$$J_2(t) + \gamma(t)N\{2,2\} + B_2(t) \tag{3.49}$$

respectively.

Further, also consider the total costs for two alternate schedules in which b_1^* crosses over to the path of b_2^* and b_2^* crosses over to the path of b_1^* after time $t-1$ given by,

$$J_1(t) + \gamma(t)N\{1,2\} + B_2(t) \tag{3.50}$$

and

$$J_2(t) + \gamma(t)N\{2,1\} + B_1(t) \tag{3.51}$$

respectively.

Then, if the original path is optimal, the total optimal cost of the original path should be better than the alternate path for of b_1^*, and

$$J_1(t) + \gamma(t)N\{1,1\} + B_1(t) < J_2(t) + \gamma(t)N\{2,1\} + B_1(t) \tag{3.52}$$

Similarly if the original path for b_2^* is optimal, then the total optimal cost for the original path should be better than the alternative path, then

$$J_2(t) + \gamma(t)N\{2,2\} + B_2(t) < J_1(t) + \gamma(t)N\{1,2\} + B_2(t) \tag{3.53}$$

Next by adding equations (3.52) and (3.53) we get a cost relationship,

$$\begin{gathered}(J_1(t) + J_2(t) + B_1(t) + B_2(t)) + \gamma(t)N\{1,1\} + \gamma(t)N\{2,2\} < \\ (J_1(t) + J_2(t) + B_1(t) + B_2(t)) + \gamma(t)N\{1,2\} + \gamma(t)N\{2,1\}\end{gathered} \tag{3.54}$$

Whence,

$$\gamma(t)N\{1,1\} + \gamma(t)N\{2,2\} < \gamma(t)N\{1,2\} + \gamma(t)N\{2,1\} \tag{3.55}$$

Now let's also consider some $x, y \in R^n$, and let $X < \min(x,y)$ and $Y > \max(x,y)$ and $X + Y = x + y$. Then we can write x, y in terms of X, Y as,

$$x = X + \delta(Y - X) = (1-\delta)X + \delta Y \qquad \delta \in (0,1) \tag{3.56}$$

and

$$y = (X + Y) - x = \delta X + (1-\delta)Y \tag{3.57}$$

Since the cost function in equation (3.2) is strictly convex, we can write the costs $N(x), N(y)$ as,

$$N(x) < (1-\delta)N(X) + \delta N(Y) \tag{3.58}$$

and

$$N(y) < \delta N(X) + (1-\delta)N(Y) \tag{3.59}$$

Whence

$$N(x) + N(y) < (1-\delta)N(X) + \delta N(Y) + \delta N(X) + (1-\delta)N(Y) = N(X) + N(Y) \quad (3.60)$$

Now by hypothesis $b_1^*(t-1) > b_2^*(t-1)$ and $b_1^*(t) < b_2^*(t)$. Then if $X = b_1^*(t) - b_1^*(t-1) + d(t)$ and $Y = b_2^*(t) - b_2^*(t-1) + d(t)$ and $\{x, y\} = \{b_1^*(t) - b_2^*(t-1) + d(t), b_2^*(t) - b_1^*(t-1) + d(t)\}$, equations (3.47), (3.56) and (3.46), (3.57) hold for the given X, Y, x, y.

Also note that the only way $X = x$ or $x = y$ is if $b_1^*(t) = b_2^*(t)$ or $b_1^*(t-1) = b_2^*(t-1)$, which is false by hypothesis. Therefore the strict inequality in equation (3.60) holds. Then by applying the same inequality as equation (3.60) to equations (3.44), (3.45),(3.47) and (3.46) we get an cost relationship equation for the period $t \in [0, t]$ as,

$$\gamma(t)N\{1,2\} + \gamma(t)N\{2,1\} < \gamma(t)N\{1,1\} + \gamma(t)N\{2,2\} \quad (3.61)$$

which contradicts the original cost relationship in equation (3.55)

Therefore it is not optimal for the battery to crossover at any time $t \in [0, T]$. Then for any time t, $b_1^*(t) < b_2^*(t)$ as required. □

3.6.2 Convergence of Finite Horizon Solutions and Renewal Points

Let b_k^τ be the optimal solution to a problem with some end battery level $k \in [0, B]$, and horizon length τ. In this section we establish that theorem 7 below shows that if the optimal schedule with terminal battery level $b(T) = 0$, saturates above ($b^*(t) = B$), or if the optimal schedule with terminal battery level $b(T) = B$, empties below ($b^*(t) = 0$) at some time $t \in (0, T)$, then both the optimal schedules will be the same at time t. As a result, the optimal schedule for any time $t' \leq t$, will also be the same. Even when the horizon is extended to some time T', using lemmas 5 and 6, theorem 7 shows that the optimal schedule before t remains the same. Therefore, we address this time or point t as a renewal point or more accurately a quasi-renewal point for a lookahead time T, since extending the horizon to T', does not affect the scheduling decisions before t.

A quasi-renewal point differs from a renewal point, since for a renewal point, the storage levels after time t where the renewal occurs, does not affect the renewal process, and any future changes in storage level does not affect the scheduling decisions for any time before t. However, for a quasi-renewal point, the storage levels up to a look ahead time $T > t$

is required and hence, it is only any change in storage level after time T that does not affect the storage schedule before the renewal time t. Thus, using the above structure we study the properties of the infinite horizon, infinite total cost problem by using the finite horizon solution having renewal points for a certain lookahead horizon.

Finally, proposition 8 and lemmas 6 and 5 state that convergence occurs if and only if the solution ending with a full battery saturates below or the solution ending with an empty battery saturates above. This means that convergence will not occur when $b^*(t) \in (0, B)$. This can be explained by the complementary slackness conditions (3.26) and (3.27), for which the dual variables $\underline{b}^*(t)$ and $\bar{b}^*(t)$ are slack when $b^*(t) \in (0, B)$. Therefore, the convergence results are based on the structural property of the slackness conditions for which, convergence can only occur when the storage level $b^*(t) = 0$ or $b^*(t) = B$. In conclusion both theorem 7 and proposition 8 show that convergence occurs in finite time provided b_1^* saturates above or b_2^* saturate below.

The theorems and lemmas below give structural properties for the convergence of the finite horizon schedule as discussed above.

Lemma 5. *If b_B^T saturates below at some time t, then the optimal solution to any problem b_j^T, where $j \in [0, B)$, also saturates below at time t, and $b_B^T(t') = b_j^T(t')$ for all time $t' \leq t$.*

Proof. Consider the optimal solutions to two problems, one with $x = B, b_B^T$ and another with $x = j < B, b_j^T$ with time horizon length T. At some time $t \in [0, T]$, if $b_B^T(t) = 0$, then at time $t, b_j^T(t) = 0$ by Theorem 2 (i.e due to monotonicity). Then by Lemma 3 we know that $b_B^T(t) = b_j^T(t)$, for all $t^{'} \leq t$ □

Lemma 6. *If b_0^T saturates above at some time t, then the optimal solution to any problem b_i^T, where $i \in (0, B]$, also saturates above at time t, and $b_0^T(t^{'}) = b_i^T(t^{'})$ for all time $t' \leq t$.*

Proof. Consider the optimal solutions for two problems, one with $x = 0, b_0^T$ and another with $x = i > 0, b_i^T$ with time horizon length T. At some time $t \in [0, T]$ if $b_0^T(t) = B$, then at that time $b_i^T(t) = B$, due to monotonicity and Lemma 3, we know that $b_0^T(t) = b_i^T(t)$, for all $t^{'} \leq t$. □

Theorem 7. *If $b_B^T(t) = B$ or $b_0^T(t) = 0$, for some $t \in [0, T]$. Then for all $T^{'} \geq T$, $b_B^{T'}(t') = b_k^{T'}(t')$ and $b_0^{T'}(t') = b_k^{T'}(t')$ for all $t^{'} \leq t$ and consequently, $g_B^{T'}(t') = g_k^{T'}(t')$ and $g_0^{T'}(t') = g_k^{T'}(t')$*

Proof. Given that b_B^T saturates below at time t, consider a time a horizon of length T, where the optimal solutions for two problems are b_B^T and b_k^T. Here $b_B^T(T) > b_k^T(T)$, and $k \in [0, B)$. Then from Lemma 5, we know that $b_B^T(t^{'}) = b_k^T(t^{'})$, for all $t^{'} \leq t$. Next consider an extended horizon up to some time $\tau = T'$, where $T' \geq T$. Then the optimal solutions for the two problems for the extended horizon are given by $b_B^{T'}$ and $b_k^{T'}$ with terminal battery levels B, k respectively, and $b_B^{T'}(T') > b_k^{T'}(T')$. Then at time T, the battery levels are $b_B^{T'}(T), b_k^{T'}(T) \in [0, B]$, and from Lemma 5 we know that for any battery capacity at time T of $b_k^{T'}$, it is optimal to saturate below at time t, giving $b_B^{T'}(t) = b_k^{T'}(t)$. Then using Lemma 3 we get $b_B^{T'}(t') = b_k^{T'}(t')$, for all $t' \leq t$.

Similarly if we consider a time horizon of length T, and the optimal solutions for two problems b_0^T and b_k^T, where $b_0^T(T) < b_k^T(T)$, and $k \in (0, B]$, given that b_0^T saturates above at time t, and extended this problem also to a time T' as above. The optimal solutions to the problems are also in the form $b_0^{T'}$ and $b_k^{T'}$. Where $b_0^{T'}(T') < b_k^{T'}(T')$, and at time $T, b_0^{T'}(T), b_k^{T'}(T) \in [0, B]$. Then from Lemma 6 we know that for any battery level at time $T(b_k^{T'})$, it is optimal to saturate above at time t. This gives $b_0^{T'}(t) = b_k^{T'}(t)$, resulting in $b_0^{T'}(t') = b_k^{T'}(t')$, for all $t' \leq t$ by applying Lemma 3.

Also note that at some time $\bar{t}$ where, $T \leq \bar{t} < T'$, if $b_B^{T'}$ saturates below at time $\bar{t}$. Then by Lemma 3, $b_B^{T'}(\bar{t}) = b_k^{T'}(\bar{t})$ and $b_B^{T'}(t') = b_k^{T'}(t')$, for all $t' \leq \bar{t}$, or if or $b_0^{T'}$ saturates above at time $\bar{t}$ $b_0^{T'}(\bar{t}) = b_k^{T'}(\bar{t})$ and $b_0^{T'}(t') = b_k^{T'}(t')$, for all $t' \leq \bar{t}$. So Theorem 7 holds for any $t' \leq t$.

Finally, since $b_B^{T'}(t') = b_k^{T'}(t')$ or $b_0^{T'}(t') = b_k^{T'}(t')$, by applying equations (3.3) and(3.4) the generation also converges giving $g_B^{T'}(t') = g_k^{T'}(t')$ or $g_0^{T'}(t') = g_k^{T'}(t')$, for all $t^{'} \leq t$

□

Proposition 8. *If* $t \in (0, T)$ *is the last point such that* $b_B^T(t) = b_0^T(t)$*, then either* $b_B^T(t) = 0$ *or* $b_0^T(t) = B$*.*

Proof. (Proof by Contradiction) The only way that Lemma 8 can be false is if $b_B^T(t) = b_0^T(t) \in (0, B)$.

Let $t_s \in [0, t)$ be a point where both $b_B^T = b_0^T$, which must exist since $b_B^T = b_0^0$. Also let $t_{bound} \in (t, T]$ be the first point where either $b_B^T(t_{bound}) = B$ or $b_0^T(t_{bound}) = 0$, which exists since $b_B^T(T) = B$ and $b_0^T(T) = 0$. At time t from equation (3.34) the marginal generation cost of both b_B^T and b_0^T is given by.

$$\gamma(t)N^{'}(g_0^*(t)) = \big[\sum_{\tau=t}^{T-1}(\underline{b_0}^*(\tau) - \bar{b_0}^*(\tau)) + \hat{e_0}^*\big]^+ \tag{3.62}$$

$$\gamma(t)N^{'}(g_B^*(t)) = \big[\sum_{\tau=t}^{T-1}(\underline{b_B}^*(\tau) - \bar{b_B}^*(\tau)) + \hat{e_B}^*\big]^+ \tag{3.63}$$

Also from the complementary slackness equations (3.6) and (3.5) we have that $\underline{b}^*, \bar{b}^*$ are inactive when $b^*(t) \in (0, B)$. Therefore for any time $t_u \in (t_s, t_{bound})$, the marginal generation cost in equation (3.62) and (3.63) are constant. So if at time t, $b_B^T(t) = b_0^T(t)$, by Theorem 7 and equation (3.3), $g_B^*(t) = g_0^*(t)$. Further, since the marginal generation cost is constant for any time $t_u \in (t_s, t_{bound})$, the generation at any t_u is given by $g_B^*(t_u) = g_0^*(t_u)$ and so $b_B^T(t_u) = b_0^T(t_u)$. Hence b_0^T, b_B^T cannot converge for any $b^*(t) \in (0, B)$. □

In conclusion the structural results show that convergence occurs at some finite lookahead T, provided the storage fully saturates at some time $t \in (0, T)$ for a charging schedule with terminal storage level $b(T) = 0$; or if the storage level fully discharges at some time $t \in (0, T)$, for a schedule with terminal storage level $b(T) = B$. This point t at which saturation or emptying occurs is known as a renewal point, and for any time $t' \leq t$ before the renewal point, both the charging and generation schedules will remain the same. Moreover, even when the lookahead is extended to some $T' > T$, the future changes in demand and pricing will not change the renewal point, yielding the same scheduling decisions for any time before the renewal point. Therefore, since future conditions such as demand changes and price fluctuations beyond the renewal point do not affect the current optimal action, the finite horizon solution can be decoupled to study the long term scheduling decisions for energy storage and generation.

3.7 Numerical Results

The optimum charging and generation schedule that minimises the generation cost was simulated by implementing the dynamic programming algorithm in Mathlab, with the optimisation carried out for both household and aggregate utility data. In this section we simulate the structural properties and show that renewal points exist when the optimal charging schedule for the storage ending full, saturates below, and the optimal charging schedule for the storage ending empty fully charges. Moreover by extending horizon we also show that future changes in demand beyond a given lookahead do not affect the scheduling decisions before the renewal point.

3.7.1 Data Set

We have used both household and aggregate price and demand utility data as input in optimising the storage and generation schedules. To simulate the energy storage problem we use real-time 30 minute aggregate state demand (MW) and pricing data($/MWh) in 2012 from the Australian Energy Market operator (AEMO). The demand and pricing data used for the simulations in this thesis are taken from the state of NSW (New South Wales) and VIC (Victoria) during the months of March and July respectively. For the household data, we have used individual household demand data taken from the Energy Disaggregation Research data set [36]. The demand data set has been recorded for 10 real households named as {house 1,2,...,10} for 119 days. The data recorded for the household uses the power data which has been recorded at intervals of 1s. We used the 1s data and taken the average demand for each household for 30 minute time slots.

For all of our simulations we assume that our cost $N(.)$ is quadratic and in the form $N(g) = a_0 + a_1 g + a_2 g^2$ for $a_2 > 0$ similar to the assumptions by Chandy et al. in [15]. Furthermore, our simulations use discrete charge levels $b^*(t) \in [0, B]$, where B is the storage capacity. The influence of this discretisation is visible for the generation schedule, especially during periods where the generation remains constant as explained in section 3.4.1.

In this as well as subsequent chapters we use the above mentioned data set and parameters for the simulations, which will be used to study and discuss the structural properties of the scheduling decisions when using energy storage.

3.7.2 Structural Properties of the Charging and Generation Schedules with Constant γ

Figures 3.2 and 3.4 show the charging and generation schedule of the 10 day horizon for house1 using a 1kWh storage device. Here $bf1$ and $Generation1$ show the charging and generation schedules when the storage level $b(T) = 0$, followed by $bf2$ and $Generation2$ which gives the respective charging and generation schedules when the storage level $b(T) =$

B. Figure 3.2 shows that the last renewal point occurs on the 9th day, when $bf1$ saturates above. Further on the same day, even when $bf1$ empties below just after the renewal point, we can see that $bf2$ stays above $bf1$. This is due to the monotonicity of the schedules in $b(T)$. So due to the monotonicity and the convergence on the 9th day, it is clearly visible that both $bf1, bf2$ have the same charging schedule before the renewal point, which is also true for the schedule in figure 3.4 which shows convergence of the generation schedule until day 9 of the horizon.

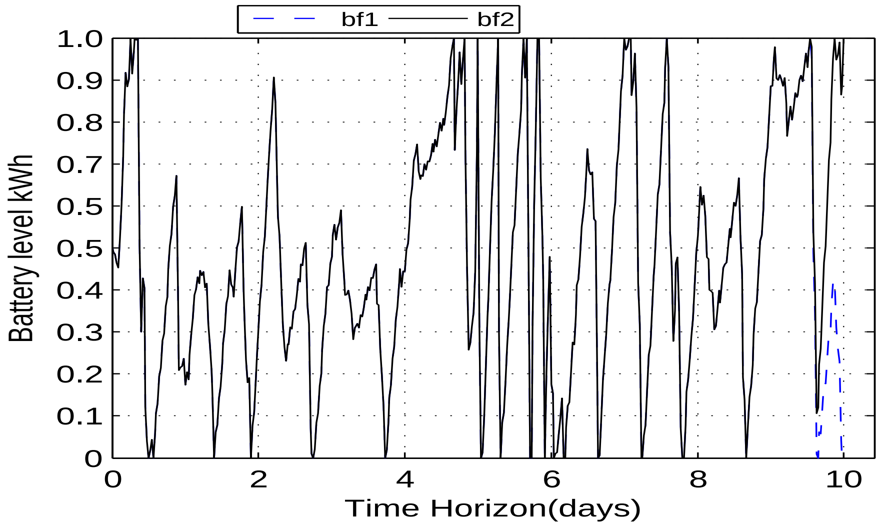

Figure 3.2: Charging schedule of house1 for a 10 day horizon using a 1kWh storage system

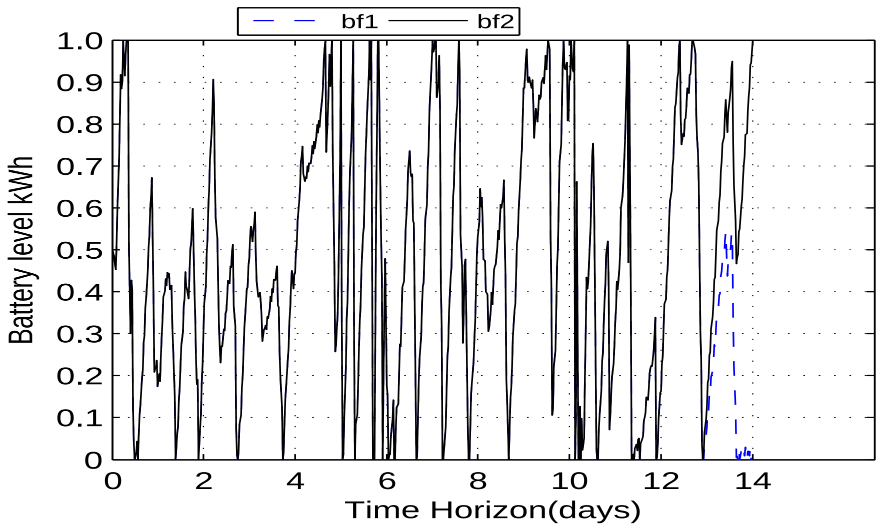

Figure 3.3: Charging schedule of house1 for a 14 day horizon using a 1kWh storage system

This behaviour is also visible for the aggregate NSW state data showing the 20 day charging and generation schedules for a 22500MWh storage system in figures 3.6 and 3.7 respectively. For the state data, the last renewal point can be seen on the 18th day, when

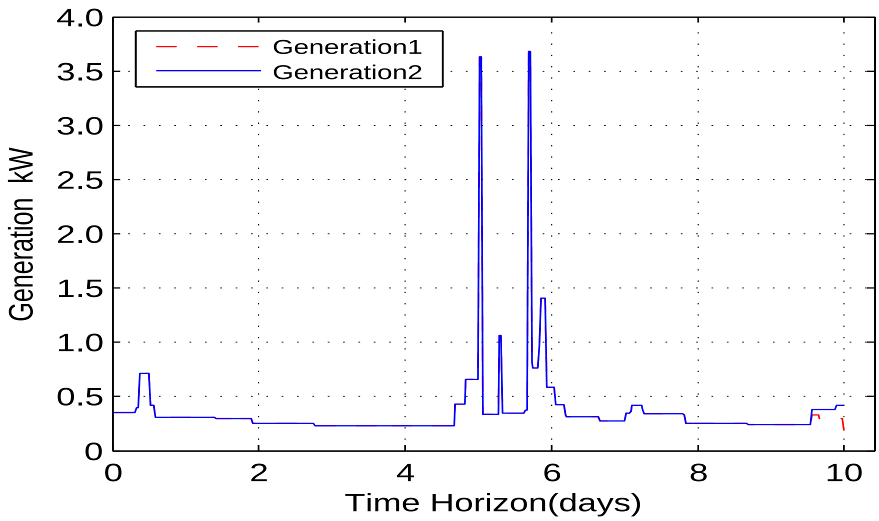

Figure 3.4: Generation schedule of house1 for a 10 day horizon using a 1kWh storage system

the storage level saturates above at $B = 22500MWh$. Therefore, the charging schedule in figure 3.6, and the generation schedule in figure 3.7 have the same solution for both $bf1$,$bf2$ and $Generation1$, $Generation2$ respectively, until the renewal point on day 18. Then since the schedules with terminal storage level $b(T) = 0$ and $b(T) = B$ converge, by monotonicity in Theorem 2, any schedule with $b(T) \in (0, B)$ also converges.

The charging and generation schedule with the same settings for an extended 14 day horizon for house1 is given in figures 3.3 and 3.5 respectively. The last renewal point for the 14 day lookahead horizon occurs on the 13th day, when $bf2$ empties below. But if we look closely at the charging and generation schedules in the above figures from day 1 to 9, it can be seen that the optimal path of the respective charging and generation schedules are the same as for the 10 day horizon in figures 3.2 and 3.4 until day 9. This allows us to observe the properties of the 14 day horizon using the 10 day horizon schedule. Similarly for the NSW state data, the extended 30 day horizon charging and generation schedule for the 22500MWh storage is given in figures 3.8 and 3.9 respectively. Here both $bf1, bf2$ have the same schedule before this last renewal point, which is seen on the 25th day of the 30 day finite horizon solution. Further, by observing the charging and generation schedules between day 1 and 18 for both the 20 and 30 day horizon aggregate NSW demand data, it can be seen that the extended horizon has the same charging and generation pattern as the 20 day horizon in figures 3.6 and 3.8. Consequently, this shows that future changes in the aggregate demand have not affected the scheduling decisions before the renewal point

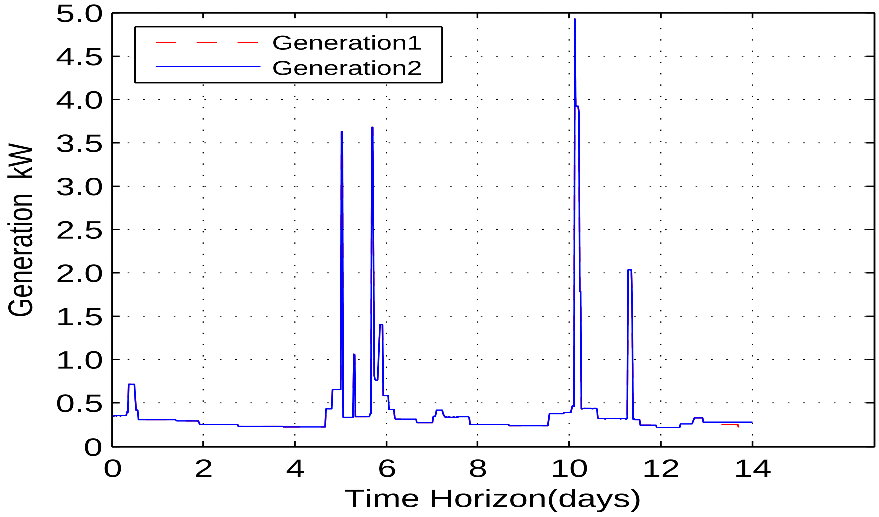

Figure 3.5: Generation schedule of house1 for a 14 day horizon using a 1kWh storage system

on day 18 for the 20 day lookahead.

Based on these numerical results, it is clearly visible that convergence occurs when $bf1$ saturates above or $bf2$ empties below, creating a renewal point. Because of this renewal point, future changes in demand will not affect the optimal scheduling decisions before the renewal point. Therefore as $T \to \infty$, if renewal points exist for some $t < T$, then the finite horizon optimal solution can be used to study the structure of the long term total generation cost minimisation problem. However, since the results above are for an ideal storage system, in subsequent chapters we will also show numerically that renewal points exist for storage devices with charging inefficiency and self-discharge, since the charging inefficiency and self-discharge affect the starvation and saturation of the energy storage.

3.7.3 Optimal Schedule for an Ideal Energy Storage System

The optimal schedule for the ideal storage given in equation (3.34), shows that the marginal generation cost is constant when $b^*(t) \in (0, B)$, and when the marginal generation cost increases, the storage device discharges from saturation to minimise cost, deciding to charge only when the marginal generation cost decreases after the storage device has fully discharged. Then under constant $\gamma(.)$, the optimal generation solution is to keep the generation constant when $b^*(t) \in (0, B)$ and to increase or decrease the generation upon fully saturating or fully discharging the storage device. The structural properties of the charging and generation schedule above are also visible for the numerical results shown

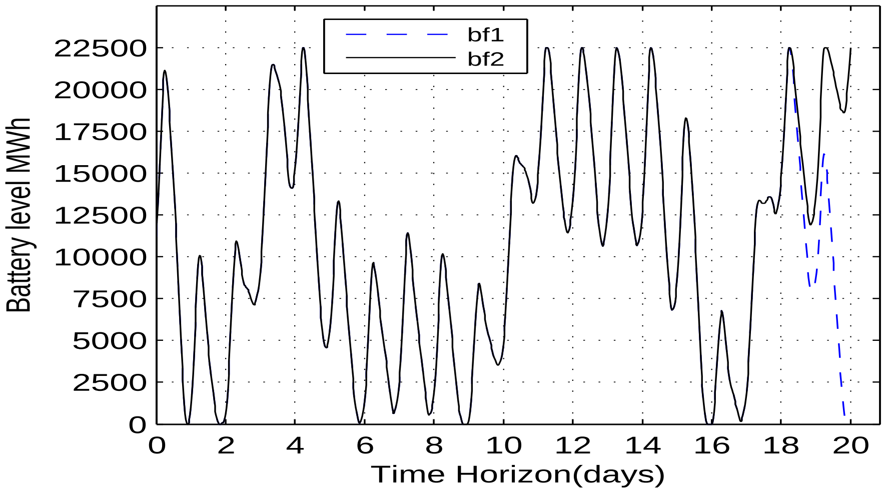

Figure 3.6: Charging schedule of NSW for a 20 day horizon using a 22500MWh storage system

in figures 3.8 and 3.9. The figures display the charging and generation schedule for the NSW aggregate state data, for a 30 day horizon using a 22500MWh storage system. Here, convergence occurs on the 25th day and therefore the scheduling decisions before the 25th day are the same for the storage system with any $b(T) \in [0, B]$.

The storage schedule on the 2nd day shows that the storage fully discharges and subsequently fully saturates once again only on the 4th day. If we observe the generation schedule in figure 3.9 for the same period, we see that the generation has a downward jump on the 2nd day when the storage fully discharges, and remains constant while $b^*(t) \in (0, B)$. Later, on the 4th day, there is an upward jump in the generation when the storage fully saturates. Notice that the generation when $b^*(t) \in (0, B)$, is not exactly constant. This slight fluctuation in generation seen when charging and discharging, is due to the discrete storage levels used during simulations. Therefore, for continuous charge levels, the scheduling would show that the generation is constant when $b^*(t) \in (0, B)$. Then based on these numerical results and the analytical results in section 3.4.1, the structure of the generation schedule when using an ideal storage device is to have constant generation when $b^*(t) \in (0, B)$, and to change the generation when the storage is fully saturated or empty.

Using the above property for the generation,subsequent chapters will compare numerically the properties of the charging and generation schedules when using storage systems with charging efficiency and self-discharge. By studying the properties of the optimal

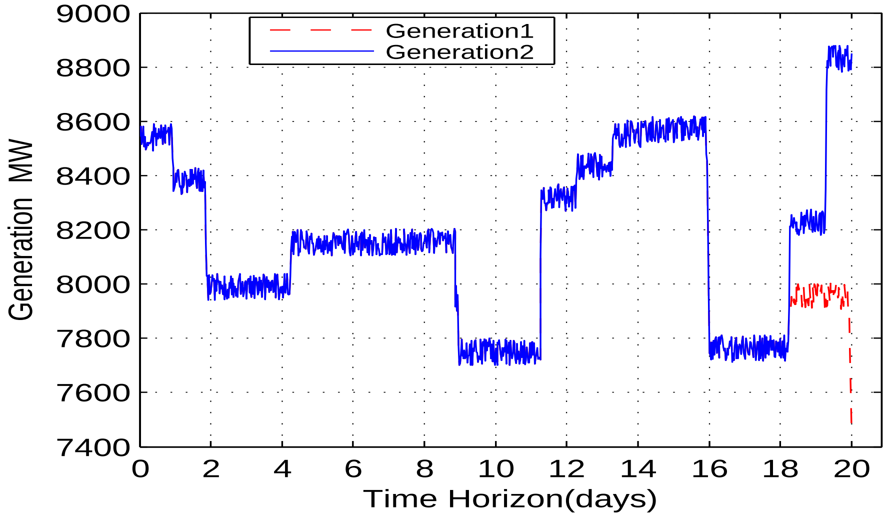

Figure 3.7: Generation schedule of NSW for a 20 day horizon using a 22500MWh storage system

solution, we will discuss the behaviour of non-ideal storage systems, when used for peak shaving with cost minimisation. Additionally, the chapters will also investigate the performance in peak shaving under arbitrary price increases, when using non-ideal storage devices to reduce the power cost for the utility and the user.

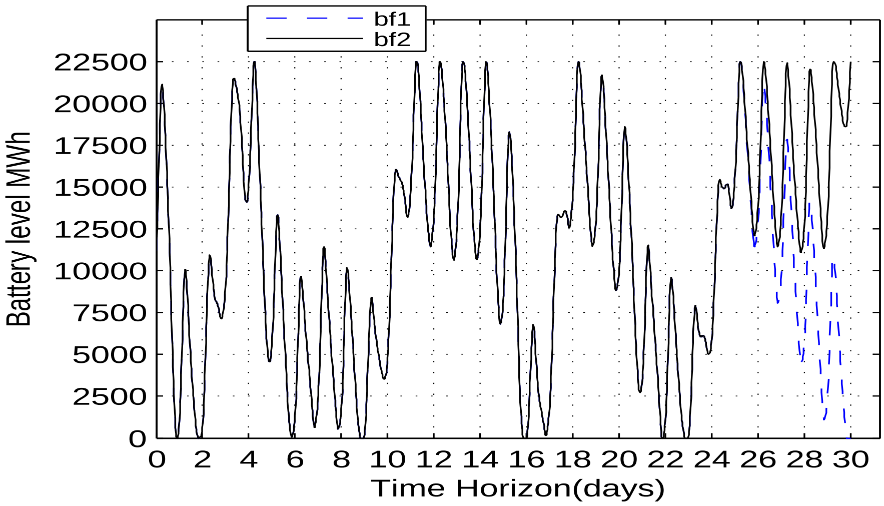

Figure 3.8: Charging schedule of NSW for a 30 day horizon using a 22500MWh storage system

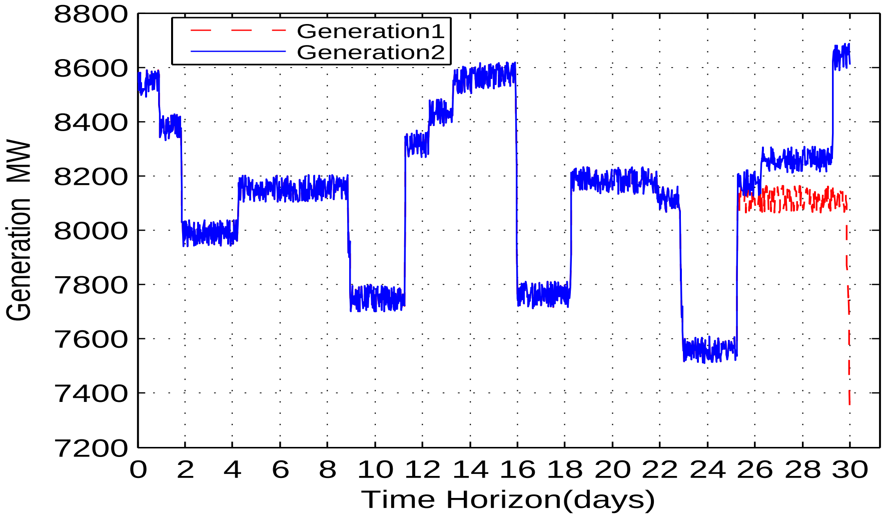

Figure 3.9: Generation schedule of NSW for a 30 day horizon using a 22500MWh storage system

Chapter 4

Energy Storage with Charging Inefficiency

This chapter extends the ideal energy storage system to incorporate charging/discharging efficiency in energy storage systems, to investigate the structural properties of the charging and generation schedule. First, we show numerically that the structural results for an ideal energy storage can be used to study the inefficient energy storage problem. Then we demonstrate numerically, the behaviour of the storage and generation schedule under real-time and arbitrary price increases. Finally we discuss the peak shaving capabilities for increasing storage capacity and storage efficiency using numerical results generated for both household and aggregate utility demand.

4.1 Energy Storage Inefficiency

The overall efficiency η of a storage system is given by the ratio between the energy input and output energy from the storage system [31]. This limits the amount of energy that can be drawn from a storage system. Most storage systems lose energy due to internal energy losses or due to losses from converting energy from its original form to a storable form and vice versa. In this chapter we model the energy loss due to conversion knows as the charging/discharging efficiency for energy storage.

4.1.1 Charging/Discharging Inefficiency

A storage device can be inefficient while charging and or discharging. The charging efficiency $\eta_c \leq 1$ of a battery is the amount of power discharged over the power drawn into the storage system. Conversely the discharging efficiency $\eta_d \leq 1$ gives the ratio of the power supplied to the load over the power drawn from the storage device. The usual reason for charging/discharging efficiency is due to conversion losses in the battery. The energy lost when converting power from the grid to a storable form of energy results in the battery being inefficient while charging. Similarly, the conversion loss from the storable form to a consumable form results in the discharging efficiency of the energy storage system. This charging and discharging inefficiency results in an overall efficiency known as the round trip efficiency η and is given by $\eta_c\eta_d \leq 1$.

In this chapter the non ideal energy storage system is modeled with both charging and discharging efficiency and the numerical results are simulated for charging efficiency of $\eta_c \leq 1$, which means that $\eta_c * originalpowerdrawn$ can only be stored in the energy storage system. The discharging efficiency of the non ideal battery is assumed to be $\eta_d = 1$ for our numerical results, allowing the power drawn from the battery to be used fully to satisfy the demand without loss. The implication of having $\eta_d = 1$, is that it is more favourable for the storage to supply power than to draw power from the grid. Table (4.1) below shows an example of the charging/discharging efficiency values for selected chemical storage systems.

Storage Type	Lead Acid	Nickel Cadmium	Sodium Sulphur	Lithium ion	Sodium Nickel Chloride
charging/ discharge Efficiency%	80	70	up to 90	95	90

Table 4.1: Efficiency values for chemical energy storage systems [1]

4.2 Verifying Solution for a Non-ideal Energy Storage System by Simulation

Since the utility or a user has the option of choosing between many types of energy storage systems with different charging/discharging inefficiencies, it is important to study the behaviour of the charging and generation schedule for these inefficient storage types. Even with inefficient storage devices, we are still interested in the long term optimal scheduling behaviour with arbitrarily increasing price, to understand the structure of the optimal schedule and to investigate the benefits of using storage system for both the utility and the user as mentioned in section 3.1. Furthermore, due to arbitrary price increases, the total cost of our model (section 3.3), which minimises the generation cost tends to infinity, as discussed in section 3.2. Therefore, the original problem of finding a solution for a system with an infinite total cost still exists.

In Chapter 3 we showed that the solution to the infinite horizon problem with unbounded cost per stage and arbitrary price increases exists, if the optimal charging schedule for the solutions to the finite horizon problem ending at $b(T) = B$ and $b(T) = 0$, both either saturate above or below for a fully efficient energy storage system. As a result we wish to do the same by numerically investigating the structure of the optimal schedule and showing that theorems 2 and 7 are true even when using an energy storage system with charging inefficiency. To demonstrate that the theorems mentioned above are true, we use dynamic programing to simulate the charging schedule of an energy storage system for the finite horizon problem with objective $\min \sum_{t=1}^{T} \gamma(t) N(g(t))$, and show that renewal points exists even when the battery is inefficient. To be more specific, we will numerically demonstrate that when the charging schedules of a storage with terminal conditions $b(T) = 0$ saturates above or $b(T) = B$ empty below, at some $t < T$; the charging schedule of the problem with $b(T') \in [0, B]$ for any $T' > T$ will also converge at t. Because of this even when the horizon is extended from T to T', the charging schedule up to time t, will be the same for both the lookaheads T and T', creating a renewal point that can be used to decouple the problem at time T. Therefore if renewal points exist even when using a battery with charging inefficiency, the solution to the infinite cost problem can be studied by observing the decoupled finite horizon problems. This allows us to investigate the structural properties of the charging and generation schedule for energy storage systems with charging inefficiency by using the optimal finite horizon solution.

4.2.1 Renewal Points with Charging Efficiency

Figures 4.1a and 4.1b show the charging schedules for a energy storage of capacity $B = 22500MWh$, with $\eta_c = 90\%$ for the March 2012 NSW demand profile for 20 and 30 day

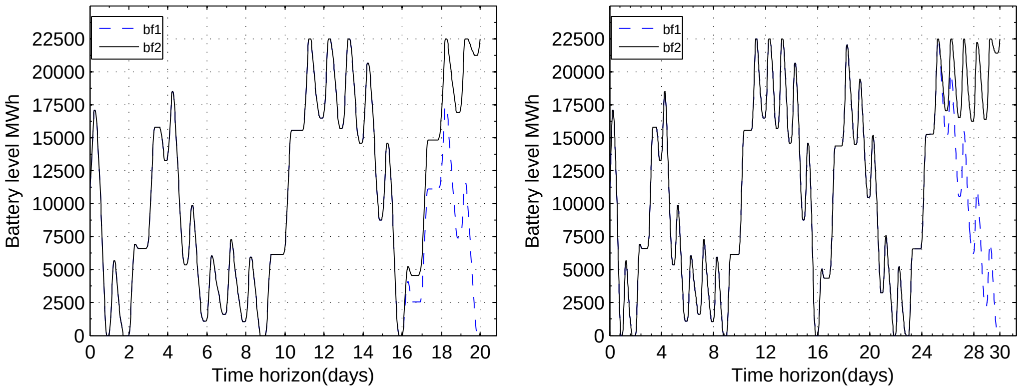

(a) 20 day charging schedule

(b) 30 day charging schedule

Figure 4.1: 20 and 30 day charging schedule for an energy storage system with charging inefficiency showing renewal points

horizons respectively. Here $bf1, bf2$, are the optimal charging schedules for a battery which terminates empty and full at the end of the horizon respectively. The 20 day schedule shows that both $bf1, bf2$ have the same charging schedule until day 16 when the storage empties below. Similarly the 30 day schedule also shows both $bf1$ and $bf2$ saturating above on the 26th day of the scheduling period. Therefore for the 20 day and 30 day horizon, we see that the respective 16th and 26th day periods are convergence points. If we also compare the scheduling behaviour of figures 4.1a and 4.1b until the 16th day, we can see that both the 20 day and the extended 30 day horizon have the exact same charging schedule This suggests, that future demand does not affect the charging schedule as long as the battery energy level converges below. This is also the case if the battery saturates above. Because of this we assume that theorems 2 and 7 are true even for an energy storage system with charging inefficiency. The above results illustrate the existence of convergence points under the conditions in theorem 7. Further simulations that we carried out on household data and other state data in Australia also have shown that renewal points can exists even for storage systems with inefficiency provided $bf1$ saturates above or $bf2$ saturates below. Therefore using these results allows us to continue studying the optimal charging and generation schedule for the infinite horizon problem by studying the decoupled finite horizon problem as done in chapter 3.

4.3 Optimal Marginal Generation Cost with Charging Inefficiency

Section 3.4 in the previous chapter proved that the marginal generation cost for a battery with charging efficiency and self discharge depend on the inefficiency, self-discharge rate, the charging and discharging constraints and the future saturation and starvation of the energy storage system. Since here we are interested in studying only the impact on the optimal schedule due to charging inefficiency we assume that $\beta = 1$. Based on this assumption the optimal schedule for an energy storage system with charging inefficiency is given by,

$$\gamma(t)N^{'}(g^{*}(t)) = \frac{1}{2}\big[(1+\eta_c)\sum_{\tau=t}^{T-1}(\underline{b}^{*}(\tau) - \bar{b}^{*}(\tau)) + \underline{C}^{*}(t) - \bar{C}^{*}(t) - \underline{D}^{*}(t) + \bar{D}^{*}(t)\big]^{+} \quad (4.1)$$

The above optimal solution and the complementary slackness conditions 3.6 and 3.5 indicates that the marginal generation cost for a battery with inefficiency is affected by its charging efficiency η_c, and that the marginal generation cost is constant for $b^{*}(t) \in (0, B)$ while the battery is charging or discharging. That is since the Lagrange multipliers $\underline{b^{*}}$ and $\bar{b^{*}}$ are inactive when the storage $b^{*}(t) \in (0, B)$ due to conditions 3.6 and 3.5, then the marginal generation cost will also be constant according to the left hand side of equation 4.1. Then using the above optimal solutions and the simulations using dynamic programming, the remainder of this chapter will focus on analysing the structural properties of the charging and generation schedule, for energy storage systems with charging inefficiency. Furthermore, based on these structural properties we will investigate the impact on peak shaving different types of energy storage systems.

4.4 Structural Properties with Charging Inefficiency

This section describes the structural properties of the charging and generation schedules energy storage systems with charging inefficiency based on the optimal behaviour shown in the previous section. Here we will numerically study the optimal scheduling behaviour when using energy storage and prove generalizations for the results based on the observed structure. To study the optimal solution we initially assume that the time varying price

$\gamma(.) = 1$. Since the time varying cost is assumed to be constant, the marginal generation cost for the problem becomes $N'(g^*(t))$ and for the simulations $N'(g^*(t)) = 2g^*(t)$. This means that the marginal cost changes purely based on the generation fluctuations due to the convexity of our cost function. Based on these characteristics we will first investigate the behaviour of the charging and generation schedule for an energy storage system with charging inefficiency using the optimal solutions obtained using dynamic programing.

4.4.1 Generation Schedule for Energy Storage Systems with Charging Inefficiency

As explained in chapter 3, the marginal generation cost for a fully efficient battery changes only when the charging/discharging rate limit is hit. Further, due to the convexity of the generation cost in $g^*(.)$, the optimal generation will also be constant while $b^*(t) \in (0, B)$, increasing and decreasing the generation only when the battery saturates or empties respectively. But this is not the case with a batteries having charging inefficiencies.

Figures 4.2 and 4.3, show the generation schedule for NSW and house1 demand profiles respectively. The NSW generation schedule is given for two energy storage systems both capacity $B = 22500MWh$ and efficiency $\eta_c = E = 0.9$ and 1 (figure 4.2). Similarly the household generation schedule is simulated for three different batteries with capacity $B = 0.5kWh$ and efficiencies $\eta_c = E = 0.8, 0.9$ and 1 (figure 4.3). Both figures show that the generation schedule for the inefficient battery fluctuates between some upper and lower value, and that during certain periods the generation and hence the marginal cost remains constant. This effects is more clearly evident by observing figure 4.2 from day 4 to 8, where the inefficient storage generation changes fluctuates between 7500MW and 8500MW, while the fully efficient energy storage generation remains constant at 8200MW. Note that the slight fluctuations in generation seen during constant marginal generation cost is due to the discrete storage levels used as explained in section 3.7.1.

To understand the behaviour of fluctuating generation further, lets first observe the charging and the generation schedules for a 22500MWh energy storage system with 90% efficiency as shown in figure 4.5. The figure shows that the generation always dips to a lower value when it starts charging and remains constant while it continues to charge. In contrast when it starts to discharge the generation increases and then remains constant while it discharges. Similar fluctuations in generation are also seen for the house1 demand

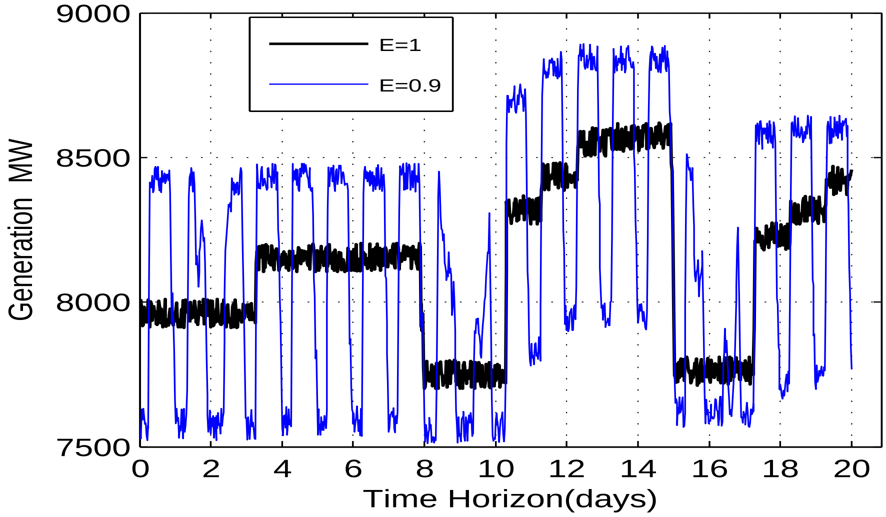

Figure 4.2: Generation schedules for fully efficient and 90% efficient energy storage systems using NSW demand profile

profile as shown in figure 4.6, for a 0.5kWh battery which is 90% efficient. The figure shows small dips in generation occurring during the charging phase and the generation increases again when the battery starts to discharge. Then based on these results for charging and generation schedule for an inefficient energy storage system and the comparison of generation schedules as shown in figure 4.2 and 4.3, it can be seen that the fluctuations occur only for the inefficient storage, and that if an efficient energy storage was used, these fluctuations will be constant. Then using these results and by using the optimal solution in section 4.3 we can say that the generation dips when the storage starts to charge and the generation jumps when the storage device starts discharging.

These bounds on generation fluctuations can be explained by solving the dual problem equations in section 3.4, as shown below

First by adding equation (3.22) with (3.23) and substituting equation (3.25) we get,

$$(1-\eta_c)(\sum_{\tau=t}^{T-1}\left[\underline{b}^*(\tau)-\bar{b}^*(\tau)\right]^+) = \underline{C}^*(t)-\bar{C}^*(t)+\underline{D}^*(t)-\bar{D}^*(t) \tag{4.2}$$

Secondly by adding equations (4.2) and (3.33) we can represent the marginal generation cost without discharging constraints as,

$$\gamma(t)N^{'}(g^*(t)) = \eta_c\sum_{\tau=t}^{T-1}\left(\underline{b}^*(\tau)-\bar{b}^*(\tau)\right)+\underline{C}^*(t)-\bar{C}^*(t) \tag{4.3}$$

Similarly by subtracting (4.2) from (3.33) we can get the marginal generation cost that

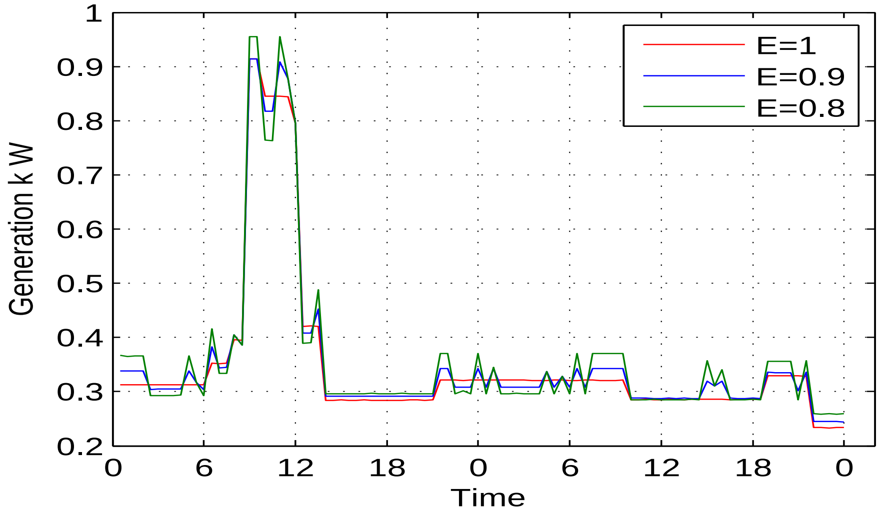

Figure 4.3: Generation schedules for fully efficient and 90% efficient energy storage systems using house1 demand profile

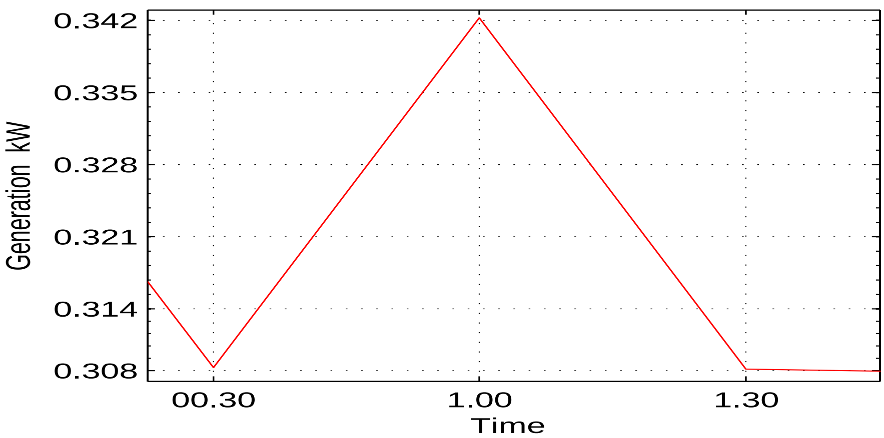

Figure 4.4: Generation schedule for a 90% efficient 0.5kWh battery for the house1 demand profile from 12.30am to 1.30am

excludes the charging constraints by,

$$\gamma(t)N^{'}(g^{*}(t)) = \sum_{\tau=t}^{T-1}\left(\underline{b}^{*}(\tau) - \bar{b}^{*}(\tau)\right) - \underline{D}^{*}(t) + \bar{D}^{*}(t) \tag{4.4}$$

Analysing both equations (4.3) and (4.4), we see that $(\underline{b}^{*}(\tau) - \bar{b}^{*}(\tau))$ increases when the battery fully saturates from complementary slackness condition (3.27), since $\bar{b}^{*}(\tau) > 0$. Similarly $\underline{b}^{*}(\tau) - \bar{b}^{*}(\tau))$, decreases when the battery full discharges based on complementary slackness conditions (3.26), since $\underline{b}^{*}(\tau) > 0$. Further, while the battery level $(b^{*}(t) \in (0, B))$, the value of $(\underline{b}^{*}(\tau) - \bar{b}^{*}(\tau))$ will remain constant, similar to the fully efficient energy storage system. Looking at equation (4.3), it can be seen that the marginal generation cost when charging is not only affected by the constraints on the battery, but it is also

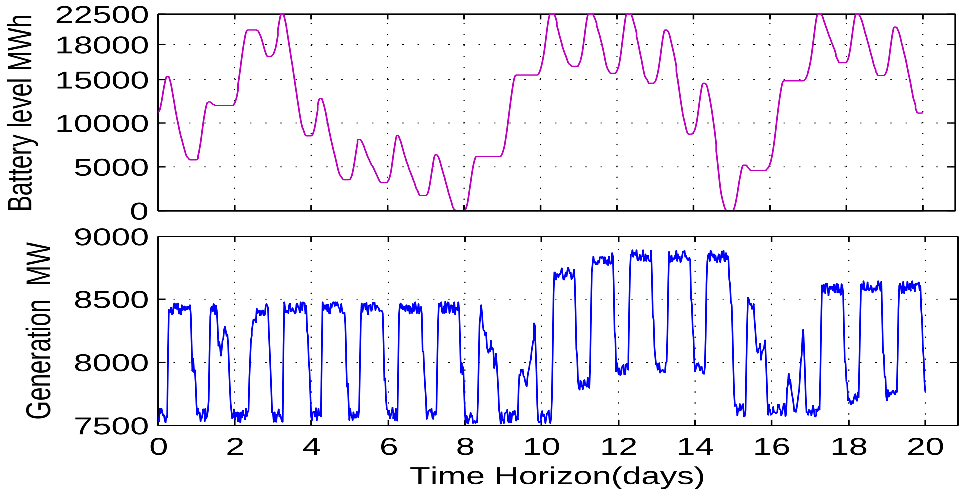

Figure 4.5: Generation and charging schedules for the NSW demand profile using a 22500MWh energy storage with 90% efficiency

affected by the charging constraints $\underline{C}, \bar{C}$ and the charging efficiency η_c. Similarly, equation (4.4) shows that the marginal generation cost and hence the optimal generation when discharging is affected by the discharging constraints $\underline{D}$ and $\bar{D}$.

Based on the on complementary slackness conditions (3.28) and (3.29), it is known that the constraints are inactive when the storage device is charging and hence the Lagrange multipliers $\underline{C} = \bar{C} = 0$. So when the marginal generation cost lower by a factor of η_c and $b^*(t) \in (0, B)$, according to equation (4.3) the battery will start to charge. And while the battery is still charging, the marginal generation cost will remain constant until either the battery fully saturates, or until it is optimal to discharge the battery before saturation. During this time, it is optimal to also decrease the generation by a factor of $1 - \eta_c$ and remain at constant generation until the battery starts to discharge. When the battery starts to discharge and $b^*(t) \in (0, B)$, this means that the marginal generation cost has increased by a factor of $1 - \eta_c$, according to equation (4.4) and complementary slackness conditions (3.30) and (3.31) showing inactive discharging constraints. So when the battery starts to discharge, due to the convexity of the generation cost in $g^*(.)$, the generation will also increase by a factor of $1 - \eta_c$ and maintain constant generation while discharging. As a result it can be seen that the generation fluctuates by $1 - \eta_c$, whenever the battery starts to charge or discharge.

An example of these bounds can be observed from the scheduling behaviour shown in figures 4.5 and 4.6. From the 4th to the 8th day in figure 4.5 when $b^*(t) \in (0, B)$,

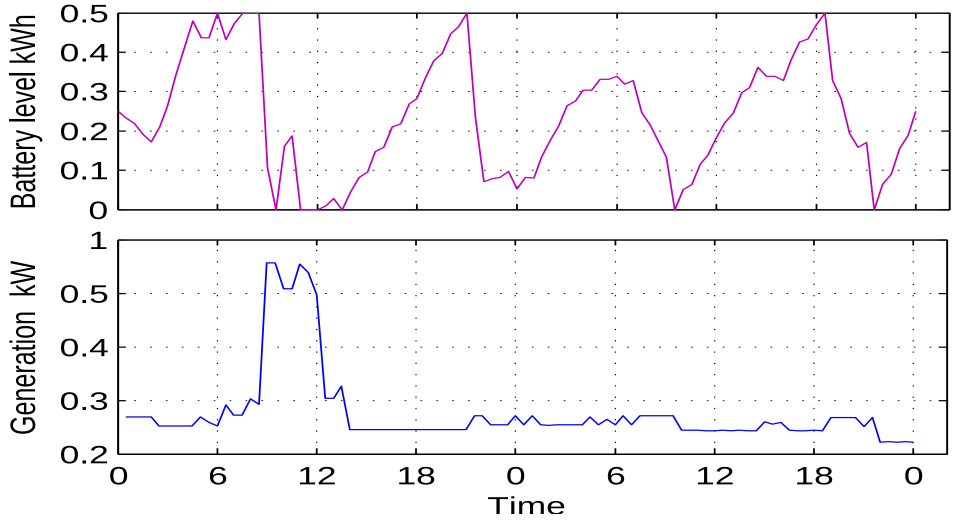

Figure 4.6: Generation and charging schedules for the house1 demand profile using a 0.5kWh battery with 90% efficiency

the generation of the energy storage system when discharging is approximately 8500MW. Subsequently, when the generation decreases to approximately 7600MW, the storage is in charging mode. This is approximately a 10% decrease in the generation for an energy storage system with efficiency $\eta_c = 0.90$. This trend is also seen for the house1 demand profile as shown in figure 4.6. Between 12midnight and 6am on day two, when $b^*(t) \in (0, B)$. The battery is seen to have high and low generations as explained earlier. If we look at the zoomed in view for the same day in figure 4.4 from 1.00 am to 1.30 am, it can be seen that the generation when the battery starts to charge decreases to $\approx$ 0.308kW from 0.342kW, which is a 10% decrease for the 90% inefficient battery used for house1.

Because of this, it can be demonstrated, that for inefficient energy storage systems, $g^*(charging) = (1-\eta_c)g^*(discharging)$, whenever the battery starts to charge or discharge when $b^*(t) \in (0, B)$ and $C^*(t) = D^*(t) \neq 0$. But if the battery does not charge or discharge and $C^*(t) = 0$ and $D^*(t) = 0$ as in figure 4.5, the complementary slackness conditions(3.28), (3.30), and the optimal solution (4.1) indicate that both the lower bound charging and discharging constraints $\underline{C}(t), \underline{D}(t)$ are active. This results in fluctuations in between the upper and lower generation values as seen on the 9th day in figure 4.5. This clearly shows that the inefficiency of the energy storage impacts the optimal generation schedule of the system and that the bounds on these fluctuations depend on the inefficiency of the battery η_c, when $b^*(t) \in (0, B)$. Furthermore as shown in figures 4.7 and 4.3, these fluctuation in generation seem to increase with increasing inefficiency, since the amount of power lost when charging the battery increases with its inefficiency.

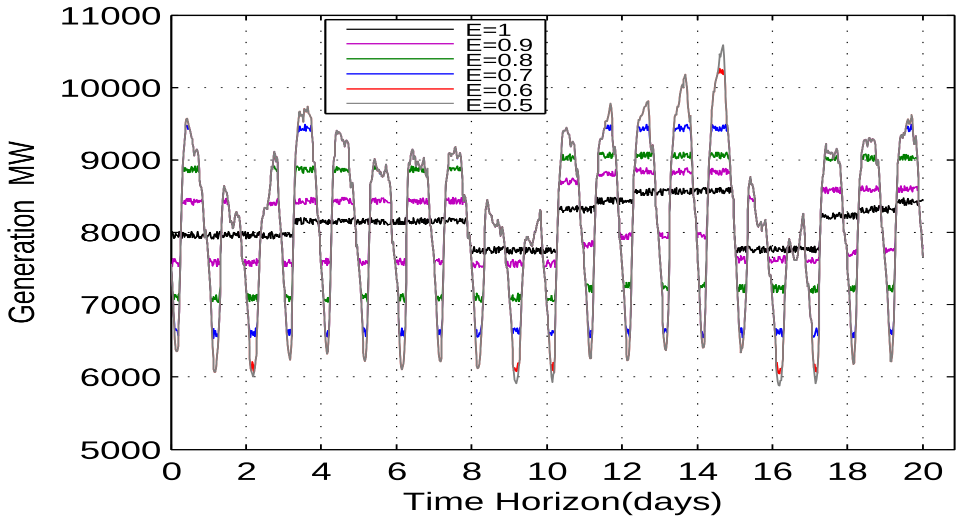

Figure 4.7: Generation schedule for 22500MWh energy storage systems with increasing inefficiency

4.4.2 Charging schedule for Energy Storage Systems with Charging Inefficiency

The charging behaviour of a storage device changes with the inefficiency of a storage system. Due to the loss in energy when charging or discharging a storage device, the charging/discharging trend will be different for storage devices when considering decreasing battery efficiency. Therefore in this section, we discuss the trend of the charging schedule for storage systems with different charging inefficiencies.

As explained in section 4.4.1, for both a fully efficient and inefficient battery, the marginal generation cost will decrease when the battery is fully discharged, and it will increase when the battery is fully saturated, causing the battery to charge and discharged based on the optimal generation. But unlike the fully efficient battery, the marginal generation cost for an inefficient battery also changes when $b^*(t) \in (0, B)$. Because of this, an inefficient battery will start to charge when the marginal generation cost decreases by a factor of $1-\eta_c$ and it will start to discharge when the marginal generation cost increases by a factor of $1 - \eta_c$. As a result, the charging schedule for an inefficient energy storage will have a different optimal path to that of the fully efficient energy storage system.

Figure 4.8 shows the charging schedule with increasing inefficiency values for an energy storage system with capacity $B = 22500MWh$. The efficiency values η_c range from a fully efficient battery to a 50% efficient battery, and is simulated for the NSW demand. The charging schedule trend in general shows that as efficiency decreases, the amount energy level in the battery and the frequency at which the energy storage is charged also decreases as expected. The reason for this trend is the power lost when charging and inefficient battery, which increases as the efficiency of the battery decreases causing the storage to have a lower usable energy storage level. Interestingly figure 4.8f shows that for our state demand profile, it is better not to charge the battery at all, but to instead satisfy the demand directly from the grid at high inefficiency values. For a particular demand profile, the decision on not charging the battery or having a lower amount of charge in the battery can also be attributed to the generation fluctuations of an inefficient energy storage explained in section 4.4.1. As seen from figure 4.7, when the inefficiency of the storage increases, so does the fluctuation in generation. But for an energy storage system with high inefficiency, these fluctuations in generations are higher and the amount of energy stored in the battery is lower. But since the optimal solution tries to minimise the cost of generation, it will not be optimal to charge a highly inefficient battery if the generation increases beyond any of the peak demand values. At this point, it will be optimal to satisfy the demand directly from the grid without using the battery. The house1 charging schedule for a 1kWh battery also shows similar behaviour as shown in figure 4.9. Remarkably, for the household demand, it is still optimal for the battery to be used even at a higher inefficiency of 50%. But since the loss of energy and fluctuation in generation increases with highly inefficient batteries, we can also expect the household data to behave similar to the state data at extremely high inefficiencies.

4.5 Peak Shaving

Reducing the peak generation in the grid by either shifting the demand or by using energy storage to supply energy during peak demand from energy stored during low peak demand is known as peak shaving. In this section, we will investigate the effects of peak shaving for increasing storage capacity and increasing inefficiency, with and without real time prices (RTP). Our aim is to be able to study the performance of peak shaving by applying the optimal control solution for energy storage devices with charging inefficiency. Based on these performance results, we will discuss properties that users and utilities need to

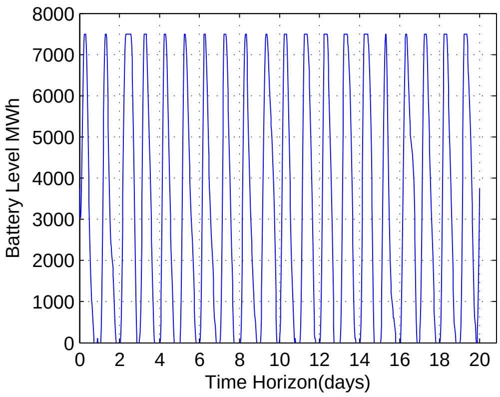

(a) Charging schedule for a 3750MWh energy storage system with 100% efficiency

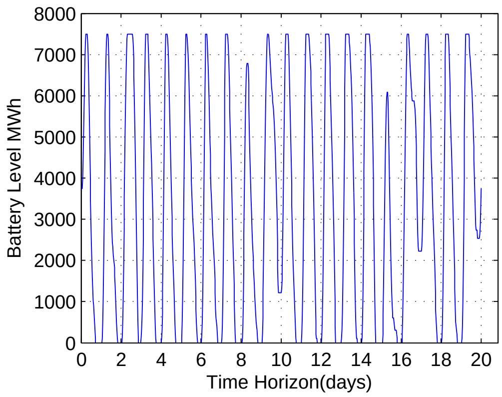

(b) Charging schedule for a 3750MWh energy storage system with 90% efficiency

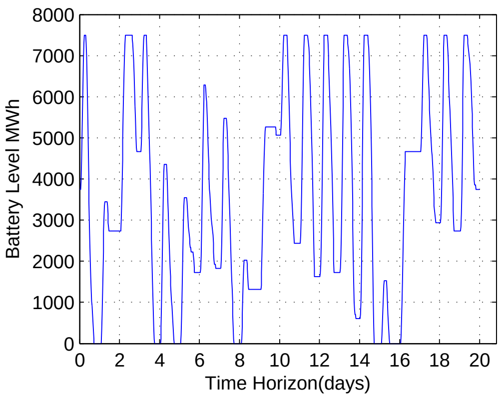

(c) Charging schedule for a 3750MWh energy storage system with 80% efficiency

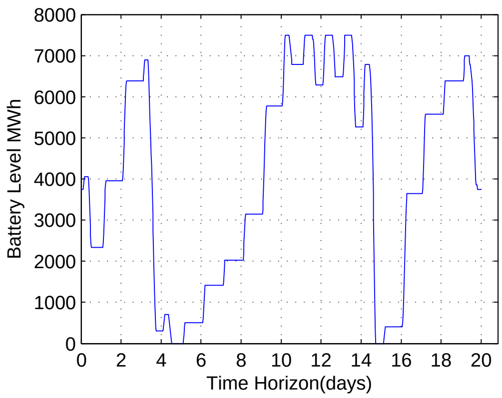

(d) Charging schedule for a 3750MWh energy storage system with 70% efficiency

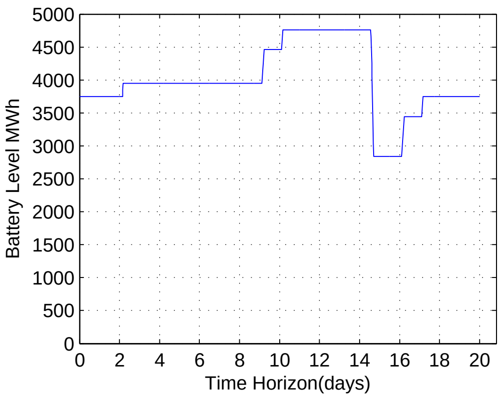

(e) Charging schedule for a 3750MWh energy storage system with 60% efficiency

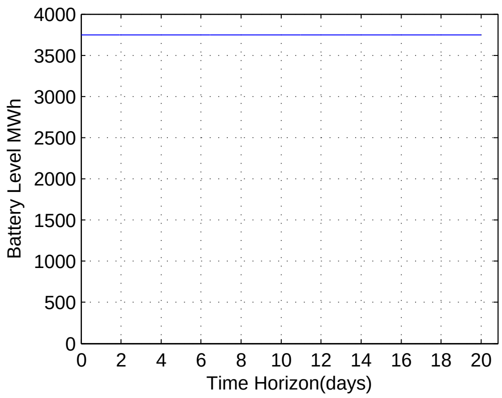

(f) Charging schedule for a 3750MWh energy storage system with 50% efficiency

Figure 4.8: Charging schedules for the NSW demand profile using 3750MWh energy storage systems with increasing inefficiency

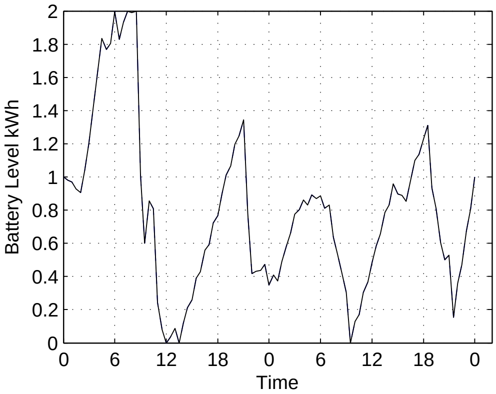

(a) Charging schedule for a 1kWh energy storage system with 100% efficiency

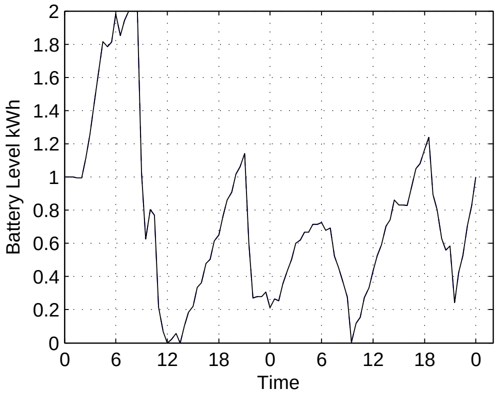

(b) Charging schedule for a 1kWh energy storage system with 90% efficiency

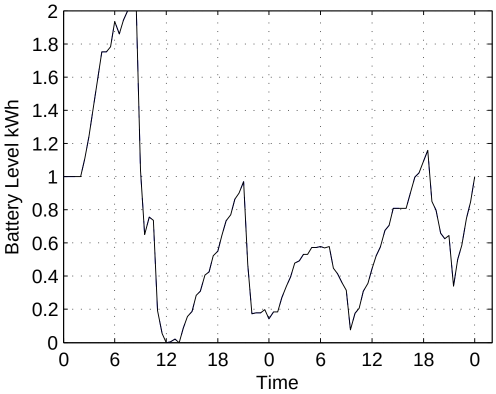

(c) Charging schedule for a 1kWh energy storage system with 80% efficiency

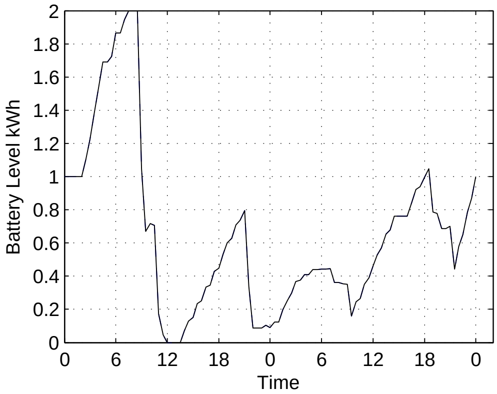

(d) Charging schedule for a 1kWh energy storage system with 70% efficiency

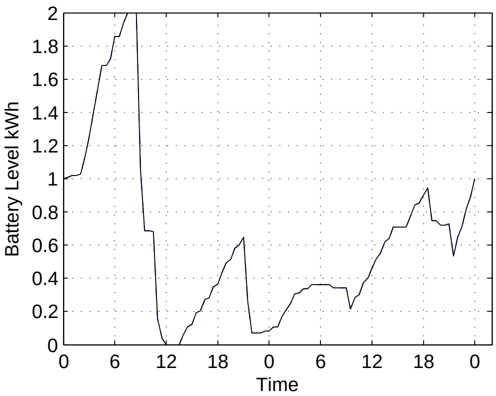

(e) Charging schedule for a 1kWh energy storage system with 60% efficiency

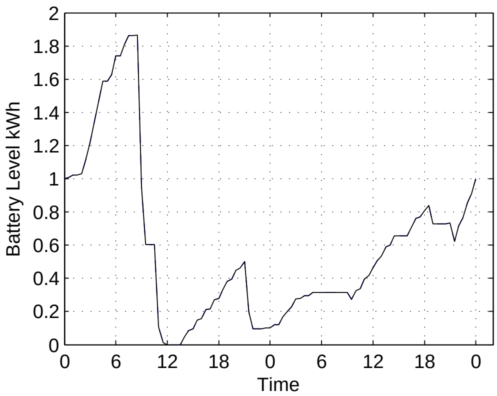

(f) Charging schedule for a 1kWh energy storage system with 50% efficiency

Figure 4.9: Charging schedules for house1 demand profile using 1kWh batteries with increasing inefficiency

consider when choosing and energy storage system for peak shaving.

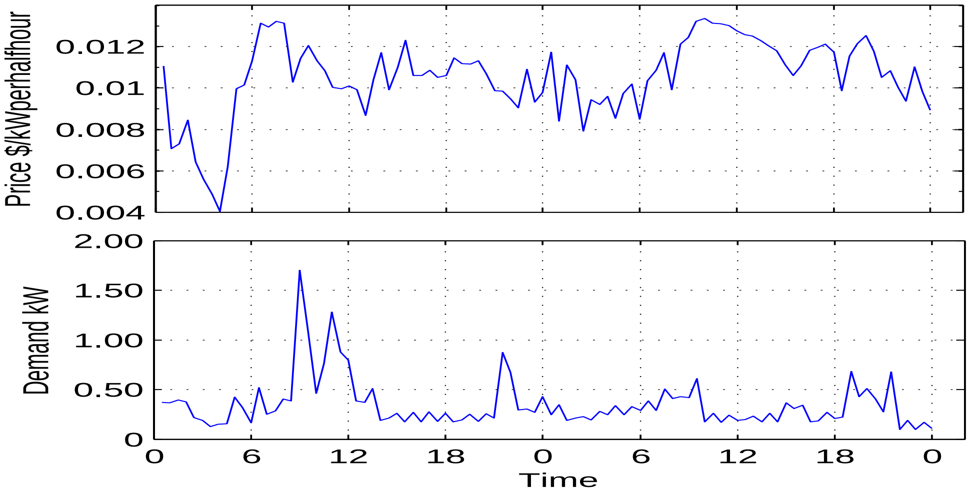

Figure 4.10: House1 demand and price curves for 2 days

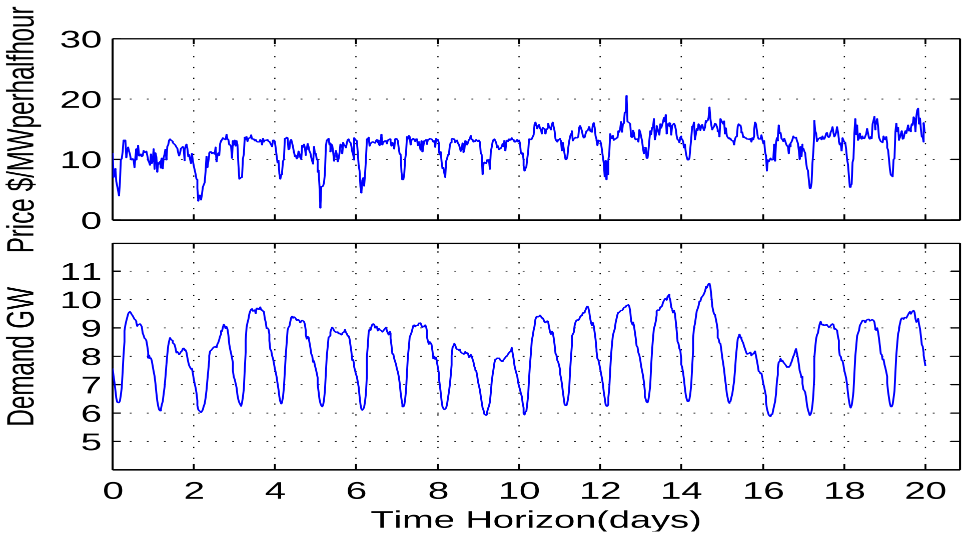

Figure 4.11: NSW demand and price curves for 20 days

4.5.1 Peak Shaving with Constant γ

The generation cost for the utility increases due to the high peak demand in the grid. This increase in peak demand requires the utility to use more expensive fast ramping generators to satisfy the user demand [23], which increasing the cost of generation and high capacity transmission and distribution networks for the utility. As a result, the utility's main objective for demand management is to minimise this generation cost by providing incentives for users to shave the peak demand in the grid [5]. Since the utility wishes to minimise the cost of generation, we will first take a look at the peak shaving performance for both the household and state demand assuming that our time varying cost $\gamma(.) = 1$ is constant. Then the generation cost to be minimised is given by $N'(g^*(.))$, where $N'(g^*(.)) = g^*(.)^2$ for the numerical results.

The demand in the grid for both house1 and NSW is given in figures 4.10 and 4.11 respectively. The peak generation in the grid due to satisfying this demand with energy storage using the optimal solution is shown in figures 4.12 and 4.13 for both NSW and house1 respectively. From the demand figures it can be seen that the highest demand of 1.702kW for the household data occurs on the first day at 9am. Similarly the NSW demand figure shows that its highest demand of 10580MW occurs on the 14th day for a 20 day horizon. Comparing the peak demand in figures 4.10 and 4.11 with the peak generation in the grid in figures 4.12 and 4.13, it can be seen that for house1, the peak generation will reduce from 1.702kW to approximately 1.4kW even for a 150Wh battery. And as the size of the battery increase, the amount of peak shaving also seems to improve substantially. As an example for a fully efficient 2kWh battery(2 car batteries, $\approx$12V, 85Ah), the peak generation reduces to approximately 0.4kW, which is an extra 1kW reduction in generation compared to the smaller battery.

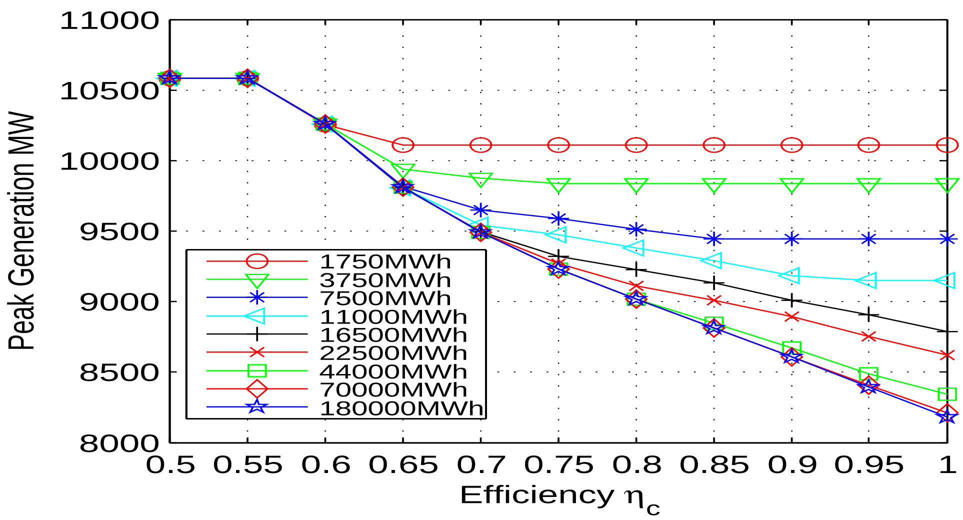

Figure 4.12: Maximum generation vs efficiency for different storage capacities using the NSW demand curve

Further, for the house1 demand, as the inefficiency of the energy storage system increases, the peak generation for the medium to large batteries increase. But this increase in peak generation is not seen for the smaller batteries. With the smaller batteries, the peak shaving achieved is seen to be constant for the range of inefficiencies provided. As

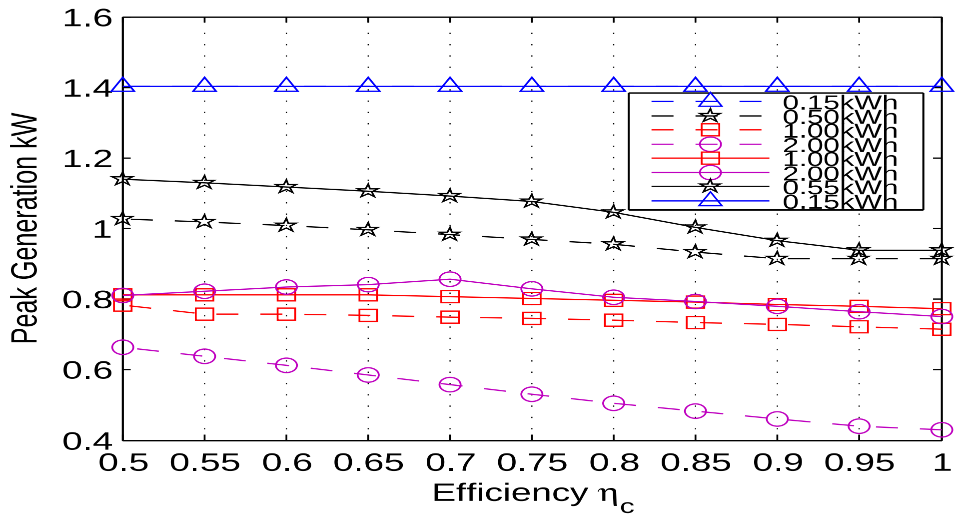

Figure 4.13: Maximum generation vs efficiency for the house1 demand profile for different battery capacities. The solid lines show the maximum generation with RTP. The dashed lines show the maximum generation without RTP

a result, the peak shaving provided by a fully efficient energy storage and a battery with higher inefficiency remains the same. Interestingly, this characteristic is also seen for the state peak generation graph shown in figure 4.12. To illustrate this further, the NSW peak generation plot shows that the same amount of peak shaving occurs for a 1750MWh energy storage system having a charging efficiency between the range of 100% and 65%. Similarly for the house1 data we see that a battery with capacity $0.15kWh$, has the same peak generation for an efficiency range from 100% to 50%. This allows inefficient(cheap) batteries to provide the same peak shaving as a larger more efficient battery. Then, if the utility provided a user with a smaller energy storage system, the utility has the option of providing a fully efficient more expensive battery or an inefficient battery of the same size purchased at a lower cost. This also benefits the user, since the batery is provided by the utility to the user. tery is provided by the utility to the user.

In addition to the above mentioned behaviour, the NSW peak generation also shows two other properties related to the storage capacity and efficiency. Figure 4.12 shows that for higher inefficiency values, the medium and large energy storage systems have the same peak generation for a given inefficiency. As an example for an inefficiency value of 80% we see that the 44000MWh, 70000MWh and 180000MWh energy storage systems have the same peak generation value of approximately 9000MW. This leads to the natural conclusion that for higher inefficiencies, increasing the capacity of the energy storage system beyond some optimal storage capacity, would not increase the peak shaving for the system. The second property seen from the state data is a trade-off between the efficiency and the capacity of the energy storage. Figure 4.12, shows this trade-off between the efficiency and the capacity an energy storage system. The same peak generation of 9000MW is seen for both a a 44000MWh, 80% efficient energy storage and a 22500MWh, 95% efficient storage system in figure 4.12. As a result the utility will have the option of choosing a smaller more efficient energy storage system or a larger storage with higher inefficiency to provide a similar amount of peak shaving in the grid. Additionally, since the cost of storage systems also depend on its capacity and inefficiency the utility is able to choose the appropriate storage characteristics to provide better peak shaving.

Even though tread-offs and mutual benefits exist between inefficient energy storages of different capacities, the total generation of the system is also a deciding factor when using energy storage for peak shaving. Because of this, the remainder of this section focuses on providing an explanation for the observed trade-offs that are re-listed below,

1. The same amount of peak shaving can be provided for a range of inefficiency values for energy storage system with smaller capacities.
2. A trade-off exists between using a large energy storage system with higher inefficiency or a smaller more efficient energy storage system, to provide the same amount of peak shaving.
3. As the efficiency of the energy storage system decreases, increasing the size of the storage not improve the peak shaving after some optimal storage size.
4. The total generation of the system increases as the inefficiency of the energy storage increases.

4.5.1.1 Behaviour of Inefficient Energy Storage

If the price is an increasing function of grid power drawn, then a battery will charge during demand troughs and discharge during peak demand periods. Because the generation cost is convex in $g^*(.)$, costing more generate an extra unit of energy, the optimal solution will minimise the total generation cost by minimising the peak generation. As a result, an inefficient energy storage will also choose to reduce the peak generation of the system by charging during low demand periods and discharging during peak demand. So for a given storage, the amount of peak shaved then depends on the amount of available energy in the battery before the peak. Therefore if the battery has an energy level E before the highest peak, it is able to discharge all or part of this energy to shave the peak in the grid. In particular, for smaller energy storage systems, this available energy before the peak is equal to the batteries capacity as shown in figures 4.14 and 4.15.

The charging schedule in figure 4.14 shows that the battery is fully saturated at 1750MWh, just before the highest demand on the 14th day, and then the battery fully discharges for the duration of the peak demand. Similarly for house1, the battery starts to charge just after 6am on the first day during a low demand period. Once the battery is fully charged, it stays charged until the demand peak at 9am, after which the battery starts to fully discharge providing the maximum possible peak shaving. These results show that smaller batteries are able to provide the maximum possible peak shaving, even with increasing inefficiency, since it is more likely to fully saturate the battery. However for larger batteries, the amount of energy lost is higher since, the battery can store more energy, causing more energy to be lost at lower efficiency values. This results in, larger batteries with higher inefficiencies to not be able to provide the same peak shaving as fully efficient battery's of the same size as shown in figure 4.12. Then as a consequence of this charging behaviour for smaller batteries, the utility is able to choose a small energy storage with higher inefficiency to provide the same amount of peak shaving. Therefore if a highly inefficient battery with smaller capacity saturates fully to provide the maximum possible peak shaving before the demand peaks, then any battery of the same capacity with higher efficiency will also provide the same peak shaving as the inefficient battery.

4.5.1.2 Capacity-Efficiency Trade-off

The trade-off between larger inefficient and smaller efficient energy storage systems can be seen from the state data in figure 4.12. Since the cost of our system relies only on a convex generation cost, the optimal solution will try to always minimise the peak generation of the system. As a result, the maximum peak shaving for a given inefficiency is achieved by trying to maximise the amount of energy stored in the battery E before the peak. Naturally, for larger energy storage systems the amount of energy that a battery can hold is larger than for a smaller energy storage systems. This means a large more efficient energy storage system would provide battery peak shaving, than a smaller energy storage

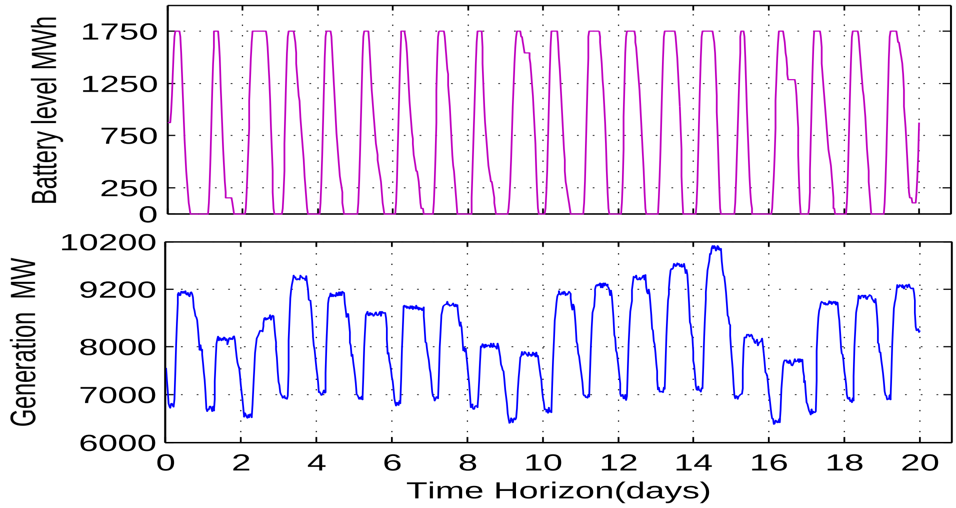

Figure 4.14: Charging and generation schedules for the NSW demand using a 1750Mwh, 90% efficient energy storage system

system for a given inefficiency.

However as the charging efficiency decreases, as discussed in section 4.4.1 the amount of power drawn by the storage and hence the energy level in the storage device $E_{storable}$ decreases. This means that for a higher inefficiency, the large battery would store less energy. Then if the amount of this energy stored for a large more inefficient battery is the same as the amount of energy stored for a smaller more efficient battery, the utility is able to achieve the same amount of peak shaving for both the larger and the smaller batteries. This property gives rise to a trade-off between battery capacities and efficiencies, allowing the utility to choose between a larger less efficient battery or a a smaller more efficient battery, depending on the pricing of the battery and the total generation cost of the system. An example of this capacity-efficiency trade-off is shown in figure 4.16. The figure shows the peak generation for each capacity and efficiency pair. As an example to reduce the speak generation of the state demand to 9.91GW, the utility is able to use either a 9000MWh storage with an efficiency of 65%, or a smaller storage with capacity 4500MWh that is 80% efficient. Similarly to achieve a higher peak shaving having a peak generation of 9.29GW, the utility can choose either a fully efficient energy storage with capacity 11000MWh, or a much larger 16500MWh storage which is 80% efficent. Therefore as explained above, a utility is able to choose a larger storage which is inefficient or a smaller more efficient storage to provide the same peak shaving. This trade-off between the battery size and efficiency for peaks shaving can be useful when purchasing a storage system for

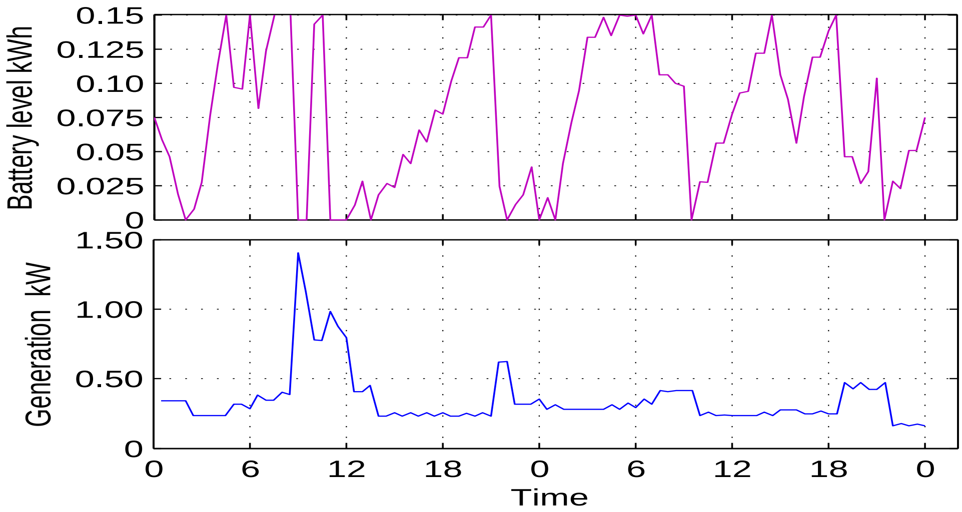

Figure 4.15: Charging and generation schedules for the house1 demand using a 0.15kWh battery with 90% efficiency

peak shaving, since the cost of the storage depends on the capacity and efficiency among others. client. Therefore as explained above, a utility is able to choose a larger storage which is inefficient or a smaller more efficient storage to provide the same peak shaving. This trade-off between the battery size and efficiency for peaks shaving can be useful when purchasing a storage system for peak shaving, since the cost of the storage depends on the capacity and efficiency among others.

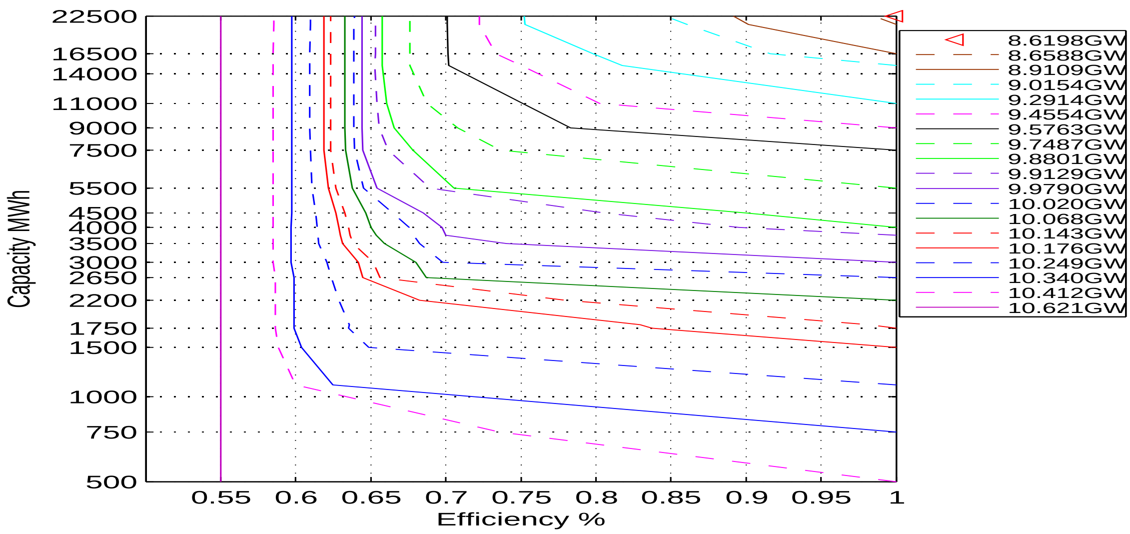

Figure 4.16: Capacity vs efficiency trade-off for peak shaving using the NSW demand profile

4.5.1.3 Characteristic of Large Capacity Energy Storage Systems at Higher Inefficiencies

A fully efficient energy storage system can achieve the maximum possible smoothing for a given storage capacity, since power is drawn from the grid, stored in the energy storage system and provided to the user without loss. But when using energy storage device with charging efficiency, a certain amount of energy is lost when charging the storage device. Therefore, the energy level in a storage system decreases, reducing the maximum smoothing and the storage capacity that achieves this smoothing. Figure 4.12 shows that for a given efficiency value, increasing the capacity of the energy storage will not improve the peak shaving beyond some optimal storage size. The figure indicates, that by using the smallest energy storage of capacity 7500MWh at 65% efficiency, the maximum possible peak shaving is achievable with a generation of 98000MWh. Therefore, even if the storage capacity was increased; for the same efficiency, the energy storage system would still provide the same amount of peak shaving. Because of this it would not be useful for this load trace to use an energy storage which is 65% efficient to have a capacity larger than 7500MWh in our simulations. This characteristic for the larger energy storage systems can be explained by considering the generation fluctuations of inefficient energy storage systems.

As discussed in section 4.4.1, an inefficient energy storage system causes the generation schedule to fluctuate between some upper and lower value depending on the inefficiency of the storage and the demand profile. Therefore, though a larger energy storage system might be able to store more energy in a battery causing the generation to increase, it is never optimal to have the peak generation to increase beyond the peak demand of the given demand profile. Because of this, for any given charging efficiency η_C, there is an optimal amount power drawn by an energy storage device as long as the peak generation does not go beyond the peak demand in the grid. Based on this, the energy storage that is just large enough to store the maximum energy level at a particular inefficiency would then be the optimal storage size. For the example given above, the 65% efficient, 7500MWh energy storage system was able to store the maximum possible energy for the NSW demand profile. As a result, when the capacity was increased, the peak shaving still remained the same. Because of this, increasing the storage capacity will not increase the peak shaving of the grid beyond some optimal storage capacity for a given efficiency.

4.5.1.4 Total Generation using Energy Storage with Charging Efficiency without Time-varying Prices

The increase in inefficiency for a battery not only reduces the amount of usable energy stored, but it also increases the total generation. This increase in the total generation is usually the result of the extra amount generated to maintain a desired energy level for a battery with charging inefficiency. Then by solving equations (3.3) and (3.4), the total generation of the inefficient energy storage system can be written as,

$$TotalGeneration = \sum_{t=1}^{T} g^*(t) = \sum_{t=1}^{T} d(t) + (1 - \eta_c) \sum_{t=1}^{T} C^*(t) \tag{4.5}$$

From equation (4.5) the total generation for a fully efficient energy storage reduces to the sum of the total demand given by $\sum_{t=1}^{T} d(t)$. But for an inefficient battery the total generation increases by $(1 - \eta_c)C^*(t)$ provided $C^*(.) > 0$, each time the energy storage charges. This increase in generation is due to the power lost when charging the storage due to the inefficiency. Table 4.2 below gives the average generation values for the NSW data with increasing inefficiencies. The table shows the change in total generation with increasing inefficiency for a storage with capacity 22500MWh. When using a fully efficient energy storage the average generation of the system is 8153MW, which is also equal to the average demand in the grid. But as the inefficiency of the storage is increased further, the average generation of the system increases until $\eta_c = 0.85$, and then decreases as the efficiency decreases beyond 85%. This decrease in total energy generated is a result of the energy storage not charging as often due to the upper bound the generation fluctuations as shown in figure 4.7. Additionally, for an efficiency 55%, the energy storage does not charge at all, resulting in the generation satisfying the demand directly from the grid. So in our simulations the 55% energy storage system has an average generation that is equal to the average demand of the NSW data.

Efficiency η_c	1	0.95	0.9	0.85	0.8	0.75	0.7	0.65	0.6	0.55
Average Generation kW	8153	8171	8183	8187	8185	8179	8170	8161	8155	8153

Table 4.2: Average generation for a 22500MWh energy storage system with increasing inefficiency

The total energy graphs for NSW and house 1 are given in figures 4.17 and 4.18 respectively. Similar to he results in table 4.2, the NSW total generation graphs show that for all storage capacities, the total generation increases up to a certain inefficiency and decreases as the efficiency decreases further. Interestingly, we see that the total generation is the highest for the more realistic efficiency values given table 4.1. This is because the storage device is fully utilised for the higher efficiency ranges. But as the the efficiency decreases further the storage device will not be fully utilised and the total power drawn from the grid decreases, reducing the total generation for lower efficiencies. In particular, our numerical simulation show that for our demand profile, it is not optimal to charge the storage device at all, but to instead satisfy the demand directly from the grid if the storage devices efficiency is lower than 55%. Because of this at the much lower range of efficiency values, a storage device will not be useful for peak shaving.

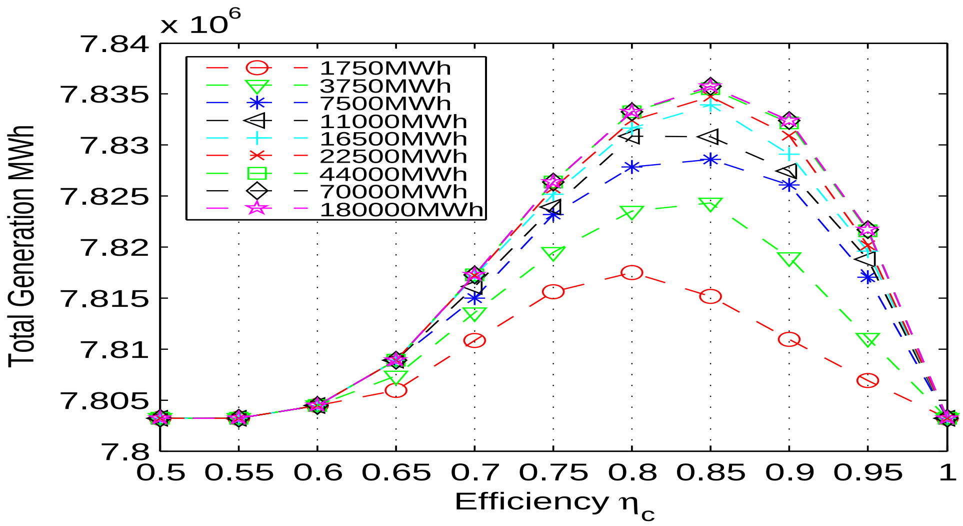

Figure 4.17: Total generation curve for the NSW demand profile using different storage capacities

Figure 4.17 also shows a reduction in the the difference between the total generation values for all energy storage systems with increasing inefficiencies. This indicates that for a given inefficiency, there is an upper bound on the total generation for a given demand profile. As an example, for an energy storage that is 75% efficient, we observe that any battery above 16500MWh would cause the grid to generate the same amount of energy to minimise the generation cost. Interestingly on comparing peak generation of the larger energy storage systems of 44000MWh,7000MWh and 180000MWh in figure 4.12 we see that the largest storage system provides battery peak shaving than the two smaller

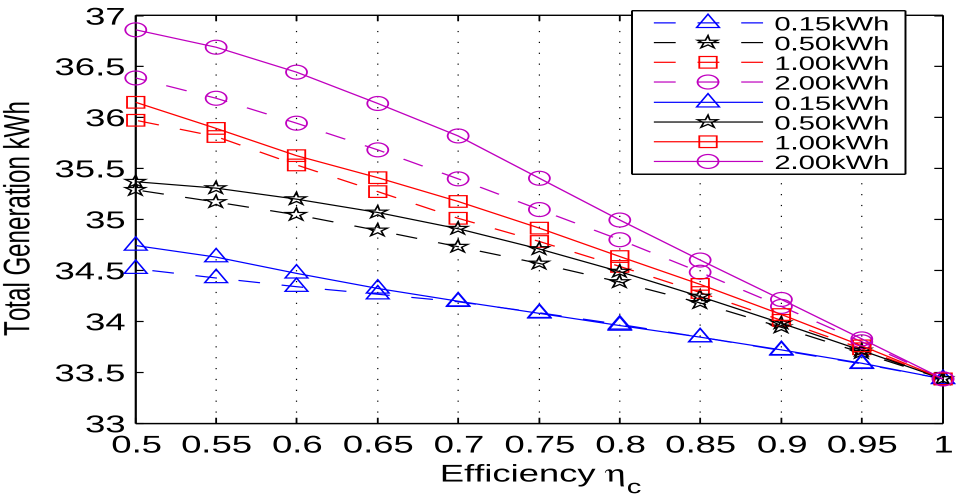

Figure 4.18: Total generation with and without RTP for the house1 demand and increasing storage capacities. The solid lines show the total generation with RTP and the dashed lines show the total generation without RTP.

storage system for efficiencies between 100% to 85% in our simulations. However, the total generation graph in figure 4.17 shows that the same amount of energy in is drawn by all three storage systems. Therefore, though larger energy storage system can reduce the peak further, the total generation graph indicates that it might be more useful to use the smaller and cheaper storage system, since it provides the same cost savings as the larger storage systems.

The house1 total generation graph in figure 4.18 shows that the total energy in the grid increasing with increasing efficiency for all energy storage devices. As expected, the larger batteries are able to store more energy and provide better peak shaving, which causes the larger storage devices to have a higher total generation than the smaller batteries. Therefore for both aggregate and individual household schedules, since the inefficiency of a battery in general increases the total amount of energy consumed, it is necessary to take into consideration the cost associated with the increase in total generation. Therefore, if the utility was to provide a user with a smaller energy storage that is inefficient, the user also has to consider the increase in total generation and cost when using the provided battery.

4.5.2 Peak shaving with Real-time Prices

It has been suggested that the utility use real-time pricing to reduce the peak demand in the grid, allowing users to shift their demand during peak periods to low peak periods [5].

The use of real-time pricing $\gamma(.) \geq 0$, changes the peak shaving and the generation schedule of the system, since the total cost of the system now depends on both the cost of generation as well as the real-time prices set by the utility given as $\sum_{t=1}^{T} \gamma(.) N(g^*(t))$. Due to these changes to the generation schedule, this section focuses on describing the peak shaving capabilities of the system with real-time prices when using inefficient energy storage.

The pricing data used for our simulations are taken from the AEMO, for NSW for the month of March 2012. The pricing data is used for both the household and state data, and is synchronized to match with the time of day for each household demand data set. In this section, we assume that the user behaviour for the house and state data are the same during the day and that the price peaks occur during peak demand, reflecting the strain on the grid. Using these assumptions we will investigate the changes to the generation focusing on the two topics given below,

1. Peak shaving for state and household demand data with real-time prices, using inefficient energy storage.
2. The total energy with real-time prices for both the state and household demand using inefficient energy storage.

4.5.2.1 Peak Shaving with Time Varying Cost

The charging of an energy storage system is influenced by the time varying cost that increases and decreases according to the demand peaks and troughs respectively. According to the demand and price profile for house1, shown in figure 4.10, the peak generation of the household without using an energy storage system is 1.702kW. This peak generation can be reduced when using energy storage systems as shown by the solid lines in the peak generation vs efficiency graph in figure 4.13. The figure shows that for the largest energy storage system of 2kWh which is fully efficient the peak can be reduced from 1.702kW to 0.75. Even when the efficiency of the 2kWh battery is 50%, the generation peak can be reduced to 0.8kW. For the same figure, the smallest energy storage system shows that it can reduce the peak generation of the grid from 1.702kW to 1.4kW. This reduction in the peak generation is also possible for batteries that are up to 50% efficient for our simulations. Because of this the household peak generation shows that with real-time energy prices, the peak generation of the grid can be reduced when using batteries with charging inefficiency. Additionally, since the same amount of peak shaving can be achieved for the smaller energy storage systems, the mutual benefit discussed in section 4.5.1.1 also applies when using real-time prices.

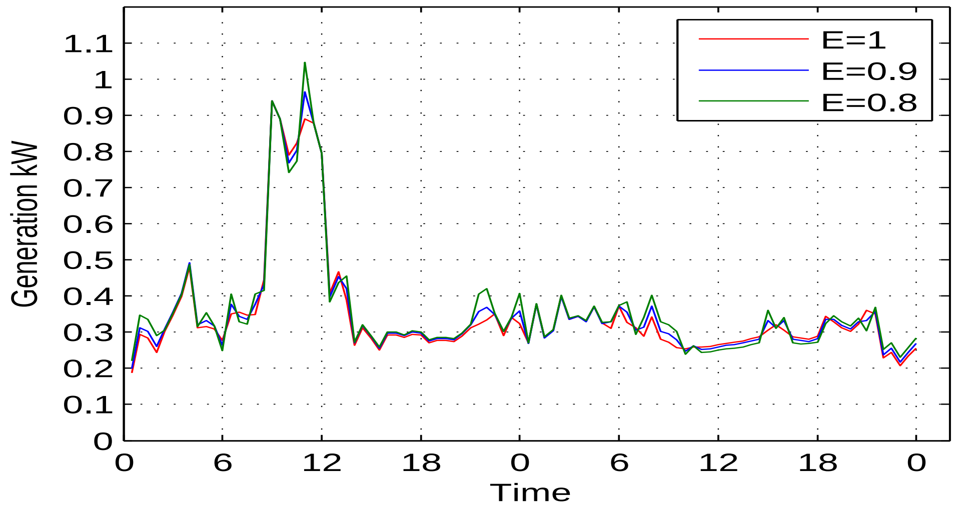

Figure 4.19: Generation schedule with RTP for the house1 demand profile using batteries capacity 0.5kWh and increasing inefficiency

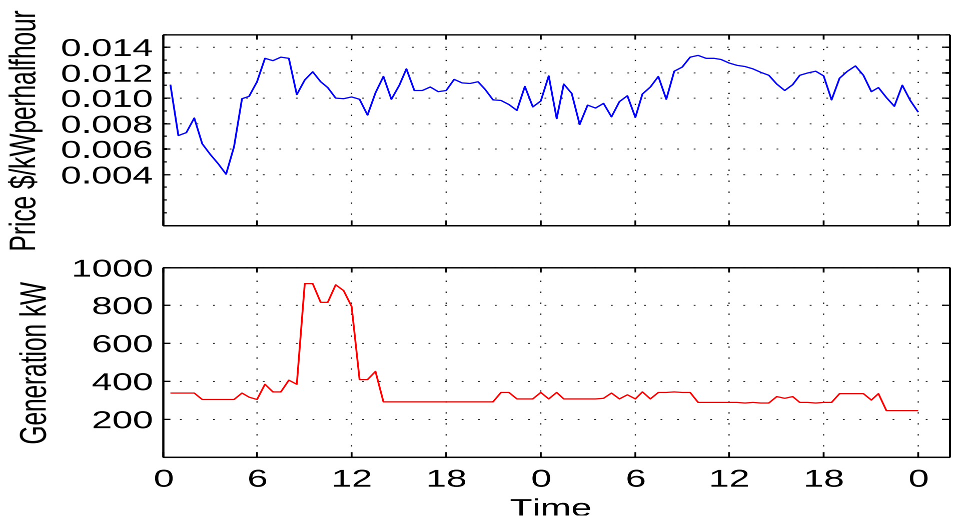

Figure 4.20: Generation schedule for the house1 using a 90% efficient battery with capacity 0.5kWh and real-time price signals

Comparing the peak shaving performance for house1, with and without time varying cost in figure 4.13 shows that the peak shaving performance without time varying cost is better than with time varying cost. This is because without time varying costs, the optimal scheduling behaviour minimises generation of the system to minimise the generation cost as explained in section 4.5.1. But with real-time prices, the optimal solution has to minimise the product of the generation cost and time varying cost $\gamma(.)$. The optimal solution in equation (4.1) shows that the generation of the system fluctuates according to the expression $N^{'}(g^*(t)) = \big[(1+\eta_c)\sum_{\tau=t}^{T-1} \underline{b}^*(\tau) - \bar{b}^*(\tau) + \underline{C}^*(t) - \bar{C}^*(t) - \underline{D}^*(t) + \bar{D}^*(t)\big]^+ / 2\gamma(t)$, and that the marginal generation cost is constant $CONST(t')$ while the battery is charging or discharging when $b^*(t') \in (0, B)$ and $t' \in (0, T)$. As a result, the generation of the system will change according to the expression $g^*(.) = CONST(.)/\gamma(.)$, in the interval that the marginal generation cost is constant.

Because of this the generation now not only depends on the the future saturation and starvation of the energy storage, but also depends on the time varying cost, which could increase the generation if it is not set to reflect the changes in demand as our price data set. As a result it is possible for the generation to increase when the time varying cost is small and increase the peak generation of the grid due to the demand price mismatch. However, though the generation in the grid increases, the optimal solution will be to still minimise the overall generation cost. An example of this behaviour can be seen from figures 4.3 and 4.19, which shows the generation schedule of a 0.5kWh battery with increasing inefficiency with and without real time prices respectively. On comparing both figures we see that with real-time prices in figure 4.20, the peak does not occur due to shaving the original demand peak, but instead occurs when charging the battery during the price and demand trough just before 12PM on the first day. This creates a higher peak that is shifted to a different time, which is a result of a not setting prices to reflect the overall demand in the grid. The implications of not setting proper pricing signals then suggests that the utility might actually end up increasing the peak in the grid due to all users charging more during low price periods. Therefore the utility needs to set prices based on the expected demand profile for users, so that the peak demand in the grid can be reduced by using energy storage. As a result, if electricity prices were set to reflect demand peak and troughs, user energy storage will help reduce the peak demand for the utility and reduce the energy bill for the user.

As previously discussed section 4.5.1.1, the smaller energy storage system provides an equal amount of peak shaving for a certain range of inefficiencies. Furthermore, the larger energy storage devices provide less peak shaving as the efficiency decreases. However, due to the pricing signals that are too low during low demand periods as shown in figure 4.10, storage systems larger than the peak demand of the household would have a higher peak generation, due to the storage system fully saturating which is an anomaly resulting in not having prices change in reference to the demand profile. Figure 4.13, shows that for the 2kWh battery the peak generation increases when the efficiency decreases to 70% and then decreases as efficiency decreases further. This characteristic for inefficient energy storage devices can by explained by the charging and generation schedules shown in figures 4.21 and 4.22 respectively. The generation schedule of the figure shows that the peak generation occurs just before 6am on the first day. During this time, the 2kWh battery fully charges for efficiencies 75% and 70% and only partially charges for a 65% efficient energy storage device. Since the energy storage only partially charges when it is 65% efficient, the peak generation of the grid will reduce. Again, this anomaly is caused by the capacity of the battery and the low time varying prices.

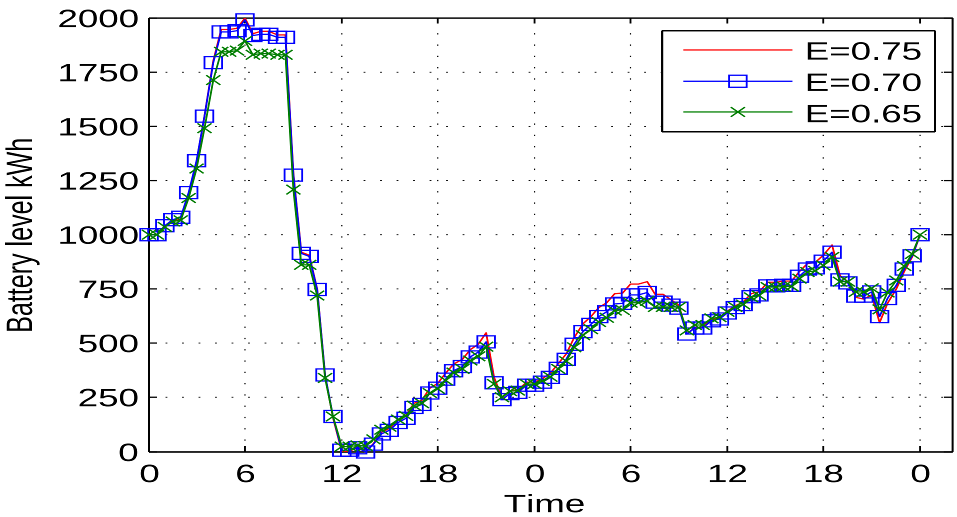

Figure 4.21: Charging schedule for the house1 demand using 2kWh batteries with increasing inefficiency

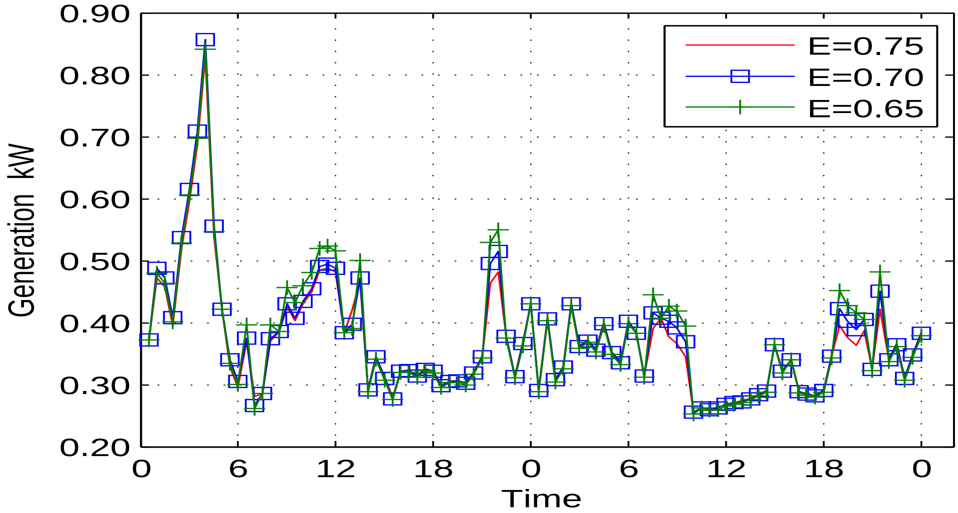

Figure 4.22: Generation schedule for the house1 demand using 2kWh batteries with increasing inefficiency

During low price periods, the energy storage system will maximise the usage of the battery, causing the system generate $g^*(t) = d(t) + b^*(t)$, where $b^*(t) \in (0, B]$. Therefore a large battery will have an energy level much higher than a small battery causing a new peak in the grid at time t. Because of this, the peak generation for the larger battery is actually caused by charging the energy storage device. If we were not using a prerecorded trace, this would push up the price at that time, and hence reduce the peak. This results in the larger battery of 2kWh increasing and decreasing (figure 4.18) its peak generation as the efficiency decreases, since the peak generation now depends on the energy level of the battery during the price troughs. In contrast for smaller batteries, since $g^*(t) = d(t)+b^*(t)$, is smaller than the original peak demand of the grid, the peak generation occurs when shaving the original peak demand of the grid.

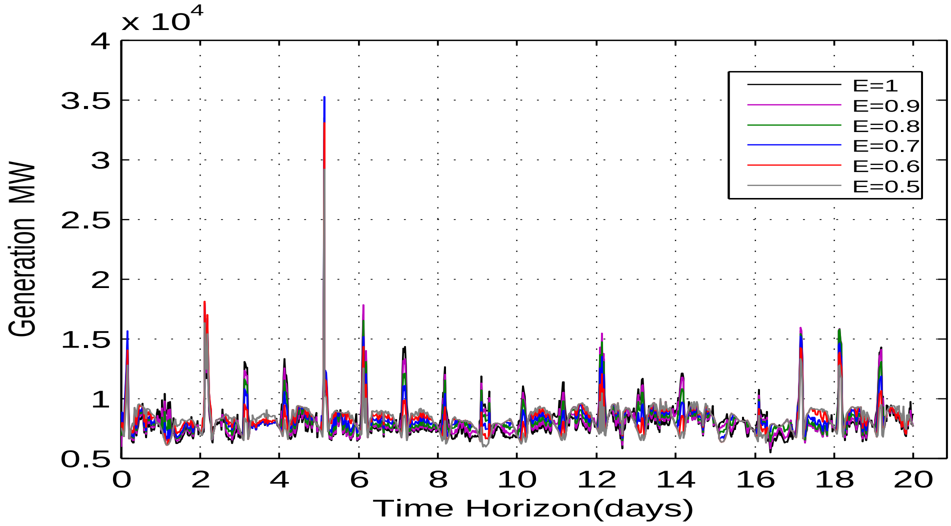

Figure 4.23: Generation schedule with RTP using the NSW demand profile, for energy storage systems with capacity 22500MWh and increasing inefficiency

The increase in peak generation due to large storage capacity and low real-time prices is also seen for the NSW demand in figure 4.11. The peak generation for NSW in figure 4.24 shows that except for the smaller energy storage of 1750MWh, all other energy storage devices have higher peak than the peak demand without energy storage. Additionally, the figure also shows that the large storage devices have a higher peak generation than the smaller energy storage devices. The NSW demand in figure 4.11 shows a peak of 10580MW on the 16th day of the 20 day horizon. However, according to figure 4.23, the peak generation when using an energy storage of 22500MWh is visible on the 5th day of the horizon. According to figure 4.11, the demand and price trough is the lowest on the 5th day for the NSW data. As a result, the peak in generation for the grid is created by charging the storage device fully. Furthermore, since the energy storage used for the simulation is much larger than the peak demand in the grid, when the storage device fully charges, the peak generation in the grid increases to a value higher than the original peak demand similar to the household data. Also since the time varying prices are extremely low on the 5th day, it is even optimal to charge the largest energy storage of 180000MWh for our simulations. Similar to the household data this proves that for larger energy storage devices, the peak in the grid is created due to charging the storage system during low price signals in the grid and not from the peak generation due to saving the actual peak demand in the grid.

Section 4.4.1, showed that without time varying costs the when using energy storage generation is bounded by the demand peaks in the grid. Similar to this, with real-time prices the marginal generation cost with energy storage is bounded by the peak marginal generation cost of the grid without energy storage. That is, $\gamma(t)N'(g^*(t)) \leq \gamma(t_1)d(t_1)$. Where $t_1 \in (0, T)$ is the time at which the marginal demand costs are maximum. Based on this and the convexity in cost, the generation is bounded by $N'(g^*(t)) \leq \gamma(t_1)d(t_1)/\gamma(t)$. Showing that the generation peaks when $\gamma(t) \leq \gamma(t_1)$ allowing the generation to actually increase beyond the demand peaks, provided that the condition also holds $g^*(.) \leq d(.)+B$ given by equation (3.4).

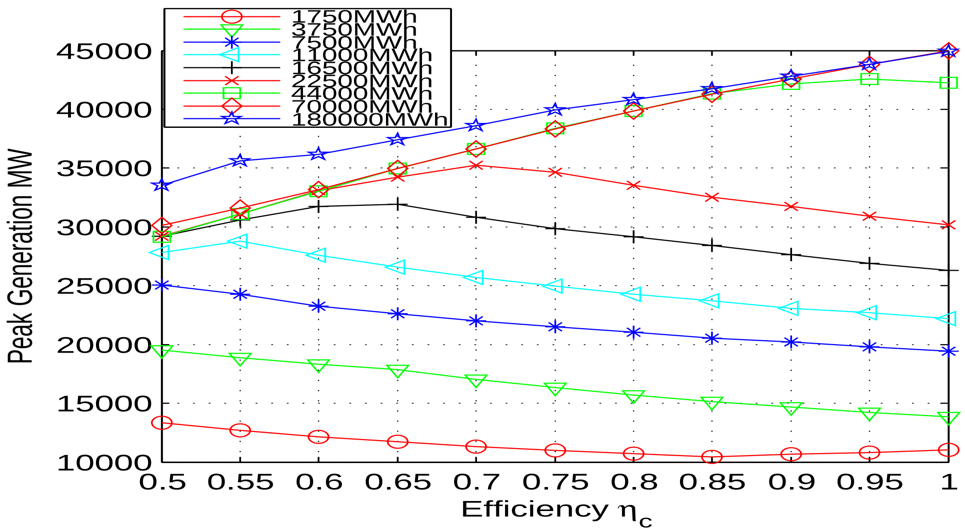

Figure 4.24: Maximum generation vs efficiency with RTP using the NSW demand profile for increasing storage capacities

In conclusion, the simulation show that the peak generation in the grid can be reduced by setting appropriate real-time prices and using the correct storage capacities. With smaller energy storage devices, it is possible for the utility to provide the user a with a battery with lower inefficiency, and still get the same amount of peak shaving, since the smaller batteries provide the same amount of peak shaving for a range of efficiency values. However, when using larger energy storage devices, the peak demand in the grid is actually created due to the charging of the storage device. This behaviour can result in the peak generation of the grid actually increasing beyond the original demand during low price and demand troughs. Furthermore, since this peak is created due to the charging of the storage device, the peak demand will shift to the the time when the low price and demand occurs within the horizon.

4.5.2.2 Total Generation with real-time prices

The inefficiency of a storage device affects the total energy consumed and the total cost for the utility and user. The NSW total generation in figure 4.25, shows the total generation of a storage device increasing with increasing inefficiency up to a certain efficiency and then decreasing when the efficiency decreases further. As an example, figure 4.25 shows the total energy generated by a 60% efficient storage of 11000MWH would be higher than a 50% storage device of the same capacity similar to the behaviour without time varying prices in section 4.5.1. This increase and decrease in generation is seen due to not charging the storage as often at higher inefficiencies due to the conversion losses. However, when comparing the total generation with and without real-time prices, the total generation with real-time prices can be higher. This is due to the system generating more depending on the price and demand fluctuations. However, though the system generates more, the optimal schedule will still minimise the overall cost for the utility and the user.

Additionally, for our simulations the artifact of the low price and large energy storage capacities show that only the smaller energy storage systems provide peak shaving. Then obviously for peak shaving and reduced total cost a utility would choose a smaller storage device to be used for the NSW state data according to our simulations. Similarly, the house1 data in figure 4.18 shows the total generation increasing with increasing efficiency for all energy storage devices. Obviously, for the total generation to decrease similar to the NSW state data, the household has to use batteries with much higher inefficiency values. Further, since the peak shaving reduces with increasing inefficiency and the total generation increases with increasing inefficiency and battery capacity, the utility has to choose an energy storage considering not only the peak shaving but also the total costs by using a larger and inefficient storage device.

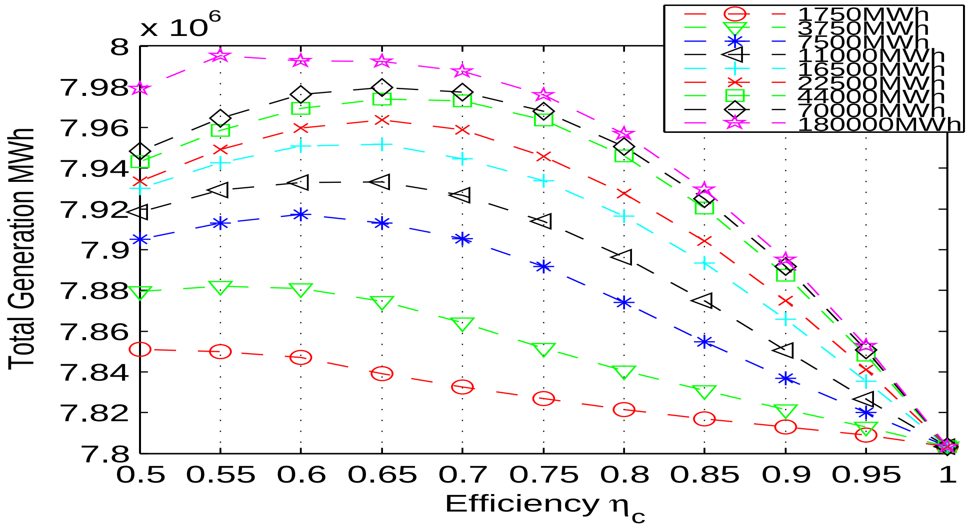

Figure 4.25: Total generation with RTP for the NSW demand using different storage capacities

4.5.3 Peak Shaving with Rapidly Increasing Prices

The increase in energy prices affect the optimal decisions on charging and discharging an energy storage device for peak shaving. This is especially true in the long term, for rapid increasing prices. Therefore this subsection gives an overview of the possible reduction in peak generation under rapid price increases. The figures 4.26 give the peak generation with exponentially increasing $\gamma(.)$, for both a small and large storage system using the NSW state demand profile. The figure shows that in general, the increase in inefficiency, reduces the peak shaving in the grid. Especially at low price increases, the peak shaving decreases for both storage capacities. In our examples for an efficiency of 50% it can be seen that the energy storage does not charge at all for the lower price increases below 10^-4. Furthermore, it can be seen that at the peak generation gap between the larger energy storage and smaller energy storage decreases faster with increasing inefficiency. At higher inefficiency values, the larger energy storage system will eventually provide the same peak shaving as the smaller storage device as shown in the figure 4.26e.

Interestingly, when the price increase is substantially high at 10^-2 per half hour, it can be seen that both small and large storage devices create a much larger peak than the original peak demand of 10580MWh. This is because at such high rates of increase, both the energy storage devices remain fully saturated for the entire horizon. As a result, the storage device will not be utilised fully at extremely high rates of increase which is an artifact of setting the terminal storage level to maximum capacity. Because of this, at such price increases, it is better for the utility to not use an energy storage device. Fortunately, for more realistic price increases, both storage devices show a reduction in peak shaving which only decreases due to the increase in efficiency of the storage device.

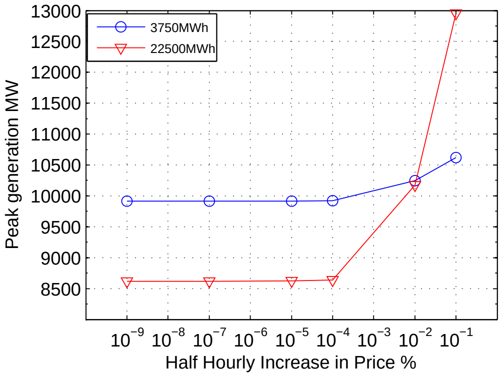

(a) Maximum generation vs price increase for fully efficient energy storage systems

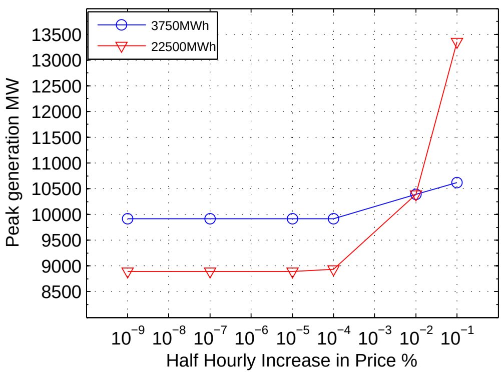

(b) Maximum generation vs price increase for 90% efficient energy storage systems

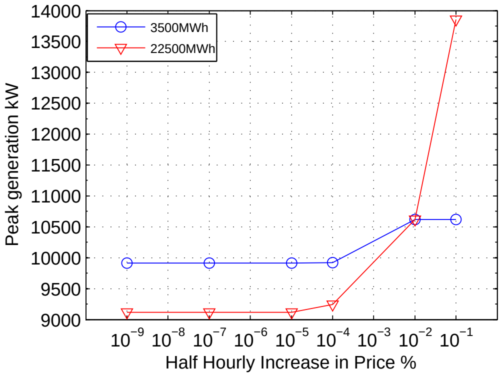

(c) Maximum generation vs price increase for 80% efficient energy storage systems

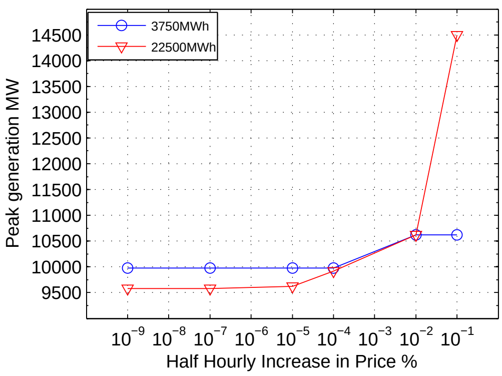

(d) Maximum generation vs price increase for 70% efficient energy storage systems

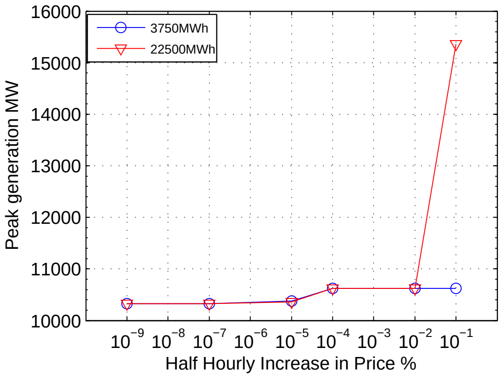

(e) Maximum generation vs price increase for 60% efficient energy storage systems

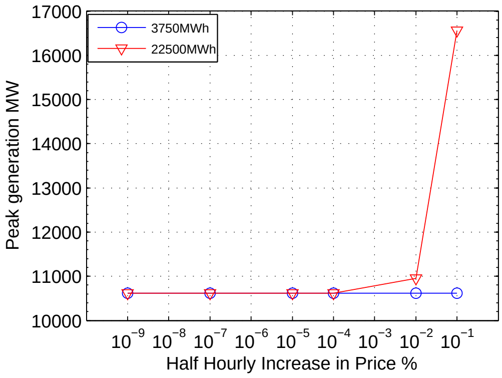

(f) Maximum generation vs price increase for 60% efficient energy storage systems

Figure 4.26: Maximum generation for rapidly increasing prices for different storage capacities and inefficiencies

Chapter 5

Energy Storage with Self-discharge

This chapter presents the structural results and optimal solution for an energy storage device with self-discharge. Using numerical results simulated using dynamic programing, the structural properties of the charging and generation schedule are discussed for increasing self-discharge and storage capacity. Further, the performance and behaviour with and without arbitrary price increases of the storage and generation schedule for peak shaving is discussed.

5.1 Self-discharge

The energy lost in a storage device during the storage phase is known as the self-discharge loss [52]. Self-discharge can occur due to chemical reactions in certain batteries or due to friction in kinetic energy storage systems such as Flywheels. This internal loss in energy can result in the storage device having a lower energy level over time. The self-discharge L, in our model gives the percentage of energy lost during some time period t, which can be hours, days or even months. We model the energy loss factor of the storage device based on the self-discharge as $\beta = 1-(L/t*100) \leq 1$, where $(\beta * b^*(t))$ gives the amount of energy remaining in the battery during each time step after self-discharge, where $b^*(t) \in [0, B]$ and B is the capacity of the storage device. Table (5.1) below gives an example of the self-discharge percentages for selected storage systems.

Type of Storage	Lead Acid	Nickel Cadmium	Lithium ion	Flywheel
Self-discharge	2 to 5% a month	5 to 20% a month	approx 1% a month	up to 2.5% of the rated power

Table 5.1: Self-discharge values for selected energy storage systems [1] [21]

5.2 Verifying Solution for an Energy Storage System with Self-discharge Losses

The self-discharge in a storage device decreases the available energy level $b^*(t)$ in a battery over time. This impacts the optimal scheduling decision for a system using energy storage which relies on storing energy to supply during peak demand and pricing periods. In particular, this loss in energy results in a change in the generation and charging behaviour of the storage for peak shaving in the grid. In chapter 3 we showed that for a system using an ideal storage device between the generator and the user to reduce cost, the long term infinite horizon, infinite cost problem can be studied using a finite horizon model, provided that the finite horizon optimal charging schedules with the terminal conditions $b(T) = 0$ and $b(T) = B$, converges at some time $t \in (0, T)$. Such a time at which convergence occurs was shown to be a renewal point for a given look ahead T at which future demand and pricing signal beyond the horizon T, will not affect the scheduling decisions before any $t' < t$. Similarly, here we will show numerically that a finite horizon model can be used to study the optimal scheduling behaviour for a storage system with self-discharge since renewal points exists even with energy losses over time.

Furthermore, since we are interested in finding the properties of the charging and generation schedules with generation cost and arbitrary price increases, the finite horizon model will allow us to decouple the long term problem to be able to numerically study the structure of the scheduling decision similar to Chapter 4. Additionally, based on these structural properties we will further investigate the impact on peak shaving with generation cost and arbitrary price increases for storage devices with increasing capacity and self-discharge percentages.

5.2.1 Renewal Points for an Energy Storage with Self-Discharge

Here we compare the charging schedule for the finite horizon problem for two different capacity storage devices with high self-discharge value between chemical storage and fly-wheels to show renewal points even at high self-discharge rates. Figures 5.1a and 5.1b show the 20 and 30 day charging schedule for a 3750MWh storage device with 5% a day self-discharge. Here $bf1$ and $bf2$ give the optimal charging solutions for the storage device with terminals energy level $b(T) = 0$ and $b(T) = B$ respectively. Where T gives the horizon length and B is the capacity of the storage device. On inspecting figure 5.1a, it can be seen that both $bf1$ and $bf2$, have the same charging schedule for any time before the 20th day when the storage saturates above. Similar behaviour is seen in figures 5.1c and 5.1d, showing the 20 and 30 day charging schedule for a 11000MWh storage device with 5% a day self-discharge respectively. In figure 5.1c, the final renewal point is seen on the 19th day when the storage fully discharges indicating that the optimal solutions converge. This convergence happens if $bf1$ saturates above or $bf2$ empties below as stated in theorem 7 in Chapter 3. This shows that convergence occurs even when using a storage device with self-discharge.

A natural result of having renewal points is that future demand and price trends beyond the look ahead point T, do not affect the scheduling decisions before the renewal point. This decoupling of the charging schedule is clearly visible if we extend the 20 day horizon and observe the scheduling behaviour for a longer 30 day time horizon. Figures 5.1b and 5.1d show this extended 30 day time horizon and its renewal points. For the smaller storage of 3750MWh figure 5.1b shows the scheduling to be the same as the 20 day schedule for the same storage device in figure 5.1a. Moreover, the 30 day charging schedule also saturates above on the 20th day, similar to the 20 day horizon in figure 5.1a.

Even with the larger 11000MWh storage, the scheduling for the 30 day horizon in figure 5.1d, shows that the storage device charges in the same pattern as its respective 20 day demand horizon in figure 5.1c and also shows that the 19th day renewal point occurs when the storage empty's below. Therefore, as expected the numerical results show that for a device with self-discharge having renewal points for the finite horizon, it is possible to decouple the long term infinite horizon problem and use the finite horizon solution to investigate the structure of the charging and generation schedules.

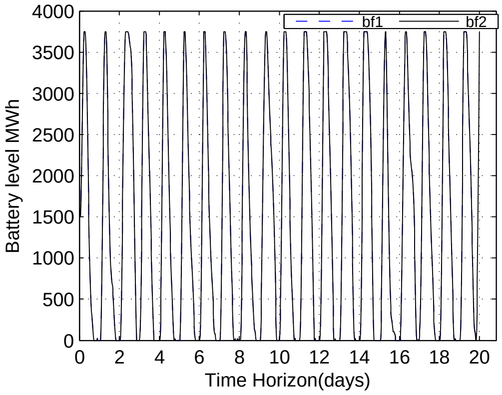

(a) The 20 day charging schedule for a 3750MWh storage system with 5% a day self-discharge

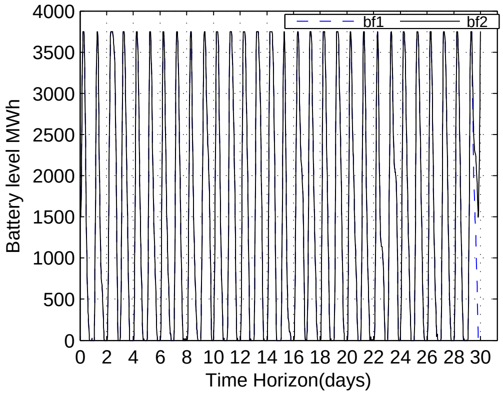

(b) The 30 day charging schedule for a 3750MWh storage system with 5% a day self-discharge

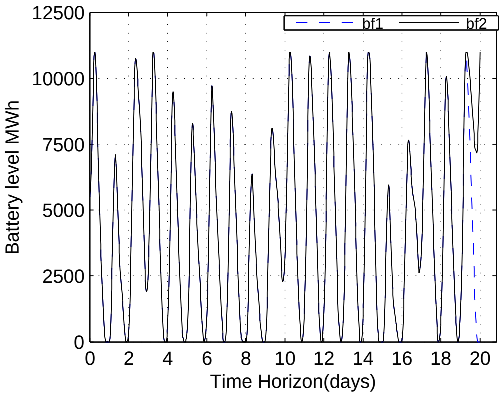

(c) The 20 day charging schedule for a 11000MWh storage system with 5% a day self-discharge

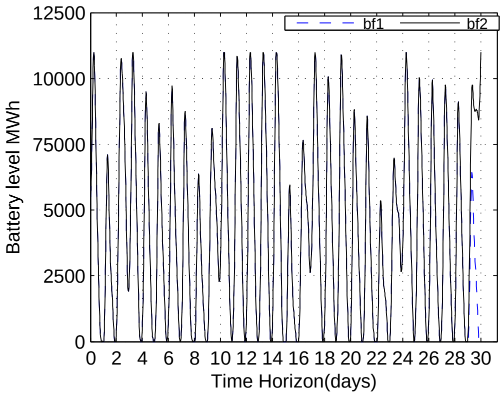

(d) The 30 day charging schedule for a 11000MWh storage system with 5% a day self-discharge

Figure 5.1: The 20 and 30 day charging schedules for energy storage systems with 5% a day self-discharge showing renewal points

5.3 Optimal Solution for an Energy Storage System with Self-discharge

The optimal marginal generation cost for an ideal energy storage, remains constant when the energy level in the battery $b^*(t) \in (0, B)$ as explained in Chapter 3. However for a storage with self-discharge, since energy is lost over time, the marginal generation cost too changes according to the equation given below,

$$\gamma(t)N^{'}(g^*(t)) = \big[\sum_{\tau=t}^{T-1} \beta^{\tau-t}(\underline{b}^*(\tau) - \bar{b}^*(\tau))\big]^+ \tag{5.1}$$

$$= \beta^{-t}\big[\sum_{\tau=t}^{T-1} \beta^{\tau}(\underline{b}^*(\tau) - \bar{b}^*(\tau))\big]^+ \tag{5.2}$$

The above equation shows that the optimal marginal generation cost is influenced by the future saturation and starvation of the storage and the self-discharge factor β. The Lagrange multipliers $\underline{b}^*(.)$ and $\bar{b}^*(.)$) are non negative only when the storage fully discharges or fully saturates respectively. This results in an increase in marginal generation cost just after saturation and a decrease in the marginal generation cost just after the storage fully discharges, similar to an ideal storage device. However, unlike the ideal storage device, the marginal generation cost for the non-ideal storage does not remain constant when $b^*(t) \in (0, B)$, but instead increases due to the self-discharge $\beta < 1$, which causes the optimal schedule to generate more to have a desired storage level due to the energy loss from the self-discharge of the battery. This causes the structure of the charging and generation schedule to change due to the self-discharge of the energy storage system.

The optimal solution5.2 shows that the marginal generation cost increase exponentially since the optimal solution $N'(g^*(t)) = \beta^{-t}\big[\sum_{\tau=t}^{T-1} \beta^{\tau}(\underline{b}^*(\tau) - \bar{b}^*(\tau))\big]^+$, increases exponentially for $b^*(t) \in (0, B)$ due to β^{-t}. However, since this exponential increase in β is very small, the increase in the marginal generation cost is also very small and linear for very small exponential increase. Because of this and due to the convexity in the marginal generation cost in $g^*(t)$ the generation schedule too will have this small exponential increase which will appear to be linear in the simulation as shown in figure 5.2 for storage systems with self-discharge.

Then, since we see that the self-discharge impacts the optimal scheduling decisions, this chapter will continue to use numerical simulations to study the structure of the storage schedule to show the charging and generation schedule trend. Furthermore, these results will be used to see how the scheduling performs with peak shaving for the utility with constant γ and with arbitrarily increasing prices.

5.4 Structural Properties

This section discusses the structural properties of the charging and generation schedules for storage devices with a range of low to high self-discharge values (5.1), based on the optimal solution and numerical results obtained using dynamic programming. In particular, we show that the self-discharge rate of the storage device affects the generation schedule so as to not have the generation constant when $b^*(.) \in (0, B)$ as an ideal energy storage device. But instead, the generation exponentially increases in the interval while the battery is charging and that the storage tends to empty more frequently and never fully saturate at high self-discharge rates.

5.4.1 Generation and Charging Schedule for Energy Storage Systems with Self-discharge

Introducing a non-ideal storage device between the utility and the user influences the amount of power drawn from the grid, and affects the optimal generation in the grid which is now not static, but instead includes a new demand which is influenced by the energy drawn and supplied by the storage device. Figure 5.2 shows the optimal scheduled generation for such energy storage devices of capacity $B = 22500MWh$ and increasing self-discharge losses. Without self-discharge, as shown in figure 5.2a an ideal energy storage system shows the generation to remain constant between periods in which the storage device is charging and $b^*(t) \in (0, B)$. Moreover by observing the charging schedule for the same storage in figure 5.3a, we see that the generation increases once the storage device fully saturates, and decreases when the energy is completely discharged from the storage, which is the behaviour seen by an ideal storage device as explained in chapter 3.

For a storage device with self-discharge, the above mentioned scheduling behaviour changes due to the change in the available energy $b^*(t)$ with time. Figure 5.2b and 5.3b shows the respective generation and charging schedules for such a 22500MWh capacity storage with a 5% a month self-discharge. Similar to an ideal energy storage system, the non-ideal storage system will increase its generation in jumps after it fully saturates, and decreases the generation in downward jumps once it fully discharges. But, within periods where $b^*(t) \in (0, B)$, the graphs shows a linear increase in the generation due to the small exponential increase of β^{-t} as explained in section 5.3. Furthermore, when the self-discharge rate increases for a similar capacity storage from 5% a month to 1.25% per half hour as shown from figures 5.2b to 5.3f this increase in generation, increases further. Especially for larger self-discharge rates such as 0.5 % per half hour of flywheels as shown in figure 5.3e, the energy storage device does not fully saturate at all, but empties more frequently than for a storage device with lower self-discharge rate as shown by the charging schedule in figure 5.3e. Then, since the storage only empties at higher rates of self-discharge, the generation schedule will always increase while the storage is charging and then decrease when the storage is empty, repeating this cycle each time the storage charges and discharges.

Figure 5.5 compares the generation schedule with time for increasing self-discharge rates when using a 22500MWh capacity energy storage system. Interestingly, for a given demand profile, it can be seen that if the ideal energy storage empties, which causes a downward jump in generation, then any energy storage with self-discharge will also have a downward jump at that particular time, which is due to the storage discharging fully. Generally, a battery will discharge during peak demand in the grid. Therefore, if it is optimal for the ideal storage system to fully discharge to reduce the peak demand, then a storage with self-discharge will also fully discharge during such peak periods. Similarly, if a storage with higher self-discharge has upward jumps in generation, which is a result of the battery being fully saturated, then any self-discharge rate less than the given self-discharge rate will also have upward jumps. This shows that if it is optimal for a storage with self-discharge to fully saturate at a particular through, then it is also optimal for a storage having a lower self-discharge rate to saturate at the same time.

Based on the numerical results and the derived optimal solution, it can be seen that a storage with self-discharge increases the generation in the grid due to the energy losses. In particular, for a storage device, the generation will not remain constant when $b^*(t) \in (0, B)$, but instead increase exponentially due to self-discharge of the storage device, that requires the battery to charge when the storage loses energy. Then using these structural properties, the remainder of this chapter will focus on understanding the impact of the optimal solution on peak shaving with constant γ and rapidly increasing prices.

5.5 Peak Shaving

The utility's motivation for providing storage is to reduce peak load on its network. However since most storage devices are not ideal and have losses due to inefficiency and self-discharge, the peak shaving benefit decreases. Similar to the discussion on peak shaving in section 4.5 on inefficient storage, this section investigates the peak shaving benefit under constant and arbitrary price increases for storage systems with self-discharge. Further, the impact of peak shaving with increasing self-discharge rates and the structural behaviour of the optimal schedule with arbitrary prices are discussed in the section.

5.5.1 Peak Shaving with Constant γ

Recall from chapter 4 that the peak demand in the grid can be reduced by using a storage device to store energy during low peak periods and use this energy to reduce the generation during the high peak demand period. When scheduling an energy storage system with self-discharge, the optimal solution needs to factor in the future saturation and starvation of the storage device and well as keep track of the energy lost due to self-discharge over the given horizon. Therefore, when shaving the peak with a storage device having self-discharge, the actual available energy for shaving the peak in the battery during peak demand periods can be less, reducing the peak shaving in the grid. Figure 5.4 shows the peak generation with increasing self-discharge rates for storage systems with a range of capacities. The self-discharge rates shown are for chemical storage systems with 5% a month(0.0003472), 20% a month(0.0013889), 5% a day(0.0010416) and 20 % a day(0.00416) self-discharge, and flywheels with 0.5 per half hour(0.005) and 1.25 per half hour(0.0125) self-discharge.

The peak generation graph shows that for relatively lower self-discharge values such as in chemical storage systems, the peak shaving increases with increasing energy storage capacity. Moreover, when the self-discharge percentage increases, the peak shaving benefit decreases, since more energy is lost during the storage phase for the higher leakage values. This results in lower energy levels in the storage devices to reduce the peak demand. However the peak generation graph also shows that for much larger energy storage systems,

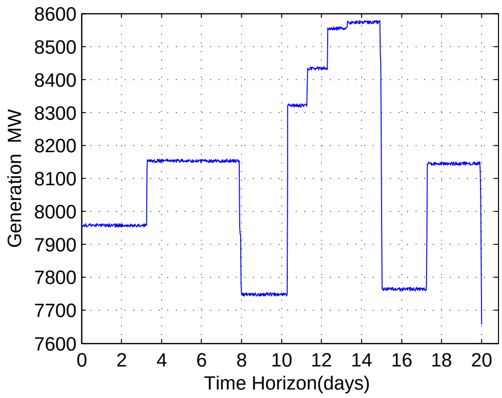

(a) Generation schedule for a 22500MWh fully efficient energy storage system

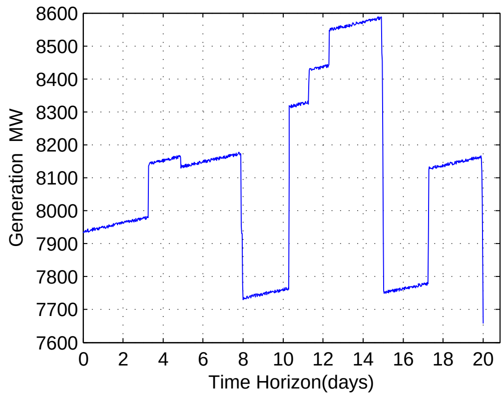

(b) Generation schedule for a 22500MWh energy storage system with 5% a month self-discharge

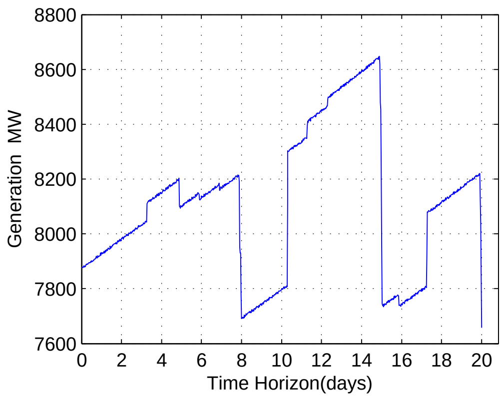

(c) Generation schedule for a 22500MWh energy storage system with 20% a month self-discharge

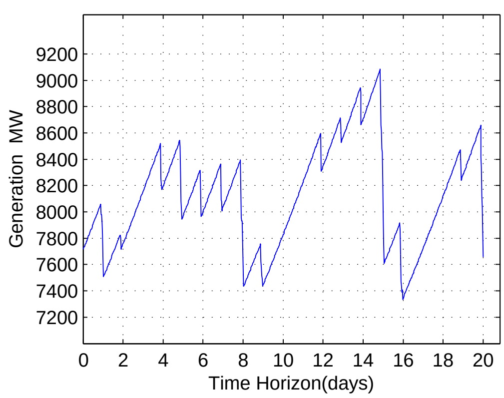

(d) Generation schedule for a 22500MWh energy storage system with 5% a day self-discharge

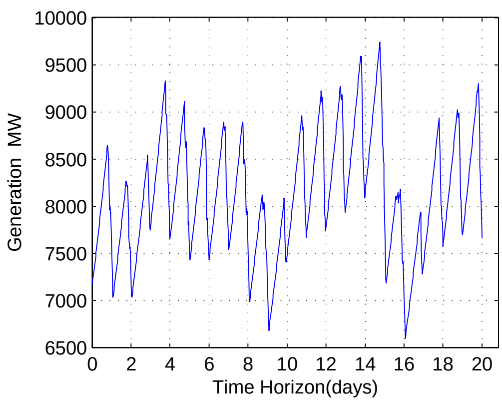

(e) Generation schedule for a 22500MWh energy storage system with 0.5% per half hour self-discharge

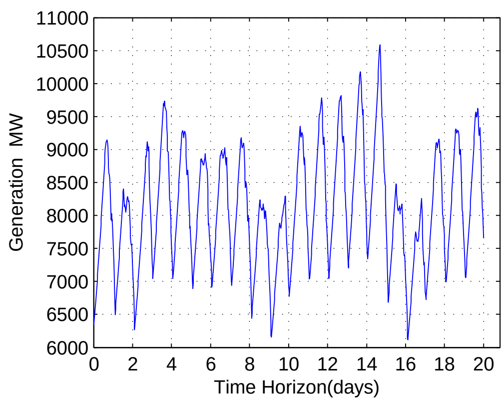

(f) Generation schedule for a 22500MWh energy storage system with 1.25% per half hour self-discharge

Figure 5.2: Generation schedule for a 22500MWh energy storage system with increasing self-discharge losses

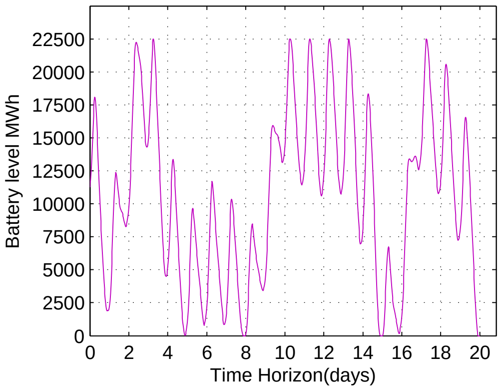

(a) Charging schedule for a 22500MWh fully efficient energy storage system

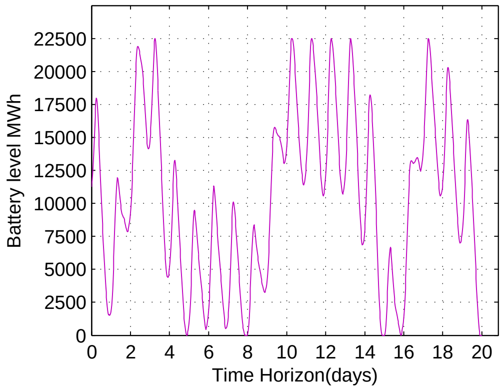

(b) Charging schedule for a 22500MWh energy storage system with 5% a month self-discharge

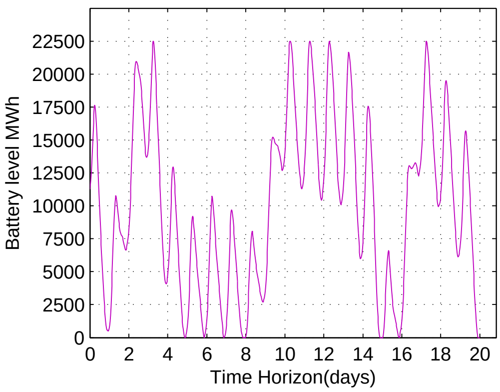

(c) Charging schedule for a 22500MWh energy storage system with 20% a month self-discharge

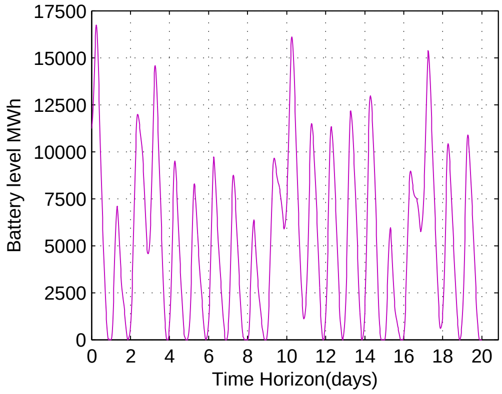

(d) Charging schedule for a 22500MWh energy storage system with 5% a day self-discharge

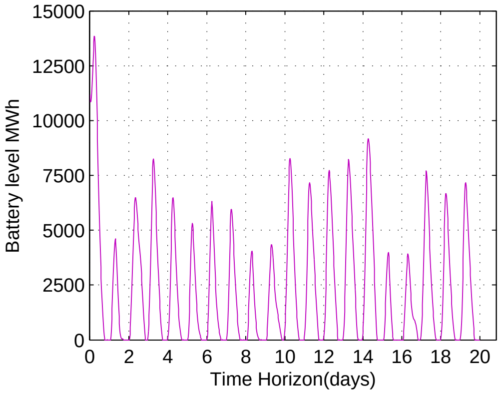

(e) Charging schedule for a 22500MWh energy storage system with 0.5% per half hour self-discharge

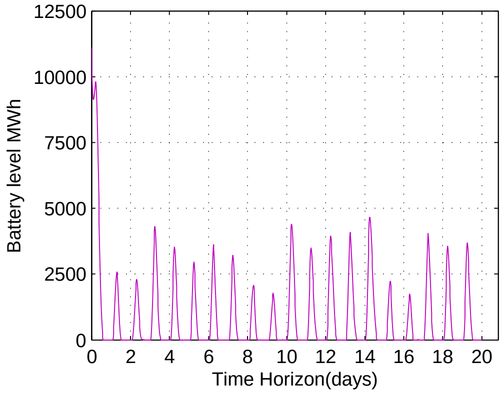

(f) Charging schedule for a 22500MWh energy storage system with 1.25% per half hour self-discharge

Figure 5.3: Charging schedule for a 22500Mwh energy storage system with increasing self-discharge losses

with higher self-discharge rates, increasing the storage capacity will not increase the peak shaving in the grid. As an example, for a 20% a day(0.00416) self-discharge rate, the 11000MWh and 22500MWh storage systems both have the same peak generation according to figure 5.4. Additionally, as the peak shaving of an energy storage increases further to 1.25% per half hour(0.0125), for our simulations we see that there is no additional peak shaving benefit, resulting in the generation being equal to the peak demand of 10580MW for the NSW data.

Figures 5.6 and 5.7 show the storage level and the generation for a 11000MWh and 22500MWh storage system with 20% a day leakage, with the storage device being half full at the start and ending empty at the end of the horizon. The generation schedules in both figures show that the peak generation occurs on the 14th day of the 20 day horizon, which is also the day in which the original peak demand of 10580MW for the NSW data occurs as shown in figure 4.11. Similar to storage devices with charging inefficiency in chapter 4, both the schedules show that for a storage device with self-discharge, there is a maximum amount of energy that can be stored in the battery, for a given demand profile to achieve maximum peak shaving. This is clearly visible by observing the charging schedules just before the peak in figures 5.6 and 5.7. The charging schedules for both figures show that on the 14th day, just before the peak, both storage devices have the same energy level of 10000MWh, which is then used to reduce the peak demand. Therefore we can see that increasing the capacity of the storage beyond a certain optimal capacity will not increase the peak shaving,especially at higher self-discharge rates. This leads to a natural result, for which larger storage devices are useful at lower leakage values, since it increases the peak shaving in the grid. However, as the self-discharge percentage increases, the effective energy level in the storage that provides the maximum peak benefit decreases. Therefore for a certain storage technology with higher self-discharge, it is better to choose the smaller or medium energy storage than a larger energy storage device of the same type.

Furthermore, figure 5.8 giving the charging schedule for the 2000MWh and 22500MWh storage systems with $b(0) = b(T) = 0$, shows the storage device discharging more often for increasing self-discharge rates. Because the storage discharges more frequently at higher self-discharge rates, the increase in generation is caused by the battery charging after it has lost energy, so that it can maintain a certain battery level $b^*(t)$ to reduce the peak demand. Moreover, this loss in energy also results in an increase in the marginal generation cost, which can be especially high for devices such as Flywheels with high self-discharge. Therefore, at higher self-discharge rates, the marginal generation and the generation of the grid increases more rapidly when $b^*(t) \in (0, B)$, minimising the the benefit of using a storage device. In our simulations of the peak generation using the NSW data in figure 5.4, we see that devices such as Flywheels with self-discharge rates above 1.25% a month will not be able to provide peak shaving due to the high energy loss rate.

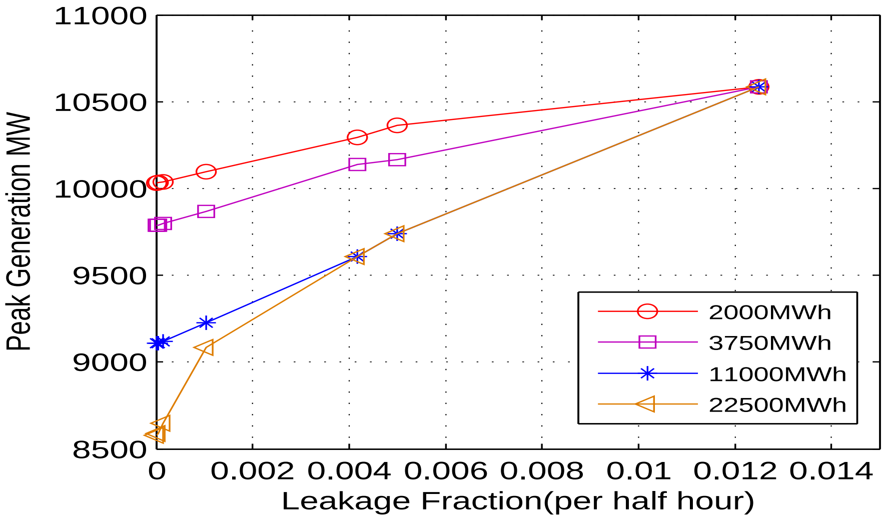

Figure 5.4: Peak generation vs self-discharge for increasing storage capacities

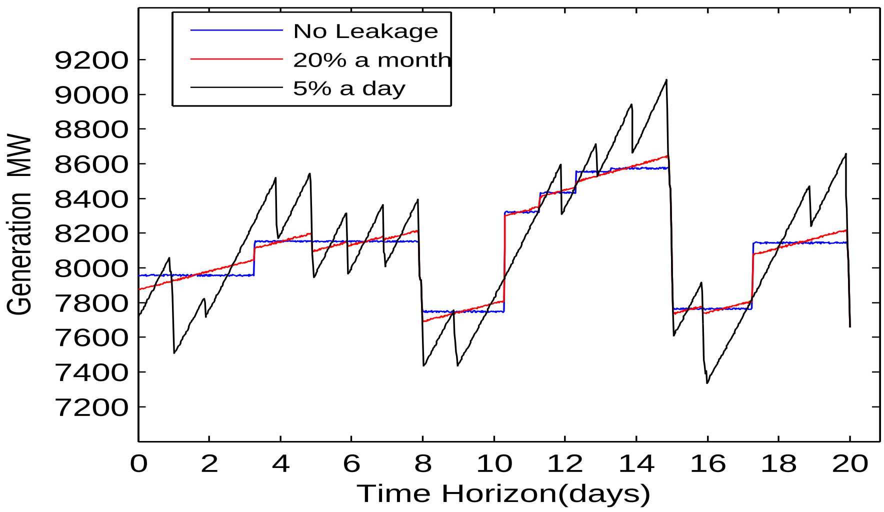

Figure 5.5: Generation schedule for a 22500MWh storage with increasing self-discharge rates

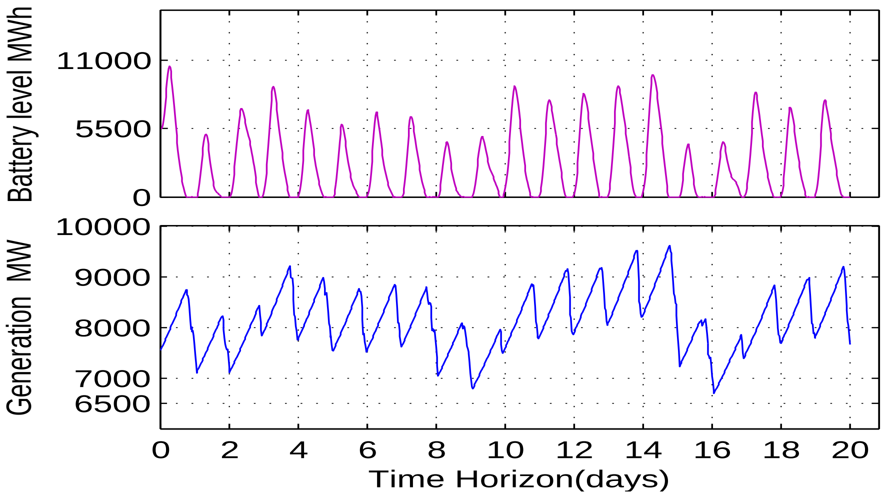

Figure 5.6: Charging and generation schedule for a 11000MWh storage system with 20% a day self-discharge

5.5.1.1 Total Generation with Constant γ

Figure 5.10 shows the total generation graph with increasing self-discharge rates for increasing storage capacities. In general, the graphs shows that the increase in self-discharge increases the total generation of the system, because the storage needs to draw more energy each time some energy is lost by the device. For the smaller energy storage systems of 2000MWh and 3750MWh, the total generation is smaller than for the larger storage systems, since the battery level is limited by its maximum storage capacity for a given self-discharge rate. However with the larger energy storage systems of 11000MWh and 22500MWh, it can be seen that for lower leakage fraction less than 0.004, the largest energy storage generates the largest amount of energy, since the storage device can store more energy for peak shaving.

Further, as the leakage fraction increases beyond 0.004, we see that both of the larger storage devices have the same total generation for the given horizon. This is because as mentioned earlier, the storage device has an optimal level of energy for a given self-discharge rate, which results in the same total generation even when the storage capacity is increases. This is evident if we observe the charging and generation schedules for both the 11000MWh and 22500MWh storage devices with 20% a day leakage in figures 5.6 and 5.7. The figures show both the storage systems having the same charging and generation schedule, which results in the total generation being the same for both the storage systems. Finally, we see that similar to the storage devices with charging inefficiency, storage devices

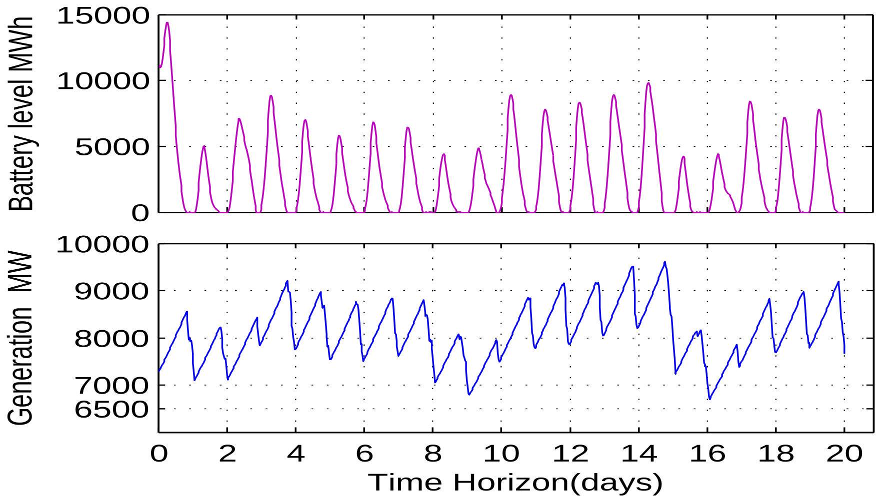

Figure 5.7: Charging and generation schedule for a 22500MWh storage system with 20% a day self-discharge

with increasing self-discharge also increase the total amount of energy generated, which results in an increase in the total cost compared to an ideal storage system.

5.5.2 Peak Shaving with Arbitrarily Increasing Prices

Generally, with an ideal storage device, the optimal solution has to take into account the future demand and the storage energy level to minimise the cost for the utility or the user. But when using a storage device with self-discharge under arbitrary price increases, the optimal solution has to now decide on the required energy level considering the energy loss caused by the self-discharge of the battery and also the increase in energy prices over the entire horizon as discussed in chapter 2. Because of this, the optimal decision of when and how much to charge the storage depends on the loss in energy and the decision on whether to charge the storage even when the prices increase.

In chapter 4, we saw that rapidly increasing prices, cause the storage devices to fully charge at extremely high price increases, which results in the storage being full all the time. Therefore at such price increases, a storage would not be useful for the utility or the user since it does not provide any peak shaving. In a similar manner, here we wish to discuss the structure of the charging and generation schedules, for storage devices with self-discharge under rapidly increasing prices by using numerically simulated data.

The graphs in figure 5.13 show the peak generation when using storage devices with increasing capacity and self-discharge percentages. Figure 5.13 shows the peak generation

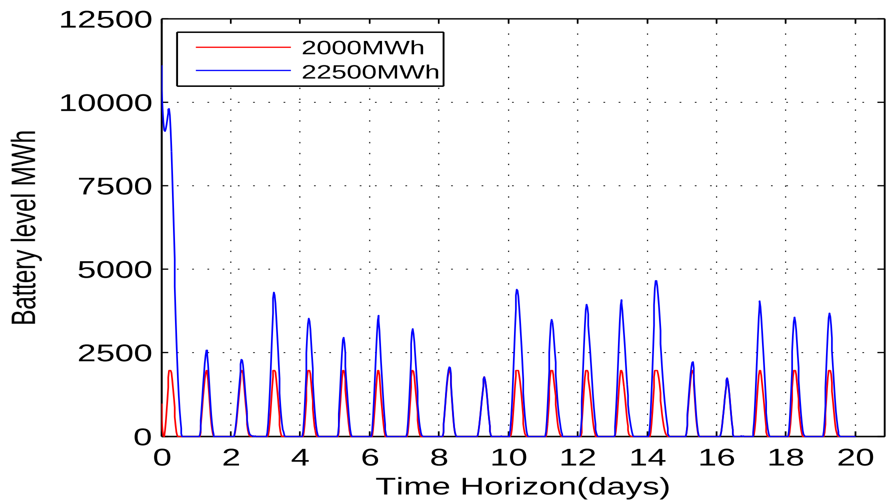

Figure 5.8: Charging schedule for 2000MWh and 22500MWh storage systems with 1.25% per half hour self-discharge

vs price increase for the July 2012 Victoria demand data [6], using energy storage devices with storage level $b(0) = b(T) = B$, and price increase $\gamma(t) = (1 + a)^t$, where $a \in (0, 0.1]$, and $t \in [0, T]$. From figure 5.13a it is clearly visible that, when there is no self-discharge and the storage is ideal, the larger the storage device, the larger the peak shaving benefit at low to moderate price increases. This is due to a larger storage system being able to store more energy to be used later during high demand and price periods. However, as the price increase becomes $\gamma(t) = (1.1)^t$, the peak generation in the grid is equal to the original peak demand of 7547MW which occurs on the 3rd day of the Victorian demand profile as shown in figure 5.11. This is because at high price increases, the storage charges up to capacity at the start of the horizon and does not utilize the storage device, but instead finds it optimal to generate just enough to satisfy the demand.

The above mentioned behaviour is also exhibited for storage devices with self-discharge as shown in figure 5.13. Figures 5.13b to 5.13f show that even with increasing self-discharge, all three storage systems fully saturates at extremely high price rates making the utility generate just enough power to satisfy the demand. Fortunately, such high price increase are not realistic, and is an artifact of our model. However, the figures also shows that for more realistic price increases between $10^{-}9$ to $10^{-}5$, the storage reduces the peak generation in the grid. This is seen for the three storage systems of capacity 3750MWh,11000MWh and 22500MWh in figures 5.13b and 5.13c showing that for low self-discharge rates and moderate price increases, having a storage device reduces the peak

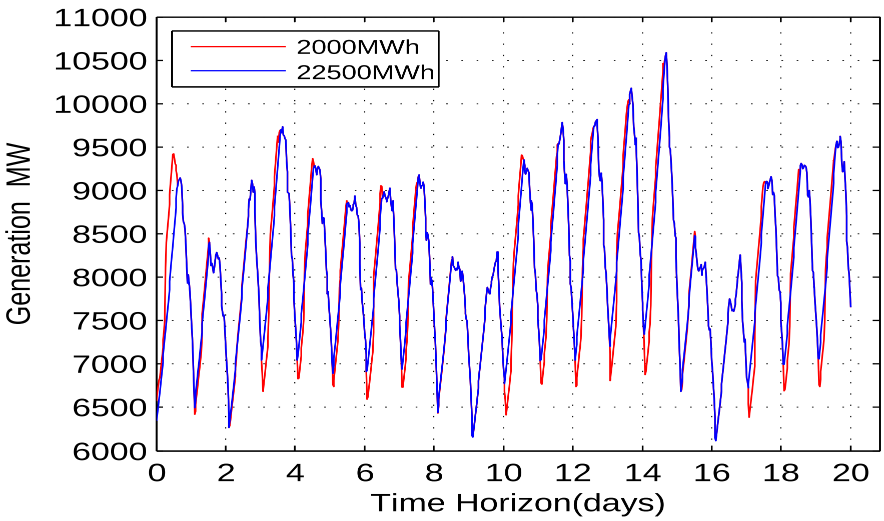

Figure 5.9: Generation schedule for 2000MWh and 22500MWh storage systems with 1.25% per half hour self-discharge

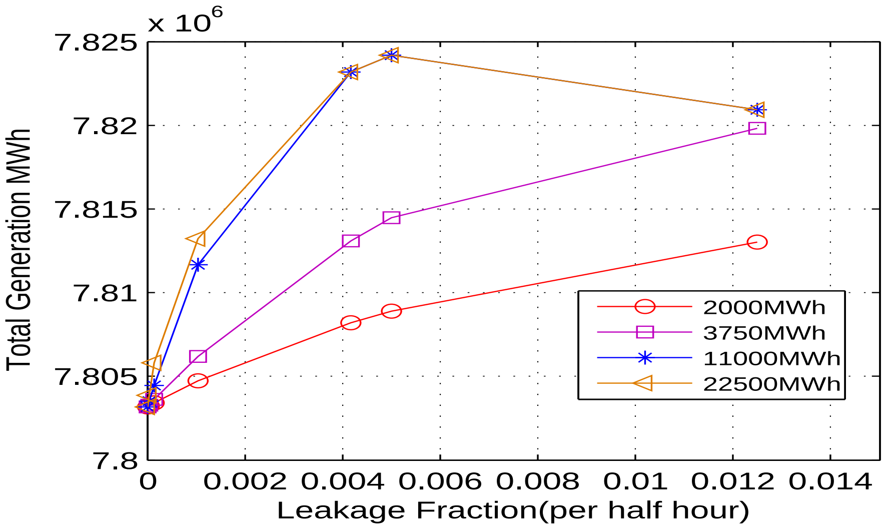

Figure 5.10: Total generation vs self-discharge for storage systems with increasing capacity

generation in the grid as expected. However, as the self-discharge of the storage systems increase, the figure 5.13 actually shows an increase in the peak generation. This increase in peak generation is due to the high loss of energy from the storage, which requires more power to be generated to maintain a desired storage level. Another observation related to increasing self-discharge is the fast increase in peak generation of larger storage systems than the smaller storage devices as seen from figures figures 5.13d to 5.13f. Since we require the storage to be fully saturated at the end of the horizon, for larger self-discharge values, the storage will try to fully use the energy in the storage system at the start of the horizon and then fully saturate at the end of the horizon as in illustrated in figure 5.12, causing a higher peak in generation.Additionally, when the self-discharge rate increases to

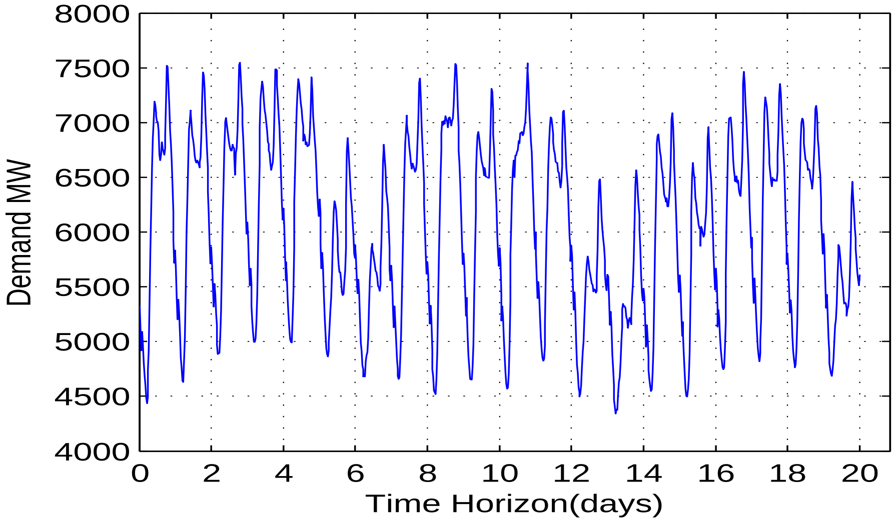

Figure 5.11: Victoria demand data for July 2012 from AEMO [6]

1.25% both the 11000MWh and 22500MWh storages both have a peak generation that is higher than the original peak demand. This behaviour is a result of us selecting to have a fully saturated storage at the end of the horizon as shown by figure 5.12, which gives the high peak shown in the peak generation figure 5.13f with rapidly increasing prices.

The graphs in figure 5.14 show the charging and generation schedule for the larger 22500MWh storage with 5% a month leakage and 1.25% per half hour leakage at 10^{-4} per half hour price increase, with the storage level being fully saturated at the end of the horizon. At a high self-discharge rate of 1.25% a month, figure 5.13f, shows the maximum peak to be higher than the original Victorian peak demand. According to figures 5.14c and 5.14d, it can be seen that this peak generation occurs due to the storage fully charging at the end of the horizon on the 20th day. If we study the generation schedule in figure 5.14d, it can be seen that in fact the generation during all other times is less than the original peak demand of 7547MW. This is true for both low and high self-discharge rates in figure 5.14. Because of this it can be said that even for higher self-discharge rates, the optimal behaviour reduces the peak in the grid for all the given storage capacities in our simulation. Therefore, the large peak generation seen for larger storage devices at higher self-discharge rates are an artifact of the condition requiring the storage to be fully saturated at the end of the horizon.

If we compare the charging schedule for the larger 22500MWh energy storage in figure 5.14 and the smaller 3750MWh storage in figure 5.15 for a self-discharge rate of 1.25% per half hour, we see that the the larger storage has more energy to reduce the peak in the grid compared to the smaller energy storage system. This means that still the larger energy storage is able to reduce the peak further than the smaller storage system. However, as the self-discharge rate increases the amount of energy in the storage decreases as seen from the same figure, compared to a storage with low self-discharge in figure 5.14a. Because of this, the amount of peak shaved also decreases at high self-discharge rates for all energy storage systems.

Interestingly, the figures in 5.13 also show dips in the peak generation at certain rates of price increases, to give the lowest peak generation for all price ranges. As an example for a 0.5% per half hour self-discharge, figure 5.13e shows the peak generation reducing to the lowest at a price increase of 10^{-3}, followed by the lowest peak generation in figure 5.13f at a price increase of $10^{-}2$. However, these dips only occur within a small range of price increase rates for a given self-discharge value, and for any rate of price increase after the dip, the generation increases. This suggests that self-discharge has the tendency to push storage levels down, while future price increases will cause current storage levels to increase. As a result, if both self-discharge and prices are balanced, the full storage capacity can be used. This can be illustrated using figures 5.16, 5.17 and 5.18 giving the charging and generation schedule for the 11000MWh storage with 0.5% self-discharge when the price increase is $10^{-4}, 10^{-3}$ and 10^{-2} respectively. The generation schedule in figures 5.17 and 5.18 for the 10^{-4} and 10^{-3} price increases shows that the peak generation occurs on the 3rd day. The charging schedule for the same day in both figures show that the storage device has a higher storage level $b^*(t)$ before the peak at a price increase of 10^{-3} compared to the same storage at a price increase of 10^{-4}. Because of this, the storage with the higher storage level at the higher price increase of 10^{-3} naturally reduces the peak generation further, compared to the storage at the lower price increase of 10^{-4}.

Recall that the optimal marginal generation cost for a storage with self-discharge, increase due to the self-discharge factor $\beta^{-t} = (1-l)^{-t}$, between $b^*(t) \in (0, B)$ according to section 5.3. Where l is the rate of self-discharge per half hour. Then with rapidly increasing prices, the optimal marginal generation cost using equation (5.2) can be written as,

$$(1+a)^t N^{'}(g^*(t)) = (1-l)^{-t} \big[\sum_{\tau=t}^{T-1} \beta^{\tau} (\underline{b}^*(\tau) - \bar{b}^*(\tau)) \big]^+ \tag{5.3}$$

Then by rearranging equation 5.3 and making $N^{'}(g^*(t))$ the subject we get,

$$N^{'}(g^*(t)) = (1+a)^{-t}(1-l)^{-t}\Big[\sum_{\tau=t}^{T-1}\beta^{\tau}(\underline{b}^*(\tau) - \bar{b}^*(\tau))\Big]^{+} \tag{5.4}$$

Considering the convexity of the marginal generation cost in $g^*(.)$, we can say that the generation, increases and decreases based on the future saturation and starvation of the storage as well as the self-discharge and rate and rapid price increase. That is from equation (5.4) we see that, the product $(1+a)^{-t}(1-l)^{-t}$ additionally influences the increase and decrease in generation. Then, when $(1+a)(1-l) = 1$, $g^*(t)$ is constant between saturation points similar to the optimal solution of an ideal storage system in section 3.4.1. Further, when the price increase is low, then $(1+a)^{-t}(1-l)^{-t}$ increases, since $(1+a)^t(1-l)^t$ decreases when $a < l$. But when $a \approx l$, the decreases in $(1+a)^t(1-l)^t$ is minimum and hence $(1+a)^{-t}(1-l)^{-t}$ is smaller, making the increase in generation smaller. Similarly, when $a > l$, which means the rate of price increase is larger than the self-discharge rate, then the product $(1+a)^t(1-l)^t$ increases, which causes the generation to decreases when $b^*(t) \in (0, B)$. Therefore during such high price increases, the generation schedule will have a downward slope as shown in figure 5.18a, which gives the generation schedule at a high price increase for a self-discharge of 0.5% every half-hour for a 11000MWh storage.

The above mentioned behaviour in the generation schedule can be illustrated using figures 5.16, 5.17 and 5.18, showing the generation and charging schedule for a 11000MWh storage with 0.5% per half hour self-discharge ($l = 0.5/100 = 0.005$) for price increases of $10^{-4}, 10^{-3}$ and 10^{-2} respectively. Here for a low price in figure 5.16, the generation increases when $b^*(t) \in (0, B)$ and the optimal solution is to discharge more often keeping the storage level low since the self-discharge rate is higher than the rate or price increase and influences the optimal decision. But as the price increases to 10^{-3}, the rate of price increase and self-discharge are approximately equal. Then the optimal decision in this case would be to minimise the generation which results in the storage having more energy which is used in reducing the peak in the grid as shown in figure 5.17.

However, when the price increase is higher than the rate of self-discharge at 10^-2, then the optimal behaviour would be to have the storage fully saturated. Because of this during this time, the storage system will saturate fully and discharge occasionally during peak demand as shown in figure 5.18, which results in a higher generation to maintain a higher energy level in the storage system. In the same figure, when $b^*(t) \in (0, B)$, the generation linearly decreases in contrast to the increase in linear generation seen for no or low price increases. Furthermore, due to the storage saturating more often and not discharging at high price increases, the generation schedule has more upward jumps each time the storage system fully saturates.

Based on thee numerical results and the optimal marginal generation cost, it can be said that at price increase rates lower than the self-discharge rates, the optimal behaviour is to discharge the storage more often to minimises the generation cost. But as the price increase rate become approximately equal to the self-discharge rate, the marginal generation cost is minimised by minimising the generation, because at such rates, the peak generation is at its lowest to providing the best peak shaving. But as the price increase rate becomes higher than the self-discharge rate, the optimal storage schedule decides on having the storage close to saturation, which results in an increase in generation.

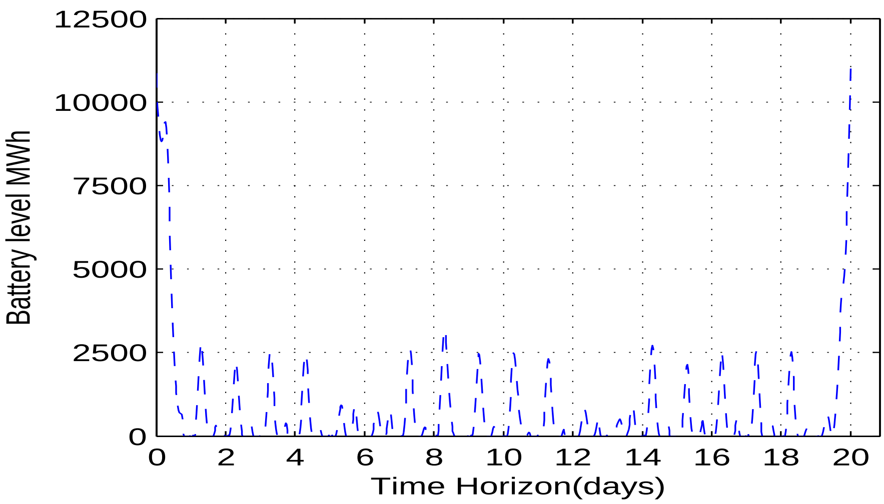

Figure 5.12: Charging schedule for a 11000MWh storage system with 1.25% per half hour self-discharge

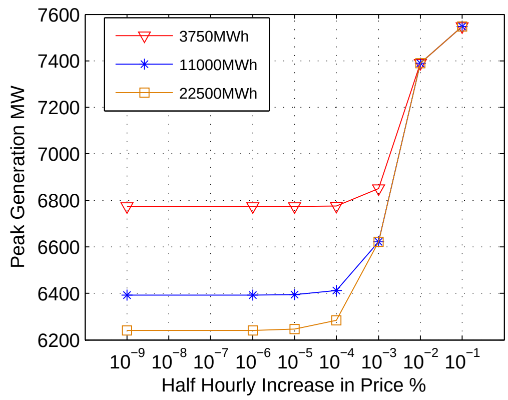

(a) Peak generation vs price increase with fully efficient storage system

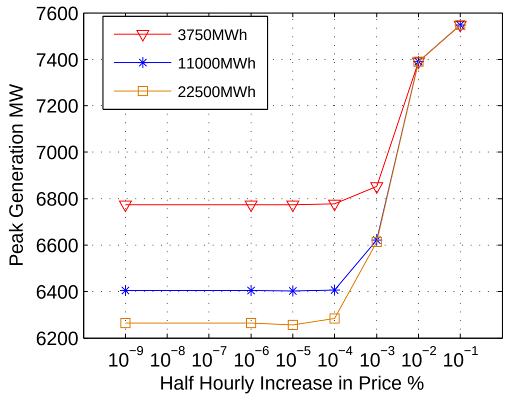

(b) Peak generation vs price increase for a storage system with 5% a month self-discharge

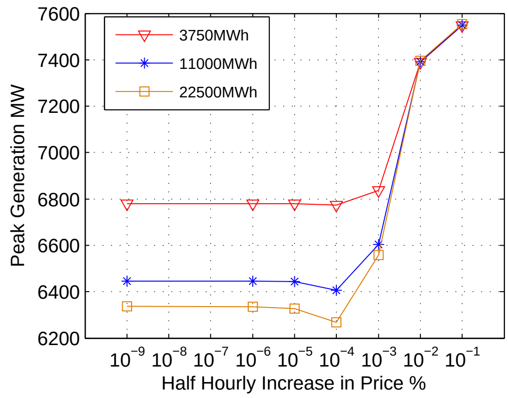

(c) Peak generation vs price increase for storage system with 20% a month self-discharge

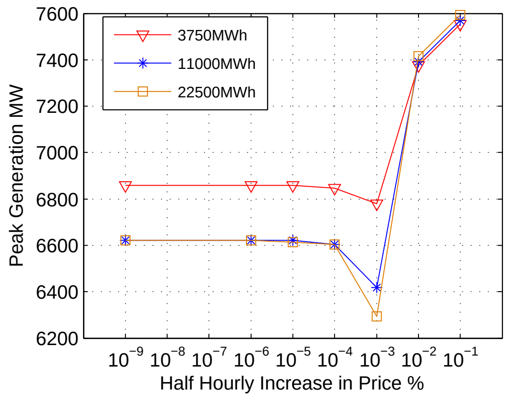

(d) Peak generation vs price increase for storage system with 5% a day self-discharge

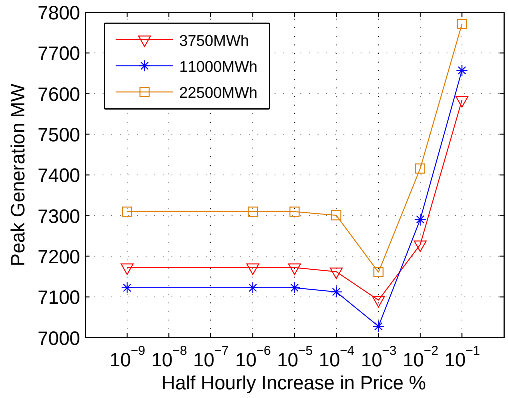

(e) Peak generation vs price increase for storage system with 0.5% per half hour self-discharge

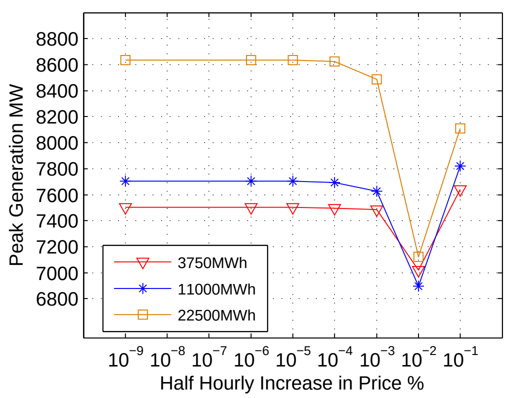

(f) Peak generation vs price increase for storage system with 1.25% per half hour self-discharge

Figure 5.13: Peak generation vs price increase for increasing self-discharge rates

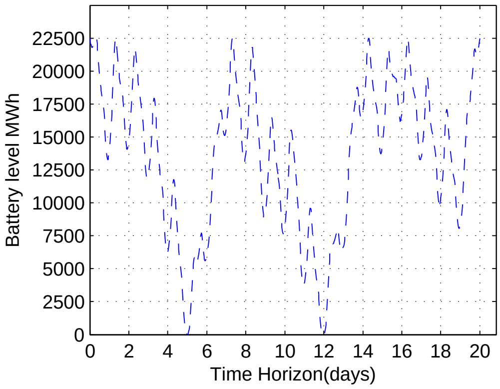

(a) Charging schedule for a 22500MWh storage system with 5% a month self-discharge

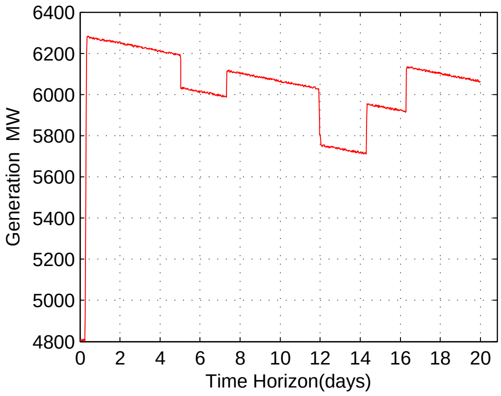

(b) Generation schedule for a 22500MWh storage system with 5% a month self-discharge

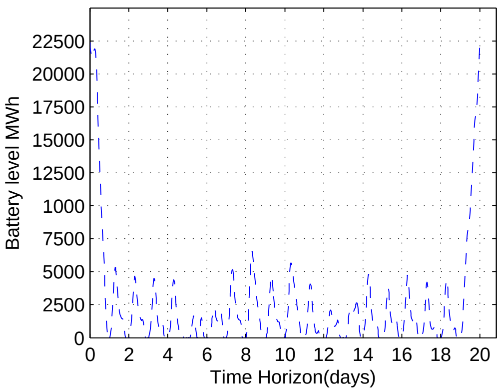

(c) Charging schedule for a 22500MWh storage system with 0.5% per half hour self-discharge

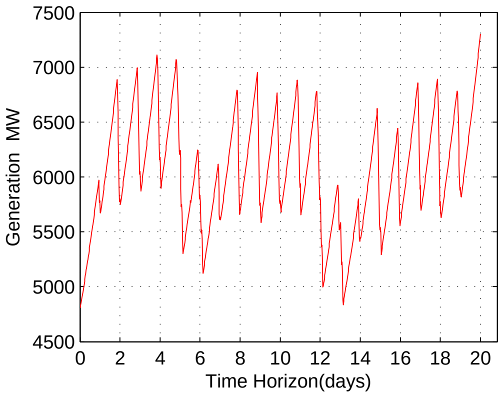

(d) Generation schedule for a 22500MWh storage system with 0.5% per half hour self-discharge

Figure 5.14: Generation and charging schedule for a 22500MWh storage system with high and low self-discharge rates

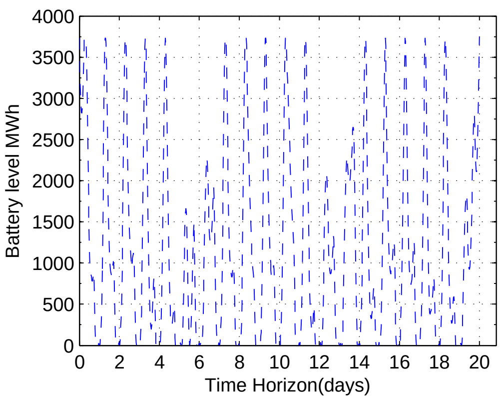

(a) Charging schedule for a 3750MWh storage system with 0.5% per half hour self-discharge

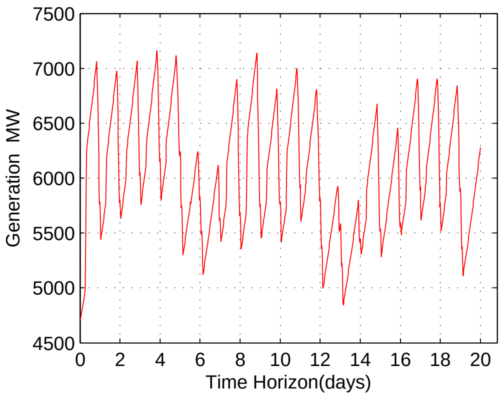

(b) Generation schedule for a 3750Wh storage with 0.5% per half hour self-discharge

Figure 5.15: Generation and charging schedule for a 3750MWh storage system with self-discharge

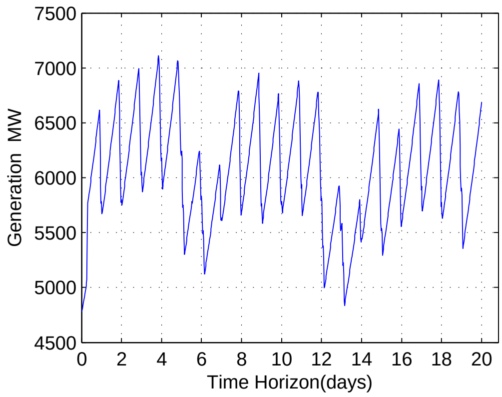

(a) Generation schedule for a 11000MWh storage system with 0.5% per half hour self-discharge and 10^{-4} per half hour price increase

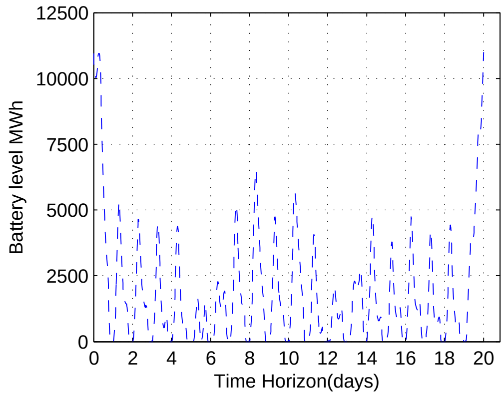

(b) Charging schedule for a 11000MWh storage system with 0.5% per half hour self-discharge and 10^{-4} per half hour price increase

Figure 5.16: Generation and charging schedule for a 11000MWh storage system with 0.5% per half hour self-discharge and 10^{-4} per half hour price increase

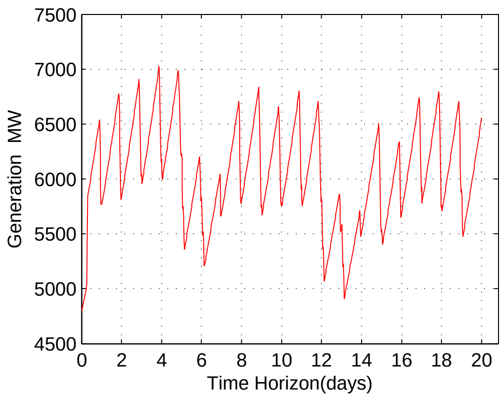

(a) Generation schedule for a 11000MWh storage system with 0.5% per half hour self-discharge and 10^{-3} per half hour price increase

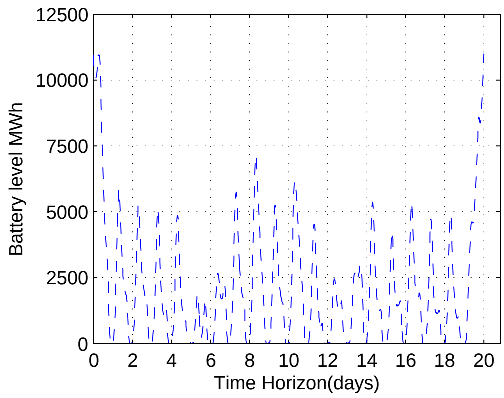

(b) Charging schedule for a 11000MWh storage system with 0.5% per half hour self-discharge and 10^{-3} per half hour price increase

Figure 5.17: Generation and charging schedule for a 11000MWh storage system with 0.5% per half hour self-discharge and 10^{-3} per half hour price increase

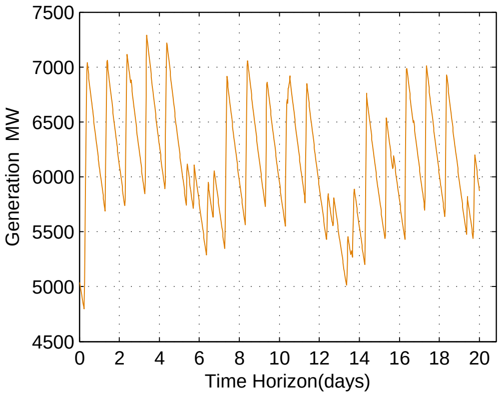

(a) Generation schedule for a 11000MWh storage system with 0.5% per half hour self-discharge and 10^{-2} per half hour price increase

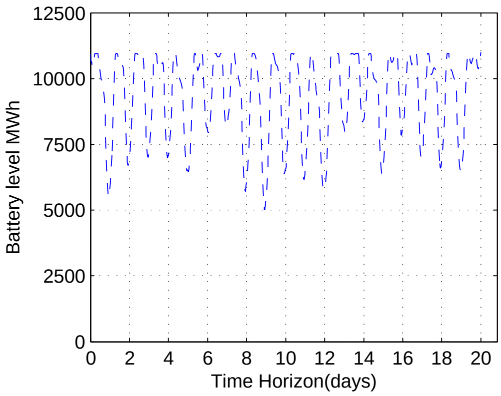

(b) Charging schedule for a 11000MWh storage system with 0.5% per half hour self-discharge and 10^{-2} per half hour price increase

Figure 5.18: Generation and charging schedule for a 11000MWh storage system with 0.5% per half hour self-discharge and 10^{-2} per half hour price increase

Chapter 6

Conclusion

In this thesis we have investigated and demonstrated structural properties of the long term optimal charging and generation schedule when using ideal and lossy energy storage systems under real-time and arbitrary price increases in the grid. Since energy prices can increase faster than inflation, the long term cost is infinite due to the unbounded average cost per stage for an infinite horizon. Because of this in this thesis we first presented an alternative method of analysing the long term cost by studying the limit of the sequence of finite horizon solution. Based on this we showed that under certain conditions, convergence occurs in finite time and that renewal points exist for which the scheduling decisions for at any point before the renewal point remains the same even when the horizon is extended to include additional demand and price fluctuations. As a result, we showed that the long term solution of the optimal schedule can be decoupled into multiple finite horizon solutions to study the optimal behaviour.

Based on the study of such a finite horizon solution with renewal points we showed that the optimal solution for an ideal energy storage will cause the marginal generation cost to only change if the storage fully saturates or empties. Further the marginal generation cost will remain constant if the storage level is between saturation and a fully discharged state. However, when the storage device is not ideal and includes charging inefficiency, the structure of the generation schedule is such that the generation will fluctuate when the storage level zero or fully saturated. Furthermore, we show that this fluctuation in generation depends on the efficiency of the storage and the future saturation and starvation of the storage system in the grid.

The study of peak shaving in the grid using inefficient energy storage showed that smaller energy storage systems have the same peak shaving for a range of inefficiency values, which allows us to suggest that under the assumption the utility is providing the user with energy storage for peak shaving, the utility has the option of providing the user with a cheaper less efficient energy storage to provide the same amount of peak shaving as a more expensive storage system with higher efficiency.

Additionally, the peak shaving behaviour with storage systems also showed that a trade-off exists between using a larger less efficient storage system or a smaller more efficient storage system for peak shaving. However, when considering the total generation of the system due to storage efficiency, it was seen that the total generation increases with increasing efficiency which introduces a conflict between the goals of reducing the peak and reducing the total energy consumptions, which needs to be considered by the user and the utility when choosing and installing an energy storage system for peak shaving and cost minimisation.

Another study on the structure of the optimal solution was carried out for storage systems with self-discharge. In contrast to the ideal and inefficient storage system, the structure of the generation schedule when using a storage system with self-discharge showed that it exponentially increased when the storage level was between the fully charged and fully discharged states. Interestingly, we also showed that with rapidly increasing prices, the optimal generation schedule exponentially decreases, when the rate of price increase is much greater than the rate of self-discharge. As a result, we see that by steadily matching the price increase with self-discharge it is possible to increase the effectiveness of peak shaving.

Based on the discussion on the structural properties of the optimal operational schedule with energy storage, we see that it is possible to utilise these properties to understand the implications and impact of the optimal schedule for different storage characteristics such as capacity, inefficiency and self-discharge. Therefore, the structural properties allow the users and utilities to understand the trade-offs that can be achieved by choosing a certain storage technology or pricing mechanism. We hope that this study encourages future research into finding structural properties for more complex storage technologies and systems.

6.1 Future Work

This thesis looked at optimising the user of a single energy storage system with inefficiency and self-discharge. As future research, it is possible to consider the effects of other characteristics of energy storage such as ramp constraints, depth of discharge and storage life cycle which limit the performance of a storage system [1, 23]. Moreover, since the cost of the storage device and the pricing mechanisms are important aspects in modeling the optimal operational schedule, future work can include a study of the storage cost and additional pricing mechanisms that benefit both the user and utility. These studies can be carried out by either using off-line algorithms as done in our thesis to understand the properties of the optimal operation or on-line studies to handle better the real-time changes in demand and pricing fluctuations.

In this thesis, chapters 4 and 5 numerically show that the monotonicity results derived in chapter 3 are true even for non-ideal storage systems. Therefore the theoretical proof of monotonicity for storage devices with inefficiency would also be an interesting direction for future work dealing with storage schedules.

Additionally, without limiting the study to a single storage system, it would be interesting to understand the structural properties of a network of energy storage system with different storage characteristics. Such distributed storage systems can be used for reducing the peak in the grid or as a method of reduce the variability of renewable generation in the grid. These extended studies using energy storage will allow the utility and the user to be able understand the implications and make better informed decisions when using energy storage in the grid.

Bibliography

[1] Review of electrical energy storage technologies and systems and of their potential for the uk. `http:/www.ensg.gov.uk/assets/dgdti00055.pdf`, 2004. [Online].

[2] A guide to understand battery specifications. `http://mit.edu/evt/summary_battery_specifications.pdf`, 2008. [Online].

[3] K. Agbossou, M. Kolhe, J. Hamelin, and T.K. Bose. Performance of a stand-alone renewable energy system based on energy storage as hydrogen. *IEEE Trans. Energy Conversion*, 19(3):633–640, 2004.

[4] E.K. Akpinar and S. Akpinar. An assessment on seasonal analysis of wind energy characteristics and wind turbine characteristics. *Energy Conversion and Management*, 46(11):1848–1867, 2005.

[5] M.H. Albadi and E.F. El-Saadany. A summary of demand response in electricity markets. *Electric Power Systems Research*, 78(11):1989 – 1996, 2008.

[6] Australian Energy Market Operator. `http://www.aemo.com.au/Electricity/Data/Price-and-Demand`. [Online].

[7] Amotz Bar-Noy, Yi Feng, Matthew P. Johnson, and Ou Liu. When to reap and when to sow - lowering peak usage with realistic batteries. In *Proceedings of the 7th international conference on Experimental algorithms*, WEA'08, pages 194–207, Berlin, Heidelberg, 2008. Springer-Verlag.

[8] G. Barbose, C. Goldman, and B. Neenan. A survey of utility experience with real time pricing. Technical report, Lawrence Berkley National Laboratory, December 2004.

[9] A.I. Bejan, RJ Gibbens, and FP Kelly. Statistical aspects of storage systems modelling in energy networks. 46th Annual Conference on Information Sciences and Systems, February 2012.

[10] Dimitri P. Bertsekas. *Dynamic Programming and Optimal Control*, volume 1. Athena Scientific, Belmont, Massachusetts, 2005.

[11] E. Bitar, R. Rajagopal, P. Khargonekar, and K. Poolla. The role of co-located storage for wind power producers in conventional electricity markets. In *American Control Conference (ACC), 2011*, pages 3886 –3891, 29 2011-july 1 2011.

[12] E. Bloustein. *Assessment of Customer Response to Real Time Pricing*. Rutgers-The State University of New Jersey, June 2005.

[13] S.P. Boyd and L. Vandenberghe. *Convex optimization*. Cambridge Univ Pr, 2004.

[14] S. Braithwait and K. Eakin. The role of demand response in electric power market design. *Edison Electric Institute*, 2002.

[15] K.M. Chandy, S.H. Low, U. Topcu, and Huan Xu. A simple optimal power flow model with energy storage. In *Decision and Control (CDC), 2010 49th IEEE Conference on*, pages 1051 –1057, December 2010.

[16] S.X. Chen, H.B. Gooi, and M.Q. Wang. Sizing of energy storage for microgrids. *Smart Grid, IEEE Transactions on*, 3(1):142 –151, March 2012.

[17] A. Cruden and GJW Dudgeon. Opportunities for energy storage operating with renewable energy systems. *Proceedings of the EESAT*, 98, 2000.

[18] M. Daoud and X. Fernando. On the communication requirements for the smart grid. *Energy and Power Engineering*, 3(1):53–60, 2011.

[19] B. Devillers and D. Gunduz. Energy harvesting communication system with battery constraint and leakage. In *2011 IEEE GLOBECOM Workshops, GC Wkshps 2011*, pages 383–388, 2011.

[20] Y.M.I. Dirickx. Turnpike theory in deterministic discrete dynamic programming with discount factor greater than one. *SIAM Journal on Applied Mathematics*, pages 467–472, 1973.

[21] EPRI. *Handbook of Energy Storage for Transmission or Distribution Applications*, 2002. [Online].

[22] A. Even, J. Neyens, and A. Demouselle. Peak shaving with batteries. In *Electricity Distribution, 1993. CIRED. 12th International Conference on*, pages 5.17/1 –5.17/6 vol.5, May 1993.

[23] A. Faghih, M. Roozbehani, and M.A. Dahleh. Optimal utilization of storage and the induced price elasticity of demand in the presence of ramp constraints. In *Decision and Control and European Control Conference (CDC-ECC), 2011 50th IEEE Conference on*, pages 842 –847, December. 2011.

[24] A. C. Fu, E. Modiano, and J. N. Tsitsiklis. Optimal energy allocation and admission control for communications satellites. *IEEE/ACM Transactions on Networking*, 11(3):488–500, 2003.

[25] N. Gast, D.C. Tomozei, and J.Y. Le Boudec. Optimal storage policies with wind forecast uncertainties. 2012.

[26] D. Gayme and U. Topcu. Optimal power flow with distributed energy storage dynamics. In *Proceedings of the American Control Conference*, pages 1536–1542, 2011.

[27] P. Harsha and M. A. Dahleh. Optimal sizing of energy storage for efficient integration of renewable energy. In *Proc. 50th IEEE Conference on Decision and Control and European Control Conference (CDC-ECC), 2011*, Orlando, FL, USA, Dec 2011.

[28] M. D. Hopkins, A. Pahwa, and T. Easton. Intelligent dispatch for distributed renewable resources. *IEEE Transactions on Smart Grid*, 3(2):1047–1054, 2012.

[29] Weihao Hu, Zhe Chen, and B. Bak-Jensen. Optimal operation strategy of battery energy storage system to real-time electricity price in denmark. In *Power and Energy Society General Meeting, 2010 IEEE*, pages 1 –7, July 2010.

[30] L. Huang, J. Walrand, and K. Ramchandran. Optimal demand response with energy storage management. *arXiv preprint arXiv:1205.4297*, 2012.

[31] H. Ibrahim, A. Ilinca, and J. Perron. Energy storage system characteristics and comparisons. *Renewable and Sustainable Energy Reviews*, 12(5):1221 – 1250, 2008.

[32] Rozanna N. Jesudasan and Lachlan L. H. Andrew. Scheduling long term energy storage. In *The fourth International Conference on Future Energy Systems (ACM e-Energy)*, Berkeley, CA, May 2013. In preperation.

[33] Rozanna N. Jesudasan, Lachlan L. H. Andrew, and Hai L. Vu. User-optimal Storage with Rising Energy Prices. Technical Report 120906A, Centre for Advanced Internet Architectures, Swinburne University of Technology, Melbourne, Australia, 06 September 2012.

[34] Rozanna N. Jesudasan, Lachlan L. H. Andrew, and Hai L. Vu. Scheduling inefficient storage. In *Proceedings of the 2013 IEEE Power & Energy Society General Meeting*, Vancouver, British Columbia, Canada, July 2013.

[35] R. J. Kerestes, G. F. Reed, and A. R. Sparacino. Economic analysis of grid level energy storage for the application of load leveling. In *IEEE Power and Energy Society General Meeting*, 2012.

[36] J.Z. Kolter and M.J. Johnson. Redd: A public data set for energy disaggregation research. In *Workshop on Data Mining Applications in Sustainability (SIGKDD), San Diego, CA*, 2011.

[37] Magnus Korpaas, Arne T. Holen, and Ragne Hildrum. Operation and sizing of energy storage for wind power plants in a market system. *International Journal of Electrical Power & Energy Systems*, 25(8):599 – 606, 2003.

[38] I. Koutsopoulos, V. Hatzi, and L. Tassiulas. Optimal energy storage control policies for the smart power grid. In *Smart Grid Communications (SmartGridComm), 2011 IEEE International Conference on*, pages 475 –480, October 2011.

[39] M. Kraning, Y. Wang, E. Akuiyibo, and S. Boyd. Operation and configuration of a storage portfolio via convex optimization. In *Proc. 18th IFAC World Congress*, pages 10487–10492, 2011.

[40] J. Lavaei and S. H. Low. Convexification of optimal power flow problem. In *2010 48th Annual Allerton Conference on Communication, Control, and Computing, Allerton 2010*, pages 223–232, 2010.

[41] J. Leadbetter and L. Swan. Battery storage system for residential electricity peak demand shaving. *Energy and Buildings*, 55:685–692, 2012.

[42] Na Li, Lijun Chen, and S.H. Low. Optimal demand response based on utility maximization in power networks. In *Power and Energy Society General Meeting, 2011 IEEE*, pages 1 –8, july 2011.

[43] B. Lin and J. Liu. Estimating coal production peak and trends of coal imports in china. *Energy Policy*, 38(1):512–519, 2010.

[44] C.E. Lin and G.L. Viviani. Hierarchical economic dispatch for piecewise quadratic cost functions. *Power Apparatus and Systems, IEEE Transactions on*, PAS-103(6):1170 –1175, june 1984.

[45] Vasilije P. Lukic. Optimal operating policy for energy storage. *IEEE transactions on power apparatus and systems*, PAS-101(9):3295–3302, 1982.

[46] D.K. Maly and K.S. Kwan. Optimal battery energy storage system (bess) charge scheduling with dynamic programming. *Science, Measurement and Technology, IEE Proceedings*, 142(6):453 –458, November 1995.

[47] A. . Mohsenian-Rad and A. Leon-Garcia. Optimal residential load control with price prediction in real-time electricity pricing environments. *IEEE Transactions on Smart Grid*, 1(2):120–133, 2010.

[48] A. Mohsenian-Rad, V.W.S. Wong, J. Jatskevich, R. Schober, and A. Leon-Garcia. Autonomous demand-side management based on game-theoretic energy consumption scheduling for the future smart grid. *Smart Grid, IEEE Transactions on*, 1(3):320 –331, dec. 2010.

[49] S. J. Moura, D. S. Callaway, H. K. Fathy, and J. L. Stein. Tradeoffs between battery energy capacity and stochastic optimal power management in plug-in hybrid electric vehicles. *Journal of Power Sources*, 195(9):2979–2988, 2010.

[50] HyungSeon Oh. Optimal planning to include storage devices in power systems. *Power Systems, IEEE Transactions on*, 26(3):1118 –1128, aug. 2011.

[51] A. Oudalov, R. Cherkaoui, and A. Beguin. Sizing and optimal operation of battery energy storage system for peak shaving application. In *Power Tech, 2007 IEEE Lausanne*, pages 621 –625, July 2007.

[52] Ter-Gazarian A. P. *Energy Storage for Power Systems*. The Institution of Engineering and Technology,London,United Kingdom, 2011.

[53] Mukund R Patel. *Wind and solar power systems: design, analysis, and operation*. CRC, 2005.

[54] M. A. A. Pedrasa, T. D. Spooner, and I. F. MacGill. Scheduling of demand side resources using binary particle swarm optimization. *IEEE Transactions on Power Systems*, 24(3):1173–1181, 2009.

[55] Q QDR. Benefits of demand response in electricity markets and recommendations for achieving them. 2006.

[56] C. Romaus, K. Gathmann, and J. Bcker. Optimal energy management for a hybrid energy storage system for electric vehicles based on stochastic dynamic programming. In *2010 IEEE Vehicle Power and Propulsion Conference, VPPC 2010*, 2010.

[57] S. Shahidinejad, S. Filizadeh, and E. Bibeau. Profile of charging load on the grid due to plug-in vehicles. *Smart Grid, IEEE Transactions on*, 3(1):135 –141, March 2012.

[58] E. Sortomme and M.A. El-Sharkawi. Optimal power flow for a system of microgrids with controllable loads and battery storage. In *Power Systems Conference and Exposition, 2009. PSCE '09. IEEE/PES*, pages 1 –5, March 2009.

[59] Han-I Su and A. El Gamal. Modeling and analysis of the role of fast-response energy storage in the smart grid. In *Communication, Control, and Computing (Allerton), 2011 49th Annual Allerton Conference on*, pages 719 –726, September 2011.

[60] J. A. Taylor, D. S. Callaway, and K. Poolla. Competitive energy storage in the presence of renewables. *IEEE Transactions on Power Systems*, 2012.

[61] Rahul Urgaonkar, Bhuvan Urgaonkar, Michael J. Neely, and Anand Sivasubramaniam. Optimal power cost management using stored energy in data centers. In

Proceedings of the ACM SIGMETRICS joint international conference on Measurement and modeling of computer systems, SIGMETRICS '11, pages 221–232, New York, NY, USA, 2011. ACM.

[62] P. Van de Ven, N. Hegde, L. Massoulie, and T. Salonidis. Optimal control of residential energy storage under price fluctuations. In *ENERGY 2011, The First International Conference on Smart Grids, Green Communications and IT Energy-aware Technologies*, pages 159–162, 2011.

[63] D. Wu, D. C. Aliprantis, and L. Ying. Load scheduling and dispatch for aggregators of plug-in electric vehicles. *IEEE Transactions on Smart Grid*, 3(1):368–376, 2012.

[64] Yixing Xu, Le Xie, and C. Singh. Optimal scheduling and operation of load aggregators with electric energy storage facing price and demand uncertainties. In *North American Power Symposium (NAPS),2011*, pages 1 –7, August 2011.

[65] L.T. Youn and S. Cho. Optimal operation of energy storage using linear programming technique. In *Proceedings of the World Congress on Engineering and Computer Science*, volume 1, 2009.